An Engineered Viral Protein Exploits LCK Kinase to Rewire T Cell Signaling Pathways

by

Yating Zheng

A dissertation submitted in partial fulfillment
of the requirements for the degree of
Doctor of Philosophy
(Pharmacology)
in the University of Michigan
2024

Doctoral Committee:

Assistant Professor Adam H. Courtney, Chair
Professor Analisa DiFeo
Professor James J. Moon
Professor Carole Parent
Professor Alan V. Smrcka

Yating Zheng

christzh@umich.edu

ORCID iD: 0000-0002-7369-8353

Dedication

This work is dedicated to my family-

My parents, Jing Liu and Xiaofeng Zheng

My grandparents Yishou Zheng, Deshen Liu, Yehui Shen, Lingsheng Bai

This work would not have been possible without their unconditional support and love.

Acknowledgements

First and foremost, I would like to express my deepest gratitude to my advisor, Dr. Adam Courtney. I am very grateful that he took me as his first graduate student and the initial 2 lab members 5 years ago. He has not only provided hands-on training but has also offered timely mentorship throughout the entirety of my Ph.D. journey. It is his sharp scientific instinct and thorough training that have enabled me to come this far and bring this project to fruition. Without his mentorship, I would not have achieved what I have today. Dr. Courtney has instructed me in all aspects, ranging from laboratory benchwork to grappling with high-level scientific inquiries, without any reserve of his knowledge. Having the opportunity to be his first graduate student and to learn directly from him has been an exceptional privilege. In my not-so-long life experience, he stands out at one of the most dedicated individuals, whose exceptional work diligence and foresight – thinking hundreds of steps ahead – are not only ambitious but also meticulous in detail. His approach to work has left an indelible mark on me and has profoundly shaped how I work – instilling diligence, perseverance, forward planning, and a focus on the present. I am also immensely grateful for his trust in my abilities to take on this exciting project, an idea he had nurtured during his postdoc at UCSF. It is because of his full-rounded support that we have managed to investigate this system from molecular cloning to translational models from scratch, in just a few short years. His professional values will undoubtedly continue to inspire me in my future endeavors, I carry the pride of having been trained by him, a foundation that has prepared

me for an intricate, challenging, and thrilling career ahead. From the depths of my heart, I wish Dr. Courtney even greater achievements in the future with the Courtney Lab.

I want to thank all the members of my dissertation committee, Dr. Carole Parent, Dr. Analisa DiFeo, Dr. Alan V. Smrcka, and Dr. James Moon for sharing valuable insights in my research projects. I would like to express my gratitude to Dr. Alan Smrcka for his guidance since my candidacy exam, where I learned to approach things more rigorously and logically. I also wish to thank Dr. Analisa DiFeo for serving as my grant-writing mentor and supporting me in my pursuit of a career that might not seem conventional but is both ambitious and promising. Additionally, I appreciate Dr. James Moon for his role as a member of my thesis committee. Pursuing cancer immunotherapy in his lab was the initial reason I wanted to come to the University of Michigan many years ago when I was still an undergraduate, and I could hardly believe that he would serve on my committee and contribute to this project.

I especially want to extend my deep gratitude to Dr. Carole Parent for her multifaceted role as my dissertation committee member, mentor during my master's research, a true friend, and a respectful advisor over the past 6 years. Carole's belief in my capabilities and integrity has been instrumental to my progress; she was the one who initially introduced to Dr. Courtney's lab, setting me on my current path. Throughout my time at the University of Michigan, Carole has provided comprehensive support, guiding me through both professional and personal challenges. The valuable experience I gained while working in Dr. Parent's lab of my master's degree instilled in me a strong work ethic, for which I am forever grateful. I will miss you Carole and I will visit you as I could in the future if I am still in this country.

I would like to thank our collaborator Dr. Weiping Zou and Dr. Jiajia Zhou for their generous support for providing the precious cancer cell lines and technical support. I am thankful

for Dr. Jiajia Zhou for generously providing in vivo knowledge he knows for me to navigate one of the most challenging parts in this project even at his busiest.

I would like to thank all the current and past members of the Courtney lab for their support including Taylor Piper, Monica Chanda, Claire Shudde, Zehui Gu, Xinyu (Ruby) Wang and Grace Aleck. Thank you, Taylor, for being as the best co-worker I have ever worked with. Your contribution to the Courtney lab as the first lab member and all the ground work you have done will be forever remembered. I want to thank Zehui for her support and contribution to the paper and Xinyu for her dedication for the tedious animal work that make this paper in shape.

I sincerely thank Dr. Stephen Fisher in the pharmacology department for his support and guidance during my year in the master's program.

Also, I want to thank Dr. Lori Isom and Dr. Emily Jutkiewicz for generously guiding me through this challenging Ph.D. journey.

I want to express my sincere gratitude to my friends for their support during my toughest times in this journey: Wenhui Wei, Yang Xu, Hao Chen, Jiayu Wang, Nora Huang, Ian Chronis, Shreeya Bakshi, Chante Liu, Chi-Chi, Tenzin Ngodup, Song Chen, Wenpu Trim, and the many others whose names I may not have mentioned. Please forgive me for any oversight. As an international student who landed in this country six years ago with an education solely in Chinese, it is through your kindness and support that I have come this far. I eagerly anticipate the exciting new chapter ahead and hope to still see all of you in the future.

I wish to extend my deepest gratitude to my parents, Jing Liu and Xiaofeng Zheng. Thank you for allowing your only child to pursue her dreams and a demanding career, despite the distance of being separated by six years across a foreign land. Your unconditional love and support have been the pillars of my journey. To my father, in particular, those six years apart have been a

significant absence, and I have missed the opportunity to see you during this time. However, I believe that we will create even more joyful memories in the years to come.

Table of Contents

List of Figures

Abstract

T cells are central mediators of human immunity that protect against infectious threats and eliminate malignant cells through a T cell response that is coordinated by specialized signaling pathways. For a T cell to attack a cancer cell, it must first become activated, proliferate, and acquire effector function. This process requires three critical signal inputs; Signal 1: Antigen; Signal 2: Co-stimulation; Signal 3: Cytokine. Once a T cell anti-tumor response is initiated, for cancer to persist, it must escape T cell mediated attack. Cancer can co-opt inhibitory T cell receptors to prevent T cell attack. Immunotherapies that block inhibitory receptors, such as PD1/L1 and CTLA4 antibodies, have revolutionized the treatment of metastatic cancer. However, many patients that fail to respond to immune checkpoint blockade do not possess an inflamed tumor and are hypothesized to require an activator that can promote a T cell response. Therefore, strategies to interface with T cell signaling pathways are necessary to effectively harness T cells as therapeutic entities for the treatment of cancer.

The TCR complex; coinhibitory and costimulatory receptors (e.g. CD28 and PD-1), as well as intracellular signaling proteins (e.g. ITK and ZAP-70) are phosphorylated by the SRC family kinase LCK. LCK kinase is basally active in resting T cells, which suggests that the recruitment of LCK activity to a protein, to induce its phosphorylation, could be a generalizable feature to be exploited for the targeted activation of T cell signaling pathways. Herpesvirus saimiri (HVS) infects T cells, expressing a tyrosine kinase interacting protein (TIP) to co-opt LCK by recruiting it to non-canonical substrates to phosphorylate and activate them. We therefore sought to

determine whether HVS TIP protein could provide a blueprint to harness LCK kinase activity to promote the activation of intracellular signaling pathways in T cells.

The basal kinase activity of LCK is regulated by the inhibitory CSK kinase that phosphorylates the C-terminal tail of LCK to stabilize its closed conformation. It has been shown that the inhibition of CSK results in increased basal LCK activity that augments the activation of T cells in response to weak or partial TCR agonists. We isolated a minimal peptide derived from the wild-type TIP protein that binds to LCK kinase. Similar to CSK inhibition, the TIP-derived minimal peptide increased LCK basal kinase activity and enhanced TCR signaling; boosting T cell responsiveness to weak antigenic stimuli ex vivo, potentially offering a new avenue for improving the efficacy of T cell-based therapies that target weakly immunogenic tumors.

The efficacy of T cell therapies can be limited if cytokine-induced JAK-STAT signaling is dysregulated or insufficient to sustain functionality. We further explored the feasibility of recruiting LCK kinase activity to non-canonical protein substrates to directly activate targeted STAT proteins in T cells. STAT activation was accomplished by engineering the HVS TIP to provide a platform for the enforced recruitment of LCK to STAT proteins. We determined that the TIP Minimal peptide that binds to LCK could be combined with STAT binding sites derived from endogenous cytokine receptors. These constructs activated targeted STAT proteins in a cytokine-independent manner. A STAT5 activator enabled CD8+ T cells to retain their functionality under suppressive culture conditions ex vivo. These findings translated to reduced tumor outgrowth in vivo due to enhanced T cell persistence and functionality.

Chapter 1 General Introduction

1.1 T Cells as Central Mediator in Cancer-Immunity Cycle

1.1.1 T Cell Development

T cells are pivotal to human immunity, acting as defenders against infectious agents, regulators of tissue homeostasis, and eliminators of cancerous cells. These roles necessitate a T cell response that entails a complex process involving signals from the T cell antigen receptor (TCR) [Signal 1], co-stimulatory molecules [Signal 2], and cytokine induced cytokine signaling [Signal 3], as well as other factors like chemokines and integrins. Such signaling instructs activated T cells to mature into distinct subtypes with specialized roles that can then migrate to tissues to exert their protective role [1]. Prior to acquiring the capacity to recognize and respond to potential threats, T cells undergo a developmental process to ensure each T cell displays a clonal TCR with minimal self-reactivity.

Lymphoid progenitors originate in the bone marrow and migrate to the thymus, where they undergo a developmental program. Early T cell progenitors known as double-negative (DN) thymocytes lack a T cell antigen receptor (TCR), and the CD4 or CD8 co-receptors. DN thymocytes can be categorized into four stages: DN1 (CD44+ CD25-), DN2 (CD44- CD25+), DN3 (CD44- CD25+), and DN4 (CD44- CD25-) [2]. Progression from double negative through DN4 involves the expression of the pre-TCR consisting of an invariant pre-TCR α-chain and a rearranged β chain [3]. Pre-TCR expression serves as a quality control checkpoint, meaning that

only the thymocytes with successful β chain gene rearrangement can be signaled through pre-TCR for proliferation and survival [4, 5]. This causes the transition of double negative thymocytes to CD4+ and CD8+ double positive (DP) thymocytes [5]. However, optimal signaling involves both a complete αβ TCR and either a CD4 (for MHC class II) or CD8 (for MHC class I) co-receptor [6]. Therefore, in the thymus, CD4+ CD8+ DP thymocytes need to make decision to eventually become either CD4+ (helper T cells) or CD8+ T cells (cytotoxic T cells). Concurrent with or following the transition to the DP state, thymocytes starts to rearrange its TCR α chain genes which results in re-arranged α chain to pair with previously formed β chain to assemble a complete αβ TCR on the DP thymocytes. The complete re-arranged αβ TCRs on CD4+ CD8+ DP thymocytes recognize self-peptides bound to major histocompatibility complex class (MHC) molecules, with specificities that resulted from somatic DNA rearrangements and chain pairing. DP cells engage with cortical thymic epithelial cells presenting self-peptides on MHC I and MHC II [7, 8]. The fate of DP thymocytes is determined by the strength of TCR signaling in response to self-peptide-MHC interactions (pMHC). Strong TCR signaling induces apoptosis (negative selection) that results in clonal deletion, a process known as central tolerance [9]. This process ensures that highly self-reactive T cells are deleted from the repertoire. Positive selection is also required, which is driven by TCR signals caused by weak interactions with pMHC. A failure to signal in response to self-pMHC results in apoptosis, a process known as death by neglect. Following positive selection, single positive (SP) CD8+ or CD4+ thymocytes emerge that are capable of recognizing MHC I or MHC II complexes, respectively [3]. These SP cells then exit the thymus to become mature CD8+ or CD4+ T cells.

1.1.2 CD8+ T Cells and CD4+ T Cells

Nearly all somatic cells express MHC I. Therefore, CD8+ T cells that recognize pMHC I act primarily in the surveillance and destruction of infected cells. This process requires the recognition of an antigenic pMHC I by a naïve CD8+ T cell and appropriate signals needed to undergo expansion and differentiation into a cytotoxic T lymphocyte (CTLs) or effector CD8+ T cell. MHC II is primarily expressed by specialized antigen presenting cells (APCs), such as dendritic cells (DCs), macrophages, and B cells [10]. CD4+ T cells develop into specialized effector subsets that coordinate pathogen elimination, including T helper type 1 (Th1), Th2, Th17, follicular helper T, whereas regulatory T (Treg) cells exert a suppressive role and act to restrain the actions of other T cells [11]. Thus CD4+ T cells subsets have distinct functions in regulating immune responses that range from promoting the expansion of CTLs and antibody production from B cells to maintenance of tissue homeostasis and are known as helper T cells (Th). Th1 cells produce Interleukin-2 (IL-2) and interferon-gamma (IFNγ) which activate macrophages and promote effector CD8+ T cell responses to mediate cellular immunity that is important to the elimination of intracellular pathogens and cancerous cells [12]. Th2 cells secrete the cytokines IL-4, IL-5, and IL-13 to help activate and recruit eosinophils, basophils, and B cells to promote humoral responses and allergic reactions [13]. Th17 cells are associated with mucosal barriers and are characterized by the production of IL-17. Th17 are involved in inflammatory responses but can also contribute to autoimmune diseases if dysregulated. Either Th1 or Th17 cells-directed response appear to promote CD8+ effector T cell responses [14, 15]. Follicular helper (Tfh) cells reside in lymphoid follicles and facilitate antibody maturation in germinal centers and are important for the development of memory B cells [16]. Regulatory T cells (Treg) are a helper T cell subset that

suppresses other immune cells, such as by producing anti-inflammatory cytokines, such as IL-10 and transforming growth factor beta (TGF-β), or by consuming IL-2 to restrain CD8+ T cells, and other suppressive mechanisms [17]. To summarize, by generating specific T cell subtypes, the immune system can fine-tune its response to specific threats and protect against inappropriate activation to prevent autoimmunity. Thus, the precise regulation of T cell activation and differentiation is crucial for overall immune homeostasis [18].

1.1.3 Signal 1: T Cell Antigen Receptor Signaling

TCR signaling is initiated when the TCR binds to a pMHC agonist. The cytoplasmic domains of the TCR-associated CD3 and ζ-chains contain motifs known as immunoreceptor tyrosine-based activation motifs (ITAMs). The tyrosine-residues within ITAMs are phosphorylated by the membrane anchored lymphocyte cell-specific protein-tyrosine kinase (LCK). LCK itself is associated with either CD4+ or CD8+ co-receptors which bind to a conserved region of MHC and facilitates recruitment of LCK to TCR:pMHC to facilitate ITAM phosphorylation. Phosphorylated ITAMS act as binding sites for the tandem SH2 domains of the ZAP-70 kinase. ZAP-70 is recruited from the cytoplasm and its autoinhibited confirmation disrupted upon ITAM binding. The recruited and partially activated ZAP-70 is then phosphorylated by LCK to stabilize its active conformation and achieve full activity. Activated ZAP-70 is then able to propagate TCR signaling by phosphorylating the linker of activated T cells (LAT). LAT functions as a signaling hub that assembles proteins needed to initiate multiple signaling pathways that are required for T cell activation and the initiation of a T cell response [19, 20]. LAT possesses four key tyrosine residues (Y132, Y171, Y191, and Y226) that are phosphorylated by ZAP-70. The tyrosine residue at position 132 (Y132), once phosphorylated,

is instrumental in the recruitment of Phospholipase C gamma (PLCγ), which generates IP3 and DAG. IP_3 diffuses through the cytoplasm and binds to the IP_3 receptor (IP_3R) on the endoplasmic reticulum (ER) which causes the release of Ca^{2+} from the ER into the cytoplasm and calcium entry from outside of the cells through the plasma membrane channels. Increased intracellular calcium levels triggers the activation of transcription factors including nuclear factor of activated T cells (NFAT). DAG within the plasma membrane activates protein kinase C (PKC). Concurrently, the connection of SOS to the phosphorylated LAT through Grb2 initiates the RAS-ERK signaling pathway. Activation of both RasGRP and SOS causes robust and persistent activation of RAS, propelling the activation of downstream signaling cascade that leads to the sequential activation of RAF, MEK, and the MAP kinase ERK (MAPK). ERK responds to a wide range signaling inputs to activates diverse transcriptional regulators to give rise to a full activation of T cells.

1.1.4 Signal 2: Signaling by the Co-Stimulatory Molecules

Signal 1 is mediated by the TCR upon. However, for sufficient T cell priming needed to initiate a T cell response, a second signal (signal 2) is required [21, 22]. Signal 2 is provided by an interaction between T cell co-stimulatory receptors and their ligands expressed on antigen-presenting cells (APCs), such as CD28 and its ligand B7-1/2 (CD80/86). These co-stimulatory receptors often colocalize with TCR at the immunological synapse between the T cell and APC to promote T cell activation [23, 24]. A lack of secondary co-stimulation can cause T cells to become anergic or unresponsive. In contrast to co-stimulatory receptors, T cell activation can also be attenuated by co-inhibitory molecules present on APCs, notably PD-1/L1 and CTLA4 [23].

Co-stimulatory and co-inhibitory receptors predominantly belong to two major superfamilies: the immunoglobulin superfamily (IgSF) and the tumor necrosis factor receptor superfamily (TNFRSF) [25, 26]. These molecules can be further grouped into specific families based on similarities in sequence, structural makeup, and functional characteristics. CD28 is found on naïve T cells and is important for the initiation of a T cell response. B7-1 and B7-2, ligands for CD28 that are expressed on APCs, are upregulated upon encountering microorganisms that activate Toll-like receptors or other pathogen sensors. However, an immune checkpoint CTLA-4 that is induced 24 to 48 hours following T cell activation binds to both B7-1/CD80 and B7-2/CD86 with higher affinity than CD28 and produces a co-inhibitory signal that attenuates T cell response [26, 27].

The intracellular domain of co-stimulatory receptors determines, at least in part, their functional outcomes. As an example, CD28 contains two motifs in its cytoplasmic tail: YMNM and PYAP. The proximal YMNM motif associates with the p85 subunit of phosphatidylinositol 3-kinase (PI3K), a common signaling intermediate, to initiate targeting of AKT (also known as protein kinase B (PKB)) that subsequently results in activation of several distal molecules. The CD28-PI3K-AKT pathway promotes T cell proliferation and survival through the activation of the downstream targets NF-kB, NFAT, BCL-XL, mTOR, GLUT1 and others [23]. In addition, both the YMNM and PYAP motifs are indispensable for the recruitment of protein kinase C θ (PKCθ) to the immunological synapse and its subsequence activation [28]. It also has been shown that CD28 also recruits the RAS guanine nucleotide exchange factor (GEF) RAS guanyl nucleotide-releasing protein (RASGRP) to the

T cell-APC interface to induce activation of RAS and the downstream phosphorylation of AKT, c-Jun N-terminal kinases (JNKs) and extracellular signal-regulated kinases (ERKs). The recruitment and activation of RASGRP seems to depend on the binding of the adaptor protein growth factor receptor-bound protein 2 (GRB2) to both the YMNM and PYAP motifs of CD28, and the recruitment of GRB2 may be the predominant signaling mechanism for IL-2 production in CD28 co-stimulated T cells [29]. In addition, the distal proline motif PYAP associates with lymphocyte cell-specific protein-tyrosine kinase (LCK) and GRB2 to enhance IL-2 induction by promoting the nuclear translocation of NFAT [28]. GRB2 is also crucial for phosphorylation of PKCθ and activation of JNKs, ERK1 and ERK2, whereas LCK promotes PKCθ activation through 3-phosphoinositide-dependent kinase 1 (PDK1) [28].

1.1.5 Signal 3: Cytokine Signaling

The third signal required to initiate a T cell response is provided by cytokines and their receptors. Cytokine-induced signaling plays essential roles in the development, differentiation, survival, and function of T cells. For example, IL-2 is indispensable to sustain T cell survival and proliferation during the priming phase of T cell activation; IL-12 and IFNγ are crucial for Th1 differentiation [30]. Most cytokines including interleukins, IFNs, and hematopoietic growth factors, activate the Janus kinase/Signal Transducers and Activators of Transcription (JAK/STAT) signaling pathways [31]. The canonical JAK/STAT signaling pathway occurs as follows: the binding of a cytokine to its receptor causes receptor dimerization. The dimerized receptor induces transphosphorylation of associated JAK kinases – JAK1, JAK2, JAK3, and Tyk2. Activated JAKs phosphorylate tyrosine residues within the cytokine receptor, creating docking sites for SH2 domain signaling proteins, primarily the STAT family of transcription

factors. The recruited STATs are then also phosphorylated by JAKs to activate them. The activated STATS then dissociate from the receptor and form homodimers or heterodimers through SH2-domain-phosphotyrosine interactions. These dimers translocate to target gene promoters, regulating the transcription of target genes.

1.1.6 The Cancer-Immunity Cycle

The immune system is a complex network of cells and tissues that act as a defense system against infection and malignancies. Two major cytotoxic cells that protect against malignant cells are natural killer (NK) cells from the innate immune system and cytotoxic CD8+ T cells from the adaptive immune system. These cells can recognize cancerous cells and become activated by them to exert killing functions [32, 33]. CD8+ T cells in particular, are capable of recognizing antigens that distinguish cancer cells from healthy tissues. Within the cancer-immunity cycle framework this process is initiated when tumor antigens (TA) are released due to tumor cell death and are captured by dendritic cells (DCs) [34, 35]. These antigens can be derived from mis-expressed or mutated proteins, which distinguishes them from normal healthy tissues. APCs, most notably DCs, can capture these antigens and traffic to lymphoid tissues where they are presented to T cells. The priming and activation of TA-specific T cells initiate a T cell-mediated anti-tumor response. Activated effector T cells traffic through the blood stream and migrate to the tumor where they then infiltrate into the TME. Activated CD8+ T cells can then recognize tumor cells through the interaction between the TCR and MHC I on the cancer cell surface that displays a TA. Cytotoxic effector T cells will then secrete cytotoxic granules that cause cancer cell death by apoptosis. There are three key components within these granules: Perforin, Granzymes, and Granulysin (only found in human but not in

mice) [36]. Perforin punctures the targeted cancer cell membrane to create pores. Granzymes are delivered into the cytoplasm of a targeted cancer cell via perforin-formed pores in the plasma membrane to initiate Caspase signaling pathway therefore to induce apoptosis; Granulysin is known to interact with the lipid bilayer to disrupt the cell membrane integrity similar as Perforin and also able to trigger apoptosis. Serglycin acts as a scaffold within the granules, connecting Perforin and Granzymes together [37]. The concurrent presence of Perforin and Granzymes is critical for potent cytolytic activity; without Granzymes, Perforin's function is inefficient, and without Perforin, Granzymes cannot enter the targeted cancer cells. Overall, apoptosis, primarily driven by CD8+ T cytotoxic T cells, is the core mechanism for cell-mediated killing of cancer cells [38, 39]. The death of the tumor cells causes the release of tumor antigens and propagates the cancer immunity cycle [40].

For cancer patients, there are many reasons for this cycle to can fail to propagate properly including poor detection of tumor antigens by DCs in the lymph node which leads to the failure in T cell priming into tumor antigen specific effector T cells, unsuccessful trafficking of T cells and infiltration into TME, poor recognition of effector T cells with tumor antigens within the TME, or inhibition of T cell activation due to an immune checkpoint mechanism [39]. Moreover, TME itself serves as an obstacle for T cells to exert their anti-tumor functions because it can establish a suppressive environment that prevents T cell function [39, 41]. Within the TME, suppressive immune cells such as Tregs and myeloid-derived suppressor cells (MDSCs) are recruited to the tumor sites to suppress effector CD8+ T cell functions from effectively recognizing and destroying tumor cells [42].

1.2 Strategies to Bolster T Cell Signaling by Targeting Intracellular Regulators

T cells are central mediators of an anti-tumor response. Cancer therefore must evade them to escape destruction by co-opting inhibitory T cell receptors to prevent T cell attack. Immunotherapies that block these inhibitory receptors that act as immune checkpoints, have revolutionized the treatment of cancer [39, 43, 44]. However, not all patients respond to these therapeutics and only a subset of cancers are treatable in this way [37, 45-48]. Many patients that fail to respond to immune checkpoint blockade do not possess an inflamed tumor and are hypothesized to require an activator that can promote a T cell response. Therefore, strategies to enhance T cell signaling to reinvigorate T cell response to boost anti-tumor immunity are being actively developed. Here, we will discuss emerging primary targets in all three T cell signaling pathways, their corresponding roles in signal transduction, and most up-to-date experimental strategies using cell-based assay and translational mouse models to bolster T cell anti-tumor response.

1.2.1 Current Strategies that Harness Signal 1

1.2.1.1 CSK: Negative Regulator in Proximal TCR Machinery

In resting cells, prior to TCR engagement, the kinase LCK is basally active and the extent of this basal activity can influence antigen recognition [49, 50]. The amount of basally active LCK is negatively regulated by the inhibitory C-terminal Src kinase (CSK). CSK phosphorylates tyrosine residues located in the C-terminal tail of Src-family kinases (SFKs). Phosphorylated Y505 within the C-terminal tail of LCK facilitates can be bound by the SH2 regulatory domain. This intramolecular interaction stabilizes a closed autoinhibited conformation. This site is dephosphorylated by the phosphatase CD45 which disrupts autoinhibition. The active form of

LCK is stabilized by trans-autophosphorylation of the activation loop within the kinase domain (Y394). Small molecule inhibition of CSK resulted in a rapid decrease in phosphorylated Y505 and a corresponding increase in LCK autophosphorylation at tyrosine 394 (Y394). This increase in active LCK levels resulted in amplified TCR signaling caused by a TCR agonist [49]. This increased signaling by the TCR sensitized naïve T cells and allowed them to become activated by weak or partial TCR agonists ex vivo [49, 51]. In contrast, the partial inhibition of LCK by PP2 had the opposite effect and reduced activation by weak TCR agonists and prevented T cell activation [49, 52, 53]. These findings have generated increased interest in investigating the translational potential by inhibiting CSK for immuno-oncology.

However, it is challenging to study the roles of CSK in T cells. CSK is ubiquitously expressed across various cell types. Embryonic lethality was observed in CSK-deficient mice due to hyperactivity of SFKs [54]. Moreover, conditional deletion of CSK in thymocytes results in TCR- and MHC-independent development of abnormal CD4+ T cells [55].

To address this, the Weiss lab generated CSK analogue sensitive (CSK^{AS}) mice by introducing bacterial artificial chromosome (BAC) transgenesis which express a mutated CSK while lacking endogenous CSK expression [56]. This mutation, marked by marked by a threonine-to-glycine substitution at position 266, affects the gatekeeper residue within the CSK ATP binding pocket, allowing for accommodation of bulky inhibitors that are unable to bind to kinases with unmodified gatekeeper residues. This mutation enables the targeted inhibition of CSK^{AS} using the small molecule 3-iodo-benzyl-PP1 (3-IB-PP1). The Weiss group has conducted a series of studies utilizing this mutant CSK mutant [49, 56]. Inhibition of this mutated CSK with the small molecule

CSK inhibitor 3-IB-PP1 allowed TCRs to become more highly activated than T cells that were not exposed to 3-IB-PP1 [49]. Inhibition of CSK^{AS} alone in thymocytes without engagement of TCR resulted in strong activation of SFKs and TCR proximal signaling [56].

These studies confirmed the negative role of CSK in the activation of T cells and suggested CSK as a potential target to regulate immune responses for cancer treatment. Mutant CSK provides the advantage of utilizing a molecule with selectivity against unmutated kinases. However, it would be more desirable to develop inhibitors that target wild-type CSK and the existing CSK inhibitor hasn't demonstrated effective in vivo inhibition of analog-sensitive CSK due to poor bioavailability.

Bristol-Myers Squibb conducted a small molecule screening using their internal kinase inhibitor collection and identified a CSK inhibitor, Compound 13. Compound 13 reduced phosphorylation of LCK Y505 - the LCK inhibitory phospho-site that promotes its closed conformation – in vivo upon oral administration of mice. They also assessed ex vivo proliferation and IL-2 secretion of CD4+ T cells by co-culturing with OKT expressing (a cognate antibody for TCR) Chinse hamster ovary (CHO) cells. Compound 13 demonstrated enhanced T cell proliferation and IL-2 production in a dose-dependent manner [57]. However, this compound 13 hasn't been evaluated in in vivo tumor model in their study.

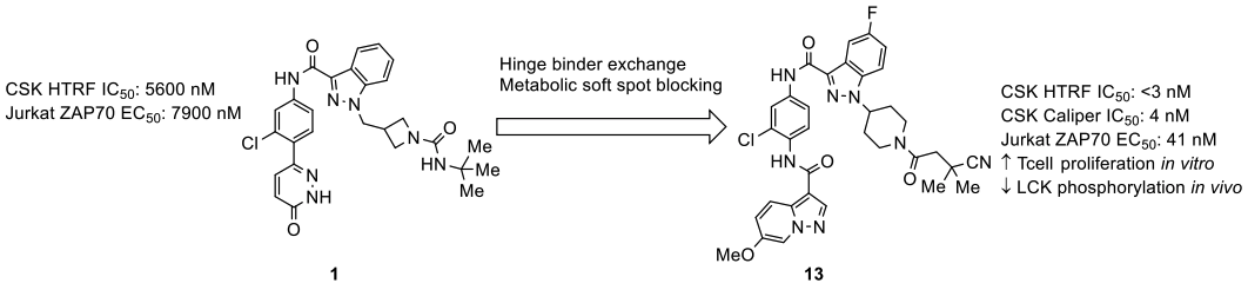

Figure 1-1

Identification of CSK inhibitor compound lead 1 and an optimized compound 13 by Bristol Myers Squibb.

Adapted from O'Malley et al, *ACS Med. Chem. Lett. 2019.*

1.2.1.2 HPK1: Intracellular T Cell Checkpoint in Proximal TCR Signaling

HPK1, also known as MAP4K1, belongs to the Ste20-related serine/threonine kinases and is predominantly expressed in hematopoietic cells. It consists of an N-terminal kinase domain, SH3-binindg proline-rich motifs, and a large citron homology domain at its C terminus, suggesting both kinase and scaffolding functions [58]. Activation of HPK1 through phosphorylation at Y381 enables it to bind and phosphorylate SLP-76, a scaffolding protein that modulates the MAPK pathway [59-61]. Within T cells, HPK1 phosphorylates the S376 site on SLP-76, which negatively regulates SLP-76 activity, which dampens TCR signaling, T cell response to antigen stimulation, and T cell-mediated immune responses against tumors [62, 63]. HPK1 Knockdown in Jurkat T cells results in enhanced TCR-induced phosphorylation of SLP-76, PLC–γ1, and ERK kinase, prolonged calcium flux, and increased cytokine production and production of antigen-specific antibodies [64]. Specifically, a SLP-76 binding protein 14-3-3tau was found to bind to SLP-76 upon TCR stimulation induced by the HPK-1-dependent phosphorylation of SLP-76 on S376 [62]. Either mutating S376 or HPK1 knockdown resulted in increased TCR-induced tyrosine phosphorylation of SLP-76 and PLC-γ1 [64, 65]. The inducible association of SLP-76 with 14-3-

3tau was reduced in HPK1-deficient T cells after TCR stimulation. HPK1 was also reported to inhibit NFAT/AP1 transcription factors in T cells [66, 67].

In another recent study, the role of HPK1 in murine CD8+ T cells was investigated using HPK1 kinase-dead knock-in mice (HPK1.kd) in which the conserved lysine in the ATP binding pocket of HPK1 was mutated to glutamic acid [61]. Compared with wild type T cells, no induction demonstrated previously by SLP-76 phosphorylation at S376 site by TCR cross-linking of HPK1.kd T cells. In HPK1.kd mice, consistent with the absence of SLP-76 S376 phosphorylation, induction of ERK1/2 phosphorylation was significantly enhanced and sustained in HPK1.kd mice relative to wild type CD8+ T cells. Furthermore, PMA-induced ERK activation which bypasses early TCR signaling, showed no discernible difference between HPK1.kd and WT mice, indicating the role of HPK1 in negatively regulating SLP-76 is TCR independent. These collective findings suggest that HPK1 is a negative regulator of TCR signaling.

Given the solid evidence that loss of HPK1 kinase activity boosted TCR signaling, Genentech investigated the anti-tumor potential by knocking out HPK1 in parallel with checkpoint inhibition. Using GL261 glioma cell model, an inflamed murine syngeneic tumor model responsive to anti-PD-L1, HPK1 knockout (HPK1.kd) mice demonstrated inhibition in tumor outgrowth associated with enhanced T cell infiltration and effector function by enhanced population of IFNγ and TNFα producing CD8+ T cells. The loss of HPK1 kinase activity was also assessed in combination with anti-PD-L1 in MC38 colon adenocarcinoma model. Treatment with anti-PD-L1 in MC38-bearing HPK1.kd mice gave rise to significant reduction in tumor growth. Many mice even exhibited a complete tumor regression and this anti-tumor effect persisted even after discontinuation of anti-

PD-L1 therapy [61]. However, HPK1.kd mice described above demonstrated modest to even non-anti-tumor effect, suggesting that the potential limitation for any selective HPK1 inhibitor as a standalone therapeutic entity. Nonetheless, those findings highlighted the crucial role of HPK1 activity in negatively regulating CD8+ effector functions, suggesting its potential as a cancer immunotherapy target [61].

To date, a couple of HPK1 inhibitors have been reported. Thienopyridines were disclosed by the University Health Network (UHN) in Toronto as a series of HPK1 inhibitors. Among them, Compound A1, a small molecule identified in the UHN patent application, demonstrated anti-tumor effect on mouse CT26 murine syngeneic colorectal carcinoma model through oral administration. Enhanced tumor inhibition was observed in combination with anti-PD-1 antibody. Anti-tumor effects of Compound K were disclosed by BMS using ex vivo culture of human T cells as well as MC38 syngeneic tumor model in combination with anti-PD-1 blockade [68]. Genentech further claimed the methods for combining an HPK1 inhibitor with a PD-1/PD-L1 axis antagonist.

1.2.1.3 DAGK: DAGK Inhibition as a Rising Strategy to Improve T Cell Activity

When TCR binds to a pMHC, it triggers the phosphorylation of the associated CD3 molecules. This ultimately, in turn, activates PLCγ, which then breaks down PIP2 into IP3 and diacylglycerol (DAG). Both IP3 and DAG act as important second messengers within the T cell. In particular, DAG plays a crucial role in initiating various downstream signaling pathways. DAG activates PKC, which can induce calcium signaling and the activation of transcription factor NFAT, as well as activate NF-kB pathway, and AP-1 mediated gene transcription for T cell activation, survival, proliferation and differentiation [69]. DAG can also activate RasGRP, which is a guanine nucleotide exchange factor (GEF) for Ras to cause its activation. Activated RAS then triggers the

activation of Ras/Raf/MEK/ERK pathway [70]. Overall, DAG mediated signaling collectively contribute to the T cell effector function. These signaling pathways converge with other vital signals to help T cells develop into effective effector cells, capable of carrying out anti-tumor responses.

The levels of diacylglycerol (DAG) are negatively regulated through phosphorylation by a family of diacylglycerol kinases (DGK), which convert DAG into phosphatidic acid (PA). In T cells, two types of DGKs, known as DGKα and DGKζ, are most abundantly expressed. These DGKs act as negative regulators that restrain TCR signaling [71, 72].

A recent study disclosed a series of first-in-class small molecules, known as the BMS-684 series, which inhibit both DGKα and DGKζ. These inhibitors were discovered through a human primary T cell phenotypic high-throughput screening, which identified them as having a unique and complementary mechanism of action (MOA) to the PD-1/PD-L1 blockade [73]. The selected compounds was confirmed through their ability to boost TCR signaling independently of PD-1 suppression, using stimuli from antigen-presenting cells that do not express PD-L1 (termed the non-PD-L1 assay). The BMS-684 compounds showed significantly enhanced IL-2 production and increased TCR signaling to a degree similar to that of anti-PD-L1 antibodies, even when PD-1 was inhibited, and this effect depended on TCR activation. In syngeneic mouse tumor models, combining DGKα/DGKζ inhibitors with anti-PD-1 therapies led to robust tumor suppression. This suggests that targeting DGKα/DGKζ could represent a new approach in T cell immune checkpoint strategies.

Concurrently, a study in another group collaborated with a key member from BMS who led the aforementioned screening study, evaluated one of the potent DGKα/ζ dual inhibitors identified from the high-throughput screening to explore if DGKs might be promising targets for boosting CD8+ T cell anti-tumor activity [74]. The DGK α/ζ inhibitor was found to strengthen TCR-induced signaling pathways downstream of DAG, leading to increased phosphorylation of PKD2 and ERK1/2, as well as boosting NF-κB and AP-1 transcriptional activities in primary human T cells. Crucially, all these effects on IL-2 production, PKD2 phosphorylation, and the activities of ERK, NF-κB, and AP-1 were dependent on the activation of the TCR. However, it was not definitively shown whether the improved anti-tumor effect of the CD8+ T cells was directly due to a reduced threshold for T cell activation by the DGK α/ζ inhibitor. This suggests that either the concept of lowering the activation threshold may not be entirely optimal for anti-tumor immunity, or perhaps a more suitable tumor model system is needed to confirm this hypothesis. Regardless, these discoveries highlight DGK α/ζ as potential therapeutic targets for magnifying tumor-specific CD8+ T cell functions.

1.2.1.4 C-Cbl and Cbl-B: Negative Regulator of Key Proximal TCR Machineries by Promoting their Ubiquitination

The E3 ubiquitin ligases Casitas B-lineage Lymphoma (Cbl) proteins, specifically c-Cbl and Cbl-b, which share common roles with abilities to interact with a range of SH2 and SH3-domain-containing proteins, enabling Cbl proteins to function as E3 ubiquitin ligases serving as negative regulators of T cell activation [75]. When TCR signaling is activated, Cbl forms complexes with multiple signaling molecules and ubiquitinates proteins, leading to their degradation and consequent suppression of signaling events [37, 76]. Cbl has been reported to promote the

attachment of ubiquitin (Ub) to the TCRζ chain, a process that necessitates a functional RING finger and the N-terminal variant SH2 domain within Cbl [77]. Mutations of TCRζ leads to a decrease in its ubiquitination, while co-expression of ZAP-70 enhances it [77]. ZAP-70 was demonstrated to act as an adaptor protein in the Cbl-mediated ubiquitination to TCRζ chain [77]. C-Cbl and Cbl-b are highly homologous but play different roles in T cells. c-Cbl primarily impacts thymic development, influencing the positive selection of thymocytes [78, 79]. Conversely, Cbl-b has a crucial role in peripheral T cell activation [80, 81]. In thymocytes, c-Cbl partners with the SRC-like adaptor protein to ubiquitinate the TCRζ chain and causes the internalization of cell surface TCR [42], whereas in mature T cells, internalization is mediated by Cbl-b [43].

Cbl was also reported to negatively regulate LCK [80]. Specifically, TCR and CD4 co-ligation in human T cells results in enhanced association between Cbl and LCK, together with LCK ubiquitination and degradation. A $Cbl^{-/-}$ T cell line showed a marked deficiency in LCK ubiquitination and increased levels of kinase-active LCK. Specifically, the LCK SH3 domain was pivotal for Cbl-LCK association and Cbl-mediated LCK degradation, with a smaller role for interactions mediated by the Cbl tyrosine kinase-binding domain. Analysis of a ZAP-70-deficient T cell line revealed that Cbl inhibited LCK-dependent MAPK activation, and an intact Cbl RING finger domain was required for such functional effect [80]. Furthermore, Cbl-b can bind to p85 subunit of PI3K. But rather than promote proteasomal degradation, Cbl-b inhibits PI3K from associating with CD28 and TCRβ following TCR activation [82]. In the context of T cell anergy, deletion of Cbl-b restored T cell responsiveness [83].

Cbl-b deficient mice demonstrate increased Th2, Th9, and Th17 cellular differentiation [84]. Furthermore, these Cbl-b deficient mice were observed to spontaneously reject UVB-induced tumors [85]. Similarly, in an adoptive transfer model where Cbl-b$^{-/-}$ CD8+ were injected TC-1 tumor bearing mice, a substantial number of mice achieve total tumor regression with enhanced proliferation of adoptively transferred CD8+ T cells. [85]. Additionally, Cbl-b-deficient CAR T against carcinoembryonic antigen demonstrated reduced exhaustion markers (PD1+ TIM3+) in MC38 syngeneic mice [86]. RNA sequencing result of tumor-infiltrating CD8+ T cells demonstrated an increase in Cbl-b expression in tumor infiltrated T cells considered as exhausted (PD-1+ Tim-3+). CRISPI-Cas9-mediated inhibition of Cbl-b restored the effector function of those exhausted T cells. The repressed tumor growth seen in Cbl-b$^{-/-}$ mice correlated with fewer PD-1+ Tim-3+ exhausted T cells [86].

The given evidence highlighted Cbl-b as an attractive target for cancer immunotherapy as an intracellular checkpoint that limits T cell activation. Nx-1607, a potent Cbl-b inhibitor developed by Nurix, is under in phase I clinical trials for various advanced solid tumors including diffuse large B-cell lymphoma. Nx-1607 has been observed to produce a dose-dependent increases in cytokine release and cell proliferation of human T cells ex vivo. Nx-1607 has demonstrated the ability to inhibit tumor growth and extend survival.

1.2.2 Current Strategies that Harness Signal 2

1.2.2.1 TRAF: An Intracellular Activation Target in Signal 2

For T cells to avoid entering a state of non-responsiveness, co-stimulation is needed during T cell priming to sustain an anti-tumor response (Signal 2). The co-stimulatory signal is delivered by various receptors, including those in the TNF receptor (TNFR) superfamily, OX40, CD27, and 4-1BB, all of which are currently being targeted by agonistic antibodies in therapeutic strategies. A shared characteristic of these TNFR receptors is their ability to recruit TNF receptor-associated factors (TRAFs) upon activation, prompting a pro-inflammatory and anti-apoptotic transcriptional response through NF-κB.

TRAF3 is required for in vivo T cell effector functions and for normal TCR/CD28 signaling. TRAF3-mediated enhancement of TCR function requires engagement of both CD3 and CD28. For T cells lacking TRAF3 that are stimulated through TCR and CD28, they exhibit not only reduced proliferation but also increased apoptosis, which is independent of both NF-κB activation and the change in pro- and anti-apoptotic proteins [87]. A recent work demonstrated that TRAF3 is recruited to the TCR/CD28 complex through interactions between the TRAF-C domain and a TRAF3 binding motif in the cytoplasmic domain of the CD28-associated adapter protein LAT [88].

Integration of the minimal TRAF-binding motif proved sufficient for the recruitment of TRAF2, a vital adaptor in 4-1BB signaling. T cells modified to include this TRAF binding sequence demonstrated enhanced persistence and expansion, both in controlled conditions and within living organisms. They also showed improved anti-tumor efficacy in a mouse model of xenograft cancer.

TRAF2 also associates with 4-1BB and OX40 [89, 90]. T cells with a dominant negative TRAF2 variant showed impaired proliferation and a reduced ability to produce cytokines such as IL-2, IL-4, and IFNγ upon stimulation through 4-1BB or OX40, indicating the important role of TRAF2 in eliciting effector T cell responses [91]. Moreover, TRAF2 is essential for memory T cell development [89]. Adoptive transfer of OVA-specific transgenic TRAF2 dominant negative T cells into recipient mice, followed by immunization with OVA and agonistic antibody to OX40, failed to generate a robust memory T cell population. This suggests that long term memory T cell survival could be dependent on TRAF [89]. Integration of the minimal TRAF-binding motif at the C-terminal of CD3ζ chain was demonstrated sufficient for the recruitment of TRAF2, which is the key adaptor molecule in 4-1BB signaling [92]. A second generation TCR-T in which CD3 ζ genes were modified to contain the intracellular domain of the 4-1BB receptor modified to include the minimal TRAF binding sequence demonstrated enhanced persistence and expansion, both in ex vivo and in vivo, and more importantly improved anti-tumor efficacy in a mouse model of xenograft cancer [92]. Altogether, these findings indicate TRAF as a promising activation target in signal 2 to reinvigorate T cell functions.

1.2.2.2 SHP1/2: Mediator to Recruit Immune-Checkpoint PD-1

The suppression of T cell activation by the inhibitory receptor PD-1 is partly mediated through its recruitment of the phosphatase SHP2, suggesting that targeting SHP2 could serve as a strategy to bolster T cell functions in cancer immunotherapy. It was expected that deletion of SHP2 would abrogate the inhibitory pathway activated downstream of PD-1 receptor. Contrary to expectations, deletion of SHP2 in T cells did not enhance anti-tumor immune responses nor did it improve the effectiveness of PD-1 antibody treatments [93]. In the ex vivo setting, SHP2 deleted CD8+ T

lymphocytes expanded only moderately better but were less polyfunctional than control cells. Mice with SHP2 deficient T cells also showed no significant improvement in controlling immunogenic tumors and respond similar to controls to anti-PD-1 treatment. Despite evidence that SHP-2 is dispensable for T cell exhaustion or PD-1 signaling, a comprehensive evaluation across specific subsets of CD8+ and CD4+ T cells is necessary to fully ascertain the role of SHP2 in T cell functioning. Even so, to date, four SHP2 allosteric inhibitors have entered clinical trials for the treatment of solid tumors [94].

In comparison to SHP2, SHP1 may show greater potential as a target in cancer immunotherapy. The cytoplasmic tails of CTLA-4 contain tyrosines that may serve as putative docking sites for SHP1, yet the combination of SHP1 inhibition with PD-1 or CTLA-4 blockade has not been explored in research to date. While clinical trials for SHP-1 inhibitors like SSG or TPI-1 have been conducted in cancer patients, they have been limited to Phase I studies focused on dosing [95]; evaluating anti-tumor outcomes was not the primary goal of these trials, and no Phase II studies have been concluded.

The underwhelming results of SSG in anti-cancer trials, both pre-clinical and clinical, have led to suggestions that the adoptive transfer approach, as demonstrated by Stromnes and colleagues, presents a more promising method for leveraging SHP1 inhibition in cancer treatment [96]. Due to SHP1's intracellular localization and the challenge of designing inhibitors selective against SHP1 without affecting SHP2 or other phosphatases, genetic modifications emerge as a more viable option for research. Incorporating a secondary knockout of SHP1 in T cells that are already

being genetically engineered could be a more advantageous than using a small molecule SHP1 inhibitor that act globally.

1.2.3 Current Strategies that Harness Signal 3

1.2.3.1 SOCS family: SOCS1 and CISH Directly Inhibit Cytokine Induced JAK/STAT Signaling

Among the Suppressors of Cytokine Signaling (SOCS) family, SOCS1 and cytokine-inducible SH2-containing protein (CISH) are predominantly associated with negative feedback mechanism of cytokine receptor signaling through JAK-STAT pathway [97]. This occurs via activation of receptor-associated Janus kinases (JAKs), which phosphorylate tyrosine residues on the receptor complex to recruit signaling molecules, including STAT proteins. Phosphorylated STAT become dimerized and translocate into the nucleus where they stimulate transcription of target genes which include SOCS genes. SOCS1 and CISH both have an SH2 domain, which is thought to compete with the binding of Janus kinases (JAKs) on activated cytokine receptors. SOCS proteins also feature a SOCS box containing binding sites for the proteins Elongin B and C, as well as a Cul box that is associated with Cullin5. This SOCS box facilitates the degradation of target proteins through a process that mimics the action of an E3 ubiquitin ligase. The process entails the assembly of Elongin B and C together with Cullin5, which then promotes the polyubiquitination and subsequent degradation of proteins bound to the SOCS molecules [98, 99].

SOCS1 has also been shown to directly inhibit JAK kinase activity by binding to the JAK activation loop through their KIR domain [100-102]. Researchers have revealed that SOCS1 knockdown can enhance anti-tumor immunity of adoptively transferred CD8+ T cells, indicating

SOCS1 as a negative regulator for effector T cell response and a potential target for anti-tumor immunity [103].

CISH has been evaluated more thoroughly for its role as an inhibitory regulator in TCR and cytokine signaling, highlighting its significance as a potential target in boosting T cell response for cancer treatment. CISH is commonly thought to inhibit TCR signaling and block STAT5 activation by competing with the activated receptor binding sites. CISH is induced in T lymphocytes after TCR stimulation or after the addition of IL-2 [104]. Instead, a recent study uncovers that the primary mechanism of action of CISH mediated suppression of T cells is through TCR signaling [104]. CISH was discovered to bind to PLCγ1 and targeted it for proteasomal degradation via polyubiquitination after TCR stimulation, which silence s TCR signaling in CD8+ T cells to maintain tumor tolerance. In the absence CISH, PLCγ1 converts PIP_3 into IP_2 and DAG, causing calcium influx and activation of PKC, which further induce activation of transcriptional activators such as NFAT and NFκB. Using gp100/pmel system, this study also explored the function of CSH effector CD8+ T cells. CISH was also found to be up-regulated in an antigen-dependent manner in tumor-specific CD8+ T cells infiltrating melanoma tumors. Deletion of CISH resulted in resulted in enhanced CD8+ T cell expansion and cytotoxic functions. CISH-deficient CD8+ T cells were able to even eliminate established tumors with enhanced expansion and functionality in vivo. By knocking down CISH in patient T cells with a short hairpin microRNA (shmiR) and co-transduced a tumor antigen specific TCR generated also generated robust anti-tumor response and enhanced T cell functions and upregulate pro-functional, proliferative and pro-survival genes (Tbx21, Cymc, and Bcl2/1, respectively), highlighting the translational potentiality of CISH as a cancer immunotherapy target to overcome tolerance enhance T cell mediated anti-

tumor immunity [104]. Another recent study also confirmed that CISH SH2 domain was essential for PLCγ1 ubiquitination and degradation in CD8+ T cells upon TCR activation [105].

Furthermore, in human T cells, knocking out CISH using CRISPR-Cas9 promoted antitumor activity by decreasing PD-1 expression levels through upregulating the level of FBX038 - a ubiquitination-regulating protein that decreases PD-1 expression [106]. CAR-T with CISH deficiency exhibited longer survival, higher level pf cytokine production and thus enhanced anti-tumor killing[106]. A recent study also showed that CISH impaired lysosomal function in activated CD4+ T cells leading to mitochondrial DNA release and increased inflammatory cytokines [107].

Altogether, these findings indicate that CISH can be potential intracellular target to inhibit for enhanced tumor specific effector CD8+ T cell functions against tumors. CISH inhibitors may complement the anti-tumor efficacy of existing cancer immunotherapies, including adoptive cell therapy with TCR, CAR-expressing T cells, cancer vaccines and checkpoint inhibitors, to improve TCR signaling within the tumor microenvironment.

1.2.3.2 STAT5: A Promising Activation Target in Cytokine Signaling

STAT5 plays a vital role in sustaining the responses of effector CD8+ T cells [108]. The functionality of CD8+ effector cells, as well as the preservation and self-renewal capacity of memory CD8+ T cells, are controlled by cytokine receptors utilizing the common gamma chain, such as those for IL-2, IL-7, and IL-15. STAT5 is a transcription factor that becomes activated through phosphorylation and dimerization following the engagement of these cytokine receptors by JAK3. A recent study demonstrated that STAT5 opposes the activity of TOX, a transcriptional

driver of tumor-specific T cell exhaustion, in CD8+ T cells [109, 110]. They found that constitutive STAT5 activity antagonized TOX-dependent epigenetic programming of exhausted CD8+ T cells to generate a durable hybrid effector/Nature Killer cell like population with enhanced tumor control, highlighting the importance of maintain STAT5 activity as a potential therapeutic approach [109].

Several groups generated different constitutively active forms of STAT5 (CASTAT5) [111]. The most widely used version is the constitutively active form of STAT5, which was developed by Kitamura and colleagues using random PCR-directed mutagenesis of STAT5a [112]. This constitutively active form of STAT5 constructs has two recurring point mutations – Histidine-299 to Arginine, and Serine-711 to Phenylalanine. This CASTAT5 is typically referred to as STAT5A1*6. They found that these two mutations alone were sufficient to trigger constitutive phosphorylation of the STAT5A1*6 construct on Tyr-694 to activate STAT5. Their further study indicated that the STAT5A1*6 construct still required tyrosine phosphorylation and thus is considered as a modestly constitutively active form of STAT5 that can be hyperactivated upon cytokine stimulation.

Therefore, therapeutic potential of the constitutively active STAT5 has started to be investigated widely. Constitutively active STAT5 in CD8+ T cells has been evaluated in an autochthonous melanoma model where CASTAT5-expressing CD8+ T effector cells infiltrate autochthonous melanomas and remain functional in the immunosuppressive tumor microenvironment. Compared with unmodified CD8+ effector T cells, CASTAT5 expressing CD8+ effector T cells develop higher cytolytic activity against antigen-expressing tumors, demonstrated by strong IFNγ

production upon re-stimulation. Adoptive transfer of CASTAT5 expressing CD8+ T cells induces tumor regression more efficiently than infusion of CD8+ effector T cells alone [113].

The presence of polyfunctional CD4+ T cells is frequently correlated with effective anti-tumor immune responses, which led to evaluating the capabilities of CASTAT5 not just in CD8+ T cells but also in combined CD4+ and CD8+ T cell therapies [114]. Introducing the aforementioned constitutively active variant of STAT5A (CASTAT5) in murine CD4+ T cells has been shown to enhance anti-tumor activity in an adoptive transfer model. In addition, the therapeutic potential of this approach was supported by outcomes from a B-cell lymphoma model in mice, where T cells were engineered to concurrently express a CD19-specific CAR and CASTAT5 resulted in the generation of multifaceted CD4+ CAR T cells. Notably, the most effective therapeutic results were seen when both CD4+ and CD8+ CAR T cells incorporated CASTAT5, indicating that CASTA5 facilitates productive CD4 help to CD8+ T cells. The study also applied CASTAT5 in primary human CD4+ T cells, highlighting its potential for clinical application [114].

Chapter 2 Development of a Viral-Derived Peptide that Activates LCK

2.1 Abstract

The anti-tumor response of cytotoxic T cells requires detection of tumor-derived antigenic peptide-MHC complex (pMHC) by the T cell antigen receptor (TCR). Some tumors do not generate a robust immune response, partly due to weak recognition of pMHC [115]. Strategies that boost TCR signaling to enhance recognition of weak pMHC could enhance recognition of poorly immunogenic tumors. To initiate TCR signaling, the SRC family kinase (SFK) LCK phosphorylates tyrosine residues on the intracellular domains of the TCR complex and the recruited ZAP-70 kinase. The activity of LCK is negatively regulated by CSK kinase. Our previous study has shown that small molecule inhibition of CSK increases LCK kinase activity and sensitizes T cells to weak antigen ex vivo [49, 51]. However, since it is a master regulator of SFKs, and its conditional deletion causes suppurative inflammation, an alternative strategy is required [116]. Because LCK is expressed only by T cells and NK cells, we sought to directly activate LCK [50]. Herpesvirus saimiri (HVS) can infect T cells and co-opt pathways needed for T cell survival and proliferation [117]. Most importantly, the HVS tyrosine kinase-interacting protein (TIP) can activate LCK [118]. We have developed a minimal LCK allosteric activator by removing the unwanted regions of TIP that could interfere with T cell functions. I have determined that this minimal LCK activator, when expressed in T cells, causes increased LCK activation, as assessed by LCK autophosphorylation. I transduced

primary mouse T cells and determined that our LCK activator could enhance TCR signaling and antigen recognition ex vivo. Therapeutic strategies that emerge from my project could provide a novel angle to develop druggable entities or cell-based therapies that address poor antigen recognition. Our strategy has the potential to improve the proportion of patients that respond poorly to current immunotherapies by providing a robust anti-tumor response.

2.2 Introduction

T cells are central mediators of human immunity that protect against infectious threats, maintain tissue homeostasis, and eliminate malignant cells through a T cell response that is coordinated by specialized signaling pathways [18]. Strategies to interface with these T cell signaling pathways are necessary to effectively harness T cells as therapeutic entities for the treatment of cancer, autoimmunity, and other human pathologies. An illustrative example is provided by the development of chimeric antigen receptor (CAR) T cells which initially fused an extracellular antibody binding domain to intracellular signaling domains derived from the T cell antigen receptor (TCR)-associated ζ chain [119, 120]. However, these first-generation CARs were an ineffective cancer treatment until a costimulatory signal provided by the intracellular domain of CD28 or 4-1BB (CD137) was incorporated into second generation CARs that were clinically approved for the treatment of B cell (CD19+) malignancies [120-122]. CARs; the TCR complex [123]; coinhibitory and costimulatory receptors, such as CD28 and PD-1 [124, 125]; as well as intracellular signaling proteins, such as ITK and ZAP-70 kinase [126, 127]; are phosphorylated by the SRC family kinase LCK. Interestingly, LCK kinase is basally active in resting T cells, which suggests that the recruitment of LCK kinase activity to a protein, to induce its phosphorylation, could be a generalizable feature to be

exploited for the targeted activation of T cell signaling pathways [50]. Indeed, the Herpesvirus saimiri (HVS) infects T cells and co-opts LCK to facilitate its reproduction by the recruitment of LCK to non-canonical substrates to phosphorylate and activate them [118]. We therefore sought to determine whether HVS could provide a blueprint to harness LCK kinase activity to promote the activation of intracellular signaling pathways in T cells.

The basal kinase activity of LCK is regulated by the inhibitory CSK kinase that phosphorylates the C-terminal tail of LCK to stabilize its closed, autoinhibited conformation [128, 129]. CSK is opposed by the tyrosine phosphatase CD45 that dephosphorylates the C-terminal tail of LCK to promote its active, open conformation that is further enhanced upon trans-autophosphorylation of the LCK activation loop [130-132]. Inhibition of CSK results in increased basal LCK kinase activity that augments the activation of T cells in response to weak or partial TCR agonists [49, 51]. The unique membrane proximal region of LCK associates with the CD4 and CD8 co-receptors [133, 134], which facilitate its recruitment to the antigen-bound TCR to promote phosphorylation of the TCR-associated ζ-chain and the recruitment of ZAP-70 kinase [135, 136]. Activated ZAP-70 phosphorylates LAT, which recruits additional signaling effectors, such as PLCγ1 and GRB2/GADS, to activate the calcium, PKC, and MAPK pathways necessary for T cell activation [137]. In comparison to the restricted substrate profile of ZAP-70, the substrate specificity of LCK is promiscuous, consistent with its capacity to phosphorylate a wider array of protein substrates [138]. These properties appear to have been exploited by HVS, which infects T cells and expresses the tyrosine kinase interacting protein (TIP). TIP is known to bind LCK and disrupt its autoinhibited conformation to cause increased basal LCK kinase activity [139-141]

I have incorporated the LCK activator into a retroviral expression system for the transduction of cell lines and primary T cells. I have optimized a procedure to transduce primary mouse T cells, improving transduction efficiency from 3% to over 90%. I have transduced my LCK activator into primary mouse T cells to evaluate TCR signaling. The LCK activator was found to boost phosphorylation of TCR signaling proteins, such as ZAP-70. I co-cultured transduced OT-I T cells with antigen presenting cells and assessed Nur77-GFP upregulation and intracellular IFNγ production as readout of T cell activation and function. In summary, my findings demonstrate that we have developed an LCK activator, that the LCK activator can be incorporated into T cells to regulate LCK activity, that the LCK activator boosts TCR signaling, and sensitizes T cells to sense and respond to weak antigens. However, our ex vivo CTL assay shows that enhancing antigen recognition might not be sufficient to enhance effector T cell killing in vitro. When incorporated in tumor specific CD8+ T cells, our TIP Minimal (LCK activator) didn't demonstrate suppression in tumor outgrowth rate. However, more study is required to evaluate the cytotoxic efficacy with LCK activator using different tumor models. Overall, we engineered a minimal TIP derived peptide that as an LCK activator which can enhance antigen recognition and lowers the threshold of T cell activation ex vivo. Moreover, the feature of enhancing basal activity of LCK kinase could be exploited, study of which will be discussed later in the next chapter.

2.3 Materials and Methods

2.3.1 Materials

2.3.1.1 Cell Lines

Phoenix cells and EL4-OVA (E.G7-OVA) cells were obtained from ATCC. B16-OVA cells were obtained from the Zou lab (U-M) (81). Jurkat T cells were obtained from the Weiss lab (UCSF). The MC38-OVA cell line has been previously described (60). Suspension cell lines were maintained in a tissue culture incubator at 37 °C with 5% CO2 in RPMI supplemented with 10% fetal bovine serum (FBS) and 2 mM glutamine. Adherent cell lines were maintained in DMEM supplemented with 10% FBS and 2 mM glutamine. E.G7-OVA cells were maintained in neomycin (G418, 500 μg/mL) supplemented RPMI culture medium (10% FBS, 2 mM glutamine).

2.3.1.2 Chemicals

PP2 (Tocris), Halt Protease Inhibitor Cocktail (Thermo Scientific), EDTA (Thermo Scientific), Propidium iodide (BioLegend), Hoechst 33342 (BioLegend), TransIT-LT1 transfection reagent (Mirus Bio), Opti-MEM (Gibco), MojoSort Streptavidin nanobeads (BioLegend), G418 (Gibco), RetroNectin (Takara), Brefeldin A (BioLegend,), NP-40 (EMD Millipore), Rat Serum (Jackson ImmunoResearch), Zombie Violet Fixable Viability Dye (BioLegend), QIAFilter plasmid purification kit (Qiagen). Synthetic peptides were synthesized by Genescript (OVA [SIINFEKL], G4 variant, and VSV [RGYVYQGL]). Tissue culture (TC) treated and non-TC treated 96-well-plates were obtained from Eppendorf and

ThermoFisher. PfuUltra II Hotstart polymerase (Strategene), DPN I (NEB), LR Clonase (ThermoFisher).

Plasmids and retroviral constructs: The WT TIP protein was synthesized as a geneblock (IDT) and cloned into a pEF6 expression vector. Truncated TIP variants were generated by PCR amplification followed by blunt end ligation. Site directed mutagenesis (Quikchange) was performed to generate STAT binding sites variants. TIP variants were transferred into the pDONR221 plasmid for Gateway cloning (ThermoFisher). MSCV_IRES_mCherry (#52114) and MSCV_IRES_Thy1.1 (#17442) were obtained from Addgene and modified to generate a destination vector by insertion of a Gateway cassette. TIP variants were transferred into MSCV destination vectors using LR clonase. The pCL_Eco plasmid was obtained from Addgene (#12371).

2.3.2 Methods

2.3.2.1 Isolation and Purification of Primary CD8+ T Cells

Primary murine CD8+ T cells were purified by negative selection using biotinylated antibodies and streptavidin-coated nano beads. Spleen and lymph nodes were ruptured in complete RPMI (Roswell Park Memorial Institute) medium [(RPMI 1640 medium, 10% fetal bovine serum (FBS), glutamine (2 mM), MEM Non-Essential Amino Acids (Gibco), Penicillin/Streptomycin (Gibco), 1 mM sodium pyruvate (Gibco), 2-Mercaptoethanol (50 μM, Gibco), HEPES (10 mM, Corning)]. Cells were washed with FACS buffer (PBS supplemented with 2% FBS and 2 mM EDTA) and combined with 5% rat serum and biotinylated antibody cocktail mix (30 μL/100x10^6 cells) [142] for 10 minutes at room temperature. Cells were

washed with flow cytometry staining (FACS) buffer and then incubated with streptavidin magnetic nanobeads (90 μL / $100x10^6$ cells) (BioLegend) for 5 minutes at room temperature and then placed in a magnet for 5 minutes. with cap off. Unwanted cell populations were discarded. Unlabeled naïve CD8+ T cells were collected and resuspended in complete RPMI medium with 10 ng/mL recombinant mouse IL-2. Naïve CD8+ T cells were activated on anti-mouse aCD3 (5 μg/mL) and aCD28 (2.5 μg/mL) coated non-TC treated plate at 37 °C for at least 24 hours before viral transduction. Primary T cells were cultured in complete RPMI medium.

2.3.2.2 Preparation of T Cell Depleted Splenocytes as Antigen Presenting Cells

To prepare T cell-depleted splenocytes as antigen presenting cells (APCs) for T cell activation assay, spleen was ruptured and red blood cells were removed using ammonium-chloride-potassium (ACK) lysis. CD4+ and CD8+ T cells were depleted using biotinylated anti-mouse CD4+ (10 μL / $100x10^6$ cells) and CD8+ (10 μL / $100x10^6$ cells) antibodies and streptavidin-coated magnetic nanobeads (20 μL /$100x10^6$ cells).

2.3.2.3 Retroviral Transduction of Primary CD8+ T Cells

Phoenix cells were added to 6-well plates and cultured overnight. The following day, cells were transfected with pCL_Eco and a viral expression vector using TransIT-LT1 reagent. After 18-24 hours, the media was removed and replaced with complete RPMI medium. Viral supernatant was collected the following day (24 hours) and centrifuged to remove cells. Primary murine CD8+ T cells were activated with plate-bound agonistic antibodies (anti-CD3

(5 μg/mL) and anti-CD28 (2.5 μg/mL)) 24 hours prior to transduction. RetroNectin (15 μg/mL) coated non-TC treated 6-well plates were combined with 1 mL viral supernatant per well and incubated at 37°C for 1 hour. 1 mL CD8+ T cell suspension (10^6 cells per well) was then added to viral supernatants and centrifuged (2000 g, 1 hour, 30°C). T cells were cultured with retroviral supernatants overnight. Total cells were counted using a Celigo imaging cytometer. Cell viability was determined by staining with Zombie Violet viability dye followed by flow cytometry analysis.

2.3.2.4 Immunoblot Analysis and Immunoprecipitation

Jurkat T cells were washed and resuspended in RPMI base medium. Plasmid DNA (10 μg) was combined with $12x10^6$ cells in 400 μL in a 0.4 cm cuvette and then electroporated using a BioRad Gene Pulser Xcell (260 V, 1250 μF). Cells were recovered into RPMI culture medium and incubated at 37°C for 48 hours. Jurkat T cells were rinsed with RPMI base medium and then resuspended at $5\text{-}10x10^6$ cells/mL before incubating at 37°C for 15 minutes. For Primary T cells, $15x10^6$ cells/mL were used. Cells were lysed through addition of lysis buffer containing a final concentration of: 1% NP-40, Na3VO4 (2 mM), NaF (10 mM), Halt Protease Inhibitor Cocktail (100X), EDTA (500 μM), PP2 (25 μM). Lysates were placed on ice for 10 minutes and centrifuged at 13,000 g to remove debris. Lysates were combined with 6x SDS sample buffer and heated at 95°C for 5 minutes before electrophoresis using NuPAGE 4-12% Bis-Tris gels (Invitrogen). Proteins were transferred to PVDF membranes (Millipore Sigma), which were then incubated with TBS-T blocking buffer (tris-buffered saline supplemented with 3% bovine serum albumin and 0.1% Tween-20). The membranes were then probed with primary antibodies (1:2000) overnight at 4°C. Blots were rinsed and incubated with HRP-conjugated secondary antibodies (1:5000). All

antibodies were diluted into TBS-T blocking buffer. Blots were imaged using chemiluminescent substrate and an iBright (Invitrogen) imaging system. Quantification was performed using iBright analysis software. For TCR stimulation of primary mouse T cells, cells were rested in RPMI medium at 37°C for 20 minutes prior to addition of anti-CD3ε antibody (2C11) followed by goat anti-Armenian hamster IgG (50 μg/mL). For immunoprecipitation (IP), $10x10^6$ Jurkat T cells were lysed and combined with 25 μL of anti-Myc tag (9E10) antibody conjugated resin (BioLegend, #658502). Samples were incubated on a rotator for 2 hours at 4°C before washing 4x with ice cold wash buffer (1/10 lysis buffer diluted with TBS). Proteins were eluted by adding 1x SDS sample buffer prior to immunoblot analysis.

2.3.2.5 T Cell Activation Assay by Imaging Cytometry

Transduced OT-I Nur77-GFP T cells were purified by positive selection using anti-Thy1.1 (CD90.1) biotinylated antibodies 24 hours after transduction. To assess T cell activation by T cell antigen receptor agonists, splenocytes were depleted of T cells using anti-CD4 and anti-CD8α biotinylated antibodies and then pulsed with peptides for 1 hour at 37°C in round bottom 96-well plates. T cells were resuspended in phenol red-free complete MEM medium and co-cultured with peptide antigen pulsed-splenocytes at a 1:1 ratio. After 6 hours of incubation (no IL-2 added), 20 μL of cells were transferred to a 96-well flat bottom plate with 180 μL PBS containing Hoechst dye (20 μM). The green and blue fluorescence channels were used to image Nur77-GFP upregulation and Hoechst positive cells (total cells) respectively. Nur77-GFP positive cells were quantified using a Celigo imaging cytometer (PerkinElmer). Data were analyzed using Celigo (V5.3) (PerkinElmer) and FlowJo (BD Biosciences) analysis software.

2.3.2.6 Cytotoxic T lymphocyte (CTL) Assay by Imaging Cytometry

Transduced OT-I Nur77-GFP T cells were harvested through anti-Thy1.1 positive selection. Cell mediated cytotoxic T lymphocytes assay was assessed using a fluorescence imaging cytometer Celigo (PerkinElmer). MC38-OVA cancer cells were added to Tissue culture-treated flat bottom 96-well plates in phenol-red free complete MEM at the density of 2,500 cells per well. The following day (24 hours), T cells were added at different effector to target (E:T) ratios and co-cultured for 16 hours at 37°C in the presence of IL-2. Cells were stained with propidium iodide (PI, 0.5 mg/μL) and Hoechst dye (20 μM) and then analyzed by the Celigo imaging cytometer to quantify activated T cells (Nur77-GFP+) and dead cells (PI+). T cell mediated cytotoxicity was quantified using the equation: $\frac{\#\text{PI+[co-culture]} - \#\text{PI+[cancer cell only]} - \#\text{PI+[T cell only]}}{\text{Total cell count [cancer cell only]}}\%$. The Celigo software application (V5.3) for expression analysis was used to collect brightfield and fluorescence images. The green and blue fluorescence channels were used to image Nur77-GFP upregulation and Hoechst positive cells (total cells) respectively as described above. The red channel was included to identify propidium iodide (PI) positive cells that were considered as dead cells. Data were analyzed using Celigo (V5.3) (PerkinElmer) and FlowJo (BD Biosciences) analysis software.

2.3.2.7 Intracellular Cytokine Release Assay and Flow Cytometric Analysis

Cells were incubated with antibodies against cell surface markers and Fc block (2.4G2) in FACS buffer for 30 minutes on ice. Cells were washed twice with FACS buffer before analysis. Antibodies are listed in previously. For intracellular IFNγ staining, splenocytes were isolated from a BoyJ (CD45.1+) mouse and red blood cells removed by ACK lysis.

Splenocytes were seeded in 96-well round bottom plates and pulsed with peptide at 37°C for 1 hour. Retrovirus-transduced CD8+ OT-I Nur77-GFP T cells (CD45.2+) were then combined and co-cultured with the peptide antigen pulsed splenocytes at a ratio of 1:4 (T cell: Antigen presenting cells) for 16 hours (300,000 T cells and 1.2 million APCs per well) in the absence of IL-2. Brefeldin A (5 μg/mL) was then added and cells incubated for 3 hours at 37°C. Cells were then washed twice with FACS buffer and stained with Zombie Violet live/dead dye. Cells were then washed twice with PBS and fixed with 2% PFA for 20 minutes. Cells were washed twice with the Perm/Wash buffer (BioLegend) and stained with anti-IFNγ and Fc block (2.4G2) in Perm/Wash Buffer at 4°C. Cells were washed twice and resuspended with FACS buffer before analysis using a Bio-Rad ZE5 flow cytometer. Data was analyzed using FlowJo software (BD Biosciences).

2.3.2.8 EL4-OVA Mouse Lymphoma Tumor Model

EL4-OVA (E.G7-OVA) cells (10^6) were subcutaneously injected into age-matched female C57BL/6J mice (6-8 weeks). On day 5 post E.G7-OVA tumor inoculation, transduced CD8+ OT-I T cells ($3x10^6$) were adoptively transferred into tumor bearing mice. Tumor size was measured every 2-3 days using calipers fitted with a Vernier scale. Tumor volume was calculated based on the formula (length x width x width)/2. For cohort studies, mice were grouped to ensure that the averaged tumor size was similar for each treatment group prior to ACT. For E.G7-OVA tumors, the averaged tumor size for each group on Day -1 was ~ 49 mm^3. Mice with tumors that were smaller than 20 mm^3 and larger than 75 mm^3 were removed.

2.3.2.9 Statistical Analysis

All statistical analyses were performed using GraphPad Prism software (V9.2.0).

2.4 Results

2.4.1 Isolation of a Minimal TIP-Derived LCK Kinase Activating Peptide

HVS can infect T cells and utilize TIP to co-opt the activity of the T cell antigen receptor (TCR) proximal tyrosine kinase LCK to remodel cellular pathways [143]. TIP binds to LCK, which phosphorylates TIP to create binding sites for the recruitment of STAT proteins [118, 144]. TIP has evolved to rewire T cell signaling pathways by co-opting LCK kinase to activate other intracellular proteins including STAT proteins (Fig. 2.1B). TIP is an integral transmembrane protein that traffics to the plasma membrane where it interacts with LCK before being subsequently trafficked to endocytic compartments along with the TCR and CD4/CD8 co-receptors, which impairs the recognition of antigen and normal T cell function [145, 146] (Fig. 2.1A). We predicted that the capacity of TIP to bind LCK and increase its basal kinase activity could be separated from its detrimental effects. Because TIP is a scaffold that exerts its effects through the recruitment and organization of signaling effector proteins, and it is thought to lack tertiary structure, we sought to isolate TIP regions that act on specific cellular targets, such as LCK.

Our initial goal was to identify a TIP variant that retained its capacity to bind LCK after removing regions of the viral protein that are known to interfere with T cell function. A series of TIP variants were evaluated that eliminated regions of TIP that cause co-receptor downregulation, as well as the transmembrane domain and an adjacent aliphatic α-helical

region that is reported to cause endocytosis (Fig. 2.1C) [145-147]. The LCK binding region of TIP that causes increased kinase activity was retained, which were mutated from tyrosine to alanine residues to prevent their phosphorylation by LCK. To assess whether these constructs increased the basal kinase activity of LCK, they were transiently transfected into Jurkat T cells and LCK autophosphorylation at Y394 was monitored by immunoblot. Unexpectedly, all constructs tested were able to robustly activate LCK, including a minimal 109 amino acid construct that lacked the transmembrane domain (Fig. 2.1D).

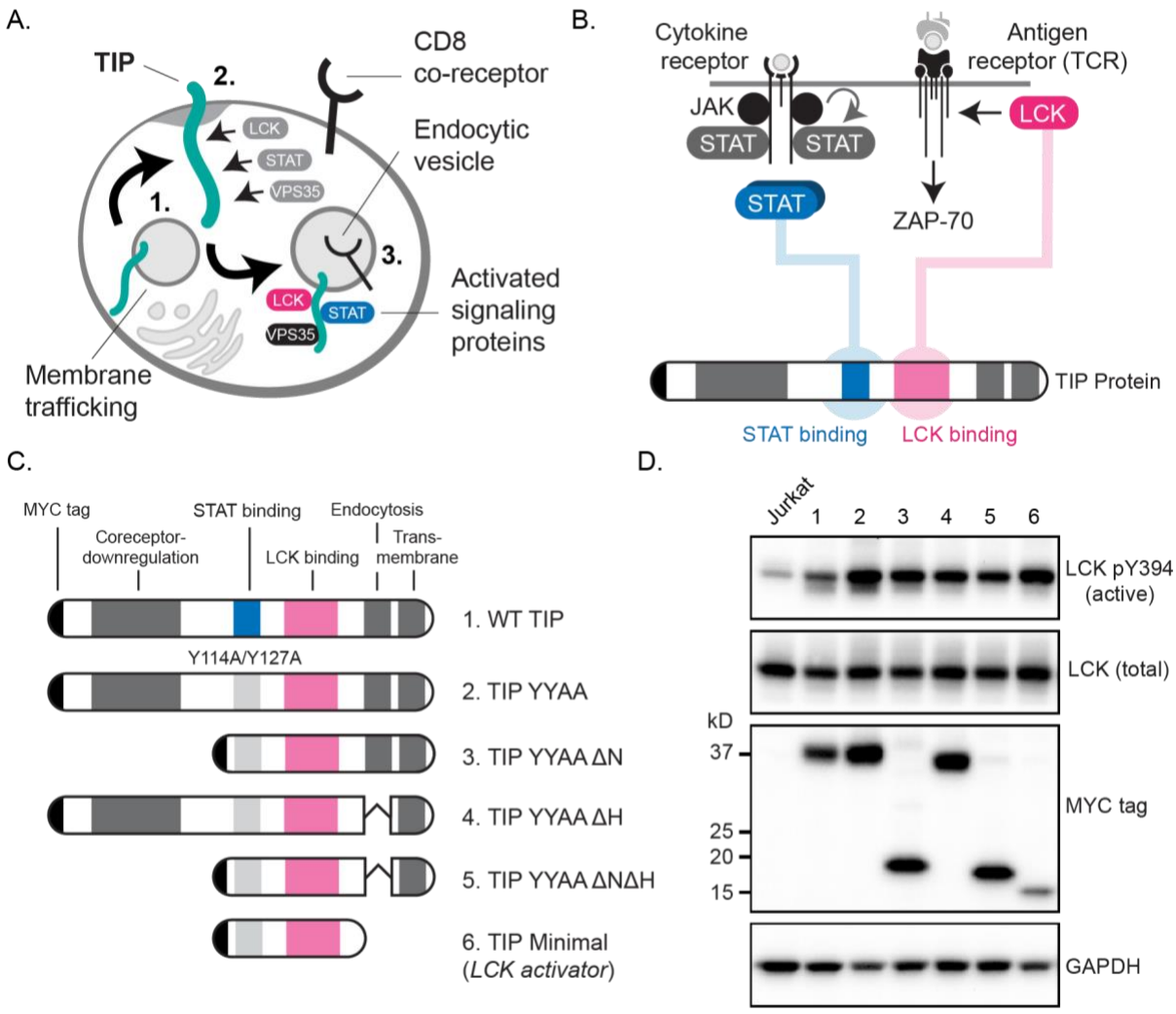

Figure 2-1

Isolation of an LCK kinase binding and activating peptide.

(A) Full-length tyrosine kinase interacting protein (TIP) co-opts cellular pathways in T cells. (B) TIP binds to and activates LCK and STAT proteins in T cells. (C) Truncated TIP protein variants were generated to isolate a minimal LCK binding region. (D) LCK autophosphorylation (pY394) was assessed in Jurkat T cells by immunoblot to determine extent of LCK activation.

2.4.2 Characterization of a Minimal TIP Variant

The increased LCK kinase activity caused by TIP is attributed to a region that is known to bind to LCK and disrupt its autoinhibited confirmation (Fig. 2.2A) [140, 148]. This is accomplished by two motifs that consist of ~ 7-10 amino acids that bind to the regulatory SH3 domain, known as SH3B, and to the kinase domain, termed CSKH due to its homology with a region of CSK [148]. We determined that mutation of these predicted LCK binding sites within the minimal TIP construct disrupted its ability to bind LCK and increase autophosphorylation (Fig. 2.2B, C).

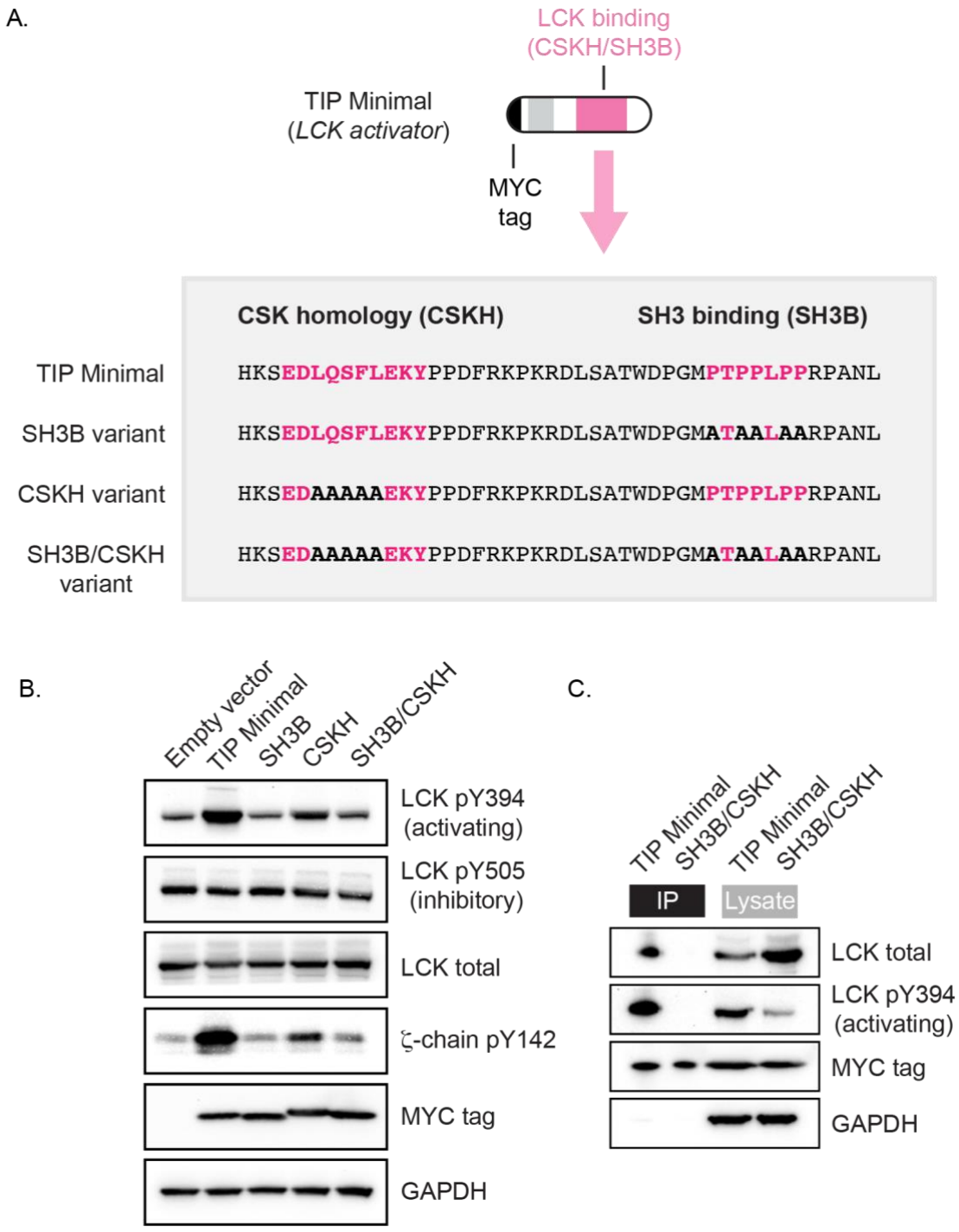

Figure 2-2

Characterization of a minimal TIP variant.

(A) Targeted mutations were introduced to annotated LCK binding sites within the TIP protein. (B) The extent of LCK activation was determined by monitoring LCK

autophosphorylation (pY394) by immunoblot. (C) Association of LCK with TIP was assessed by co-immunoprecipitation of LCK following TIP pulldown by anti-MYC beads. SH3B/CSKH denote regions of TIP annotated to bind LCK kinase that were disrupted. Data are representative of three independent experiments.

2.4.3 TIP Derived Peptides are Delivered into Primary T Cells with High Efficiency

To further assess the ability of TIP derived peptides in primary T cells to exploits LCK kinase activity, I optimized a platform to deliver our TIP derived viral peptides into primary T cells using a retrovirus expression system with stably high transduction efficiency (detailed methods are discussed in the method section). The transduction efficiency of TIP derived viral peptides including TIP Minimal (LCK activator), TIP Minimal derived STAT5 activator (will discuss in chapter 3) and a constitutive active STAT5 mutant (will discuss in chapter 4) including the empty vector control were assessed using flow cytometry. Since all the construct has a Thy1.1 (CD90.1) marker followed by Internal Ribosome Entry Site (IRES), the transduction efficiency was quantified by gating on the percentage of Thy1.1+ cells within the live CD8+ T cells (Fig. 2.3A, B, C). TIP derived peptide demonstrates almost 100% transduction efficiency compared with CD8+ T cells that were activated by anti-CD3/CD28 antibodies without retroviral transduction demonstrated by the quantification (Fig. 2.3B, C).

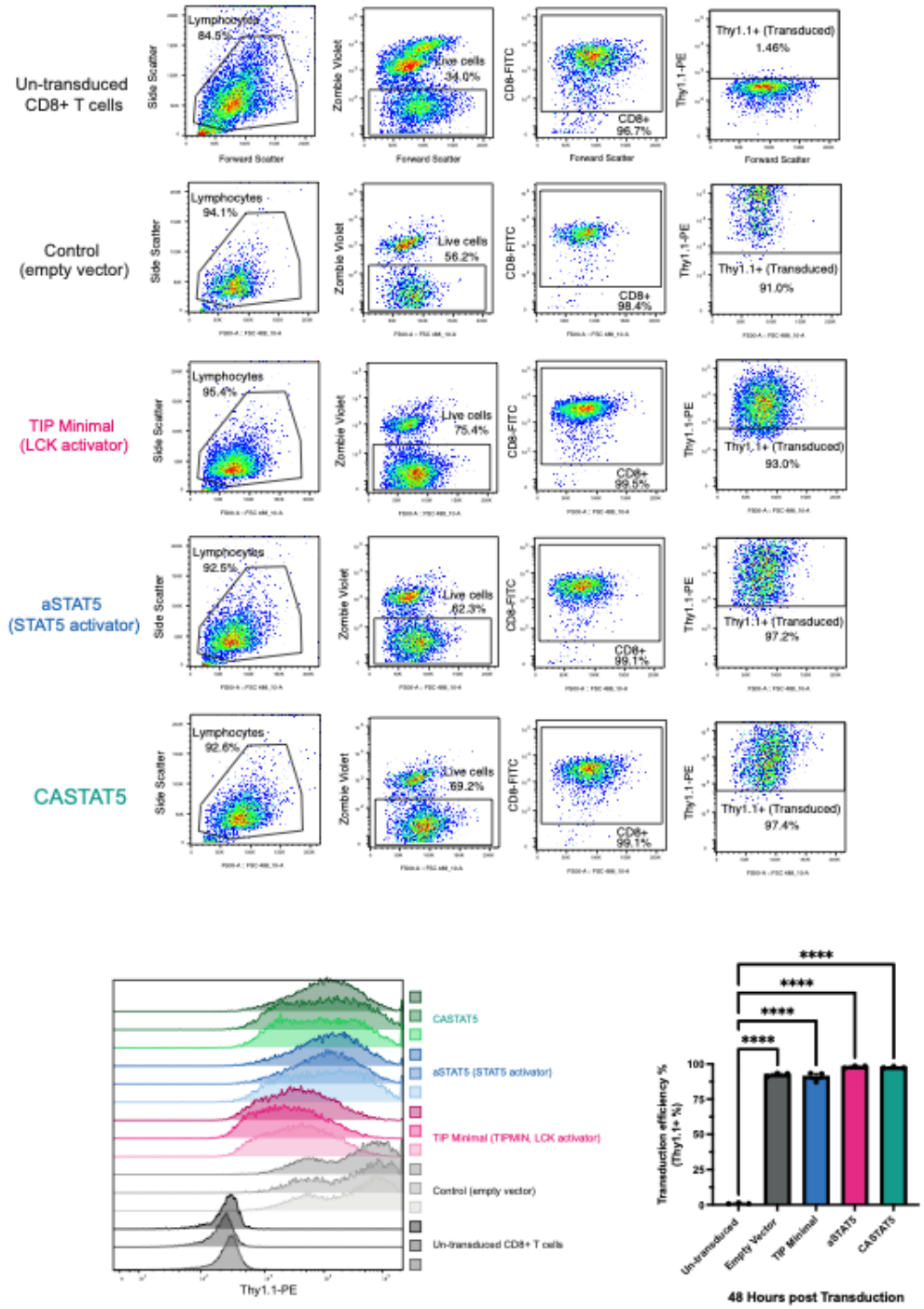

Figure 2-3

Delivery of TIP derived viral peptide into primary T cells using retroviral system.

(A) Representative flow cytometry data. Gating strategy: Lymphocytes (FSC/SSC) > Live (Zombie Violet -) > CD8+ (FITC+) > Thy1.1 (PE+). (B) Histogram from flow cytometry of

three biological replicates. (C) Quantification of transduction efficiency 48 hours post transduction (72 hours post T cells being activated by anti-CD3/CD28) assessed by percentage of Thy1.1+ cells among Live CD8+ T cells. **** $p < 0.0001$(One-Way ANOVA with Sidak's multiple comparisons test).

2.4.4 TIP Minimal Enhances LCK Activation and TCR Signaling in Primary T Cells

We had previously observed that increased basal LCK kinase activity, caused by inhibition of its negative regulator CSK, could augment TCR signaling and prime T cells to become more readily activated by weak TCR agonists [49, 51]. I therefore assessed whether the minimal TIP construct could enhance LCK activation in primary T cells. The minimal TIP construct was incorporated into primary mouse CD8+ T cells by retroviral transduction and these cells were expanded ex vivo. T cells were stimulated by an anti-CD3 agonistic antibody and protein phosphorylation was assessed by immunoblot. The LCK activator was observed to cause increased LCK autophosphorylation (pY394) in comparison to T cells transduced with an empty vector control (Fig. 2.4A). I evaluated phosphorylation of ZAP-70 Y319 because it is an LCK substrate and found that the LCK activator caused this site to be phosphorylated to a greater extent following TCR stimulation (Fig. 2.4B). These findings were consistent with increased basal LCK activity caused by the minimal TIP construct (denoted as LCK activator).

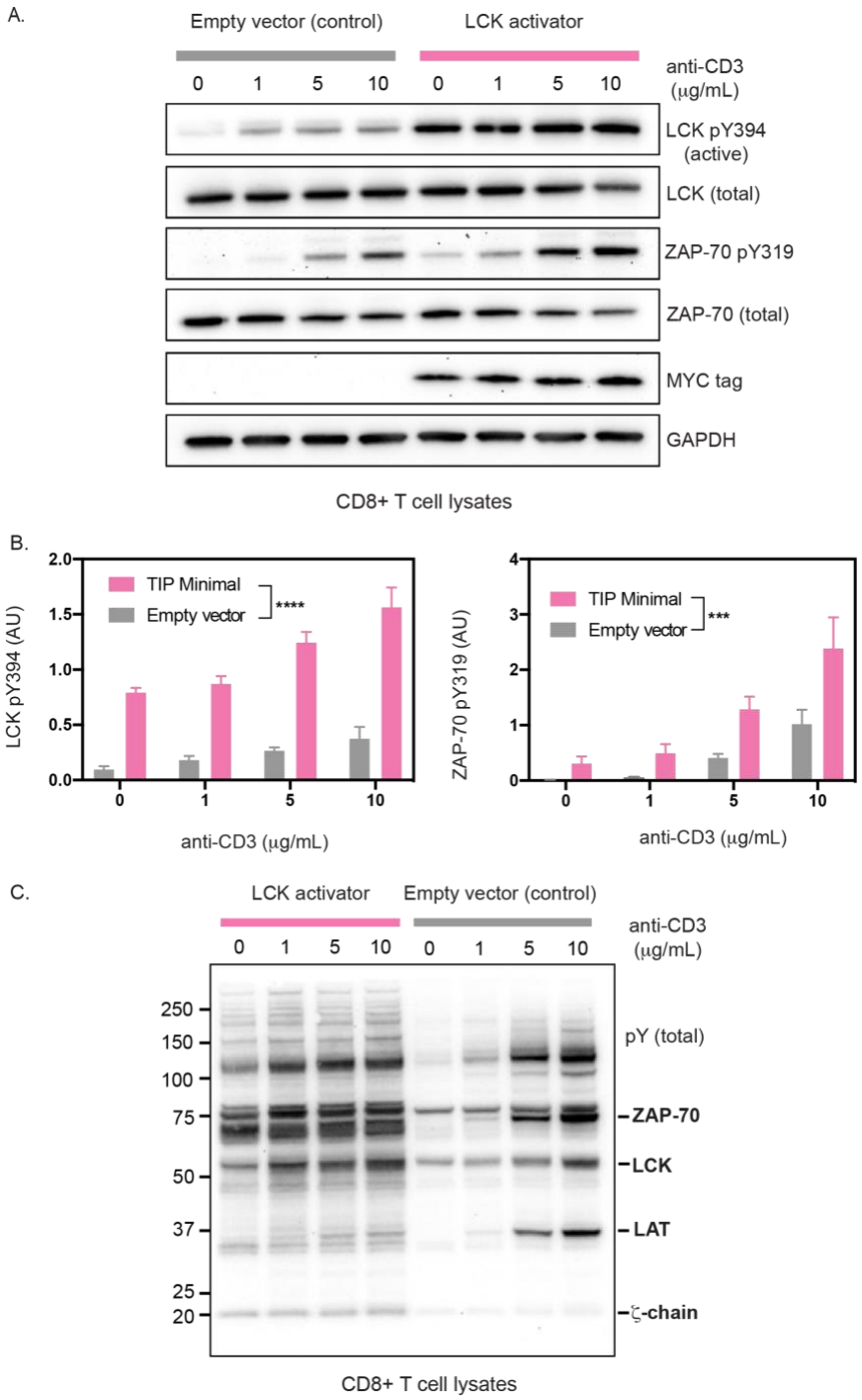

Figure 2-4

TIP Minimal enhances basal LCK activity and TCR signaling.

(A) Primary CD8+ T cells were transduced and treated with a TCR agonist (anti-CD3ε) and extent of LCK and ZAP-70 phosphorylation was assessed by immunoblot. (B) Protein

phosphorylation was quantified and normalized to total protein. Error bars represent the means ± SEM, n=3. *** $p < 0.001$, **** $p < 0.0001$ (Two-Way ANOVA). (C) Primary CD8+ T cells were transduced and treated with a TCR agonist (anti-CD3ε) and total phosphor tyrosine level was assessed using 4G10 antibody by immunoblot. All immunoblots are representative of three independent experiments (n=3).

2.4.5 TIP Derived Peptides Do Not Downregulate TCRβ or CD8α Receptor

The regions of TIP that causes co-receptor downregulation, as well as the transmembrane domain and an adjacent aliphatic a-helical region that is reported to cause endocytosis were reported [145, 147, 149]. To determine that if the TIP Minimal, TIP derived LCK activator causes receptor downregulation or not after removing all the unwanted regions, we stained the cells against T cell receptor and CD8 co-receptor. Unlike the full-length TIP, expression of the LCK activator by primary CD8+ T cells did not result in downregulation of the TCR or CD8 co-receptor (Fig. 2.5A, B).

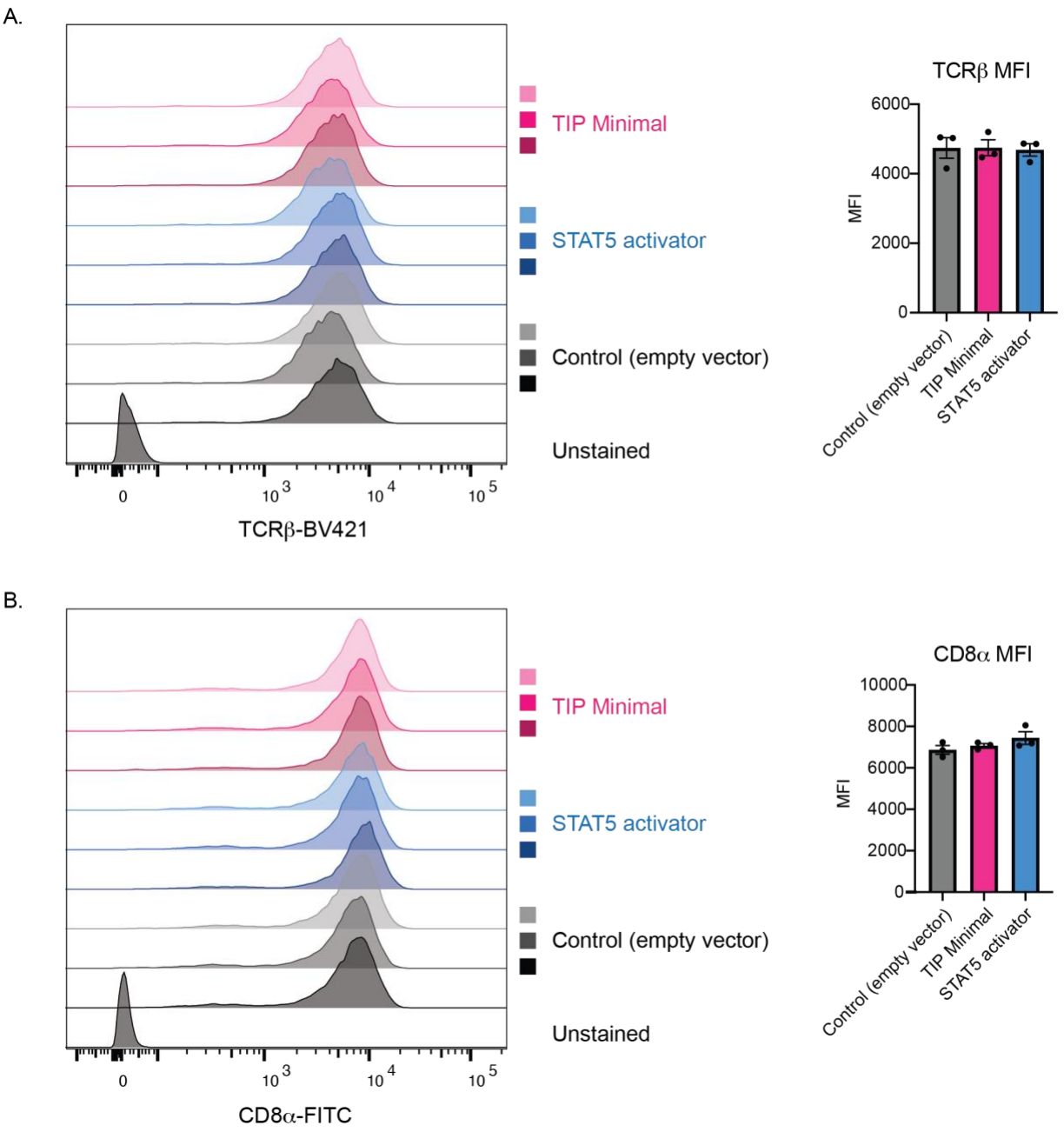

Figure 2-5

TCRβ and CD8α receptor levels are not downregulated by TIP derived peptides

(A) Primary CD8+ T cells were transduced with empty vector control, TIP Minimal and TIP derived STAT5 activator, respectively. Live intact cells were stained with antibodies against CD8α

and assessed by flow cytometry (n=3, means ± SEM). (B) TCRβ was assessed by flow cytometry (n=3, means ± SEM).

2.4.6 LCK Activator Lowers the Threshold for T cell Activation

We next determined whether the TIP-derived LCK activator could enhance T cell activation caused by weak TCR agonists similar to CSK inhibition [49, 51]. Primary CD8+ T cells were isolated from OT-I Nur77-GFP transgenic mice transduced with the LCK activator or an empty vector control and co-cultured with peptide-pulsed T cell depleted splenocytes (Fig. 2.6A) for 6 hours. The OT-I TCR recognizes a peptide derived from ovalbumin (OVA) and the Nur77-GFP reporter provides a readout of OT-I TCR-induced signaling which was used to quantify the extent of T cell activation [150-152]. To assess whether increased TCR signaling enhanced T cell activation caused by weak agonists, the degree of GFP induction caused by OVA, a strong TCR agonist, was contrasted with the G4 variant peptide, a weak agonist [153]. The LCK activator was observed to increase the number of T cells activated by the weak G4 agonist, whereas a similar increase did not occur in response to the strong OVA agonist (Fig. 2.6B, C, D, E, F). The LCK activator caused a dose-dependent increase in T cell activation in response to the G4 peptide, with the EC50 reduced by approximately 10-fold (Fig. 2.6D).

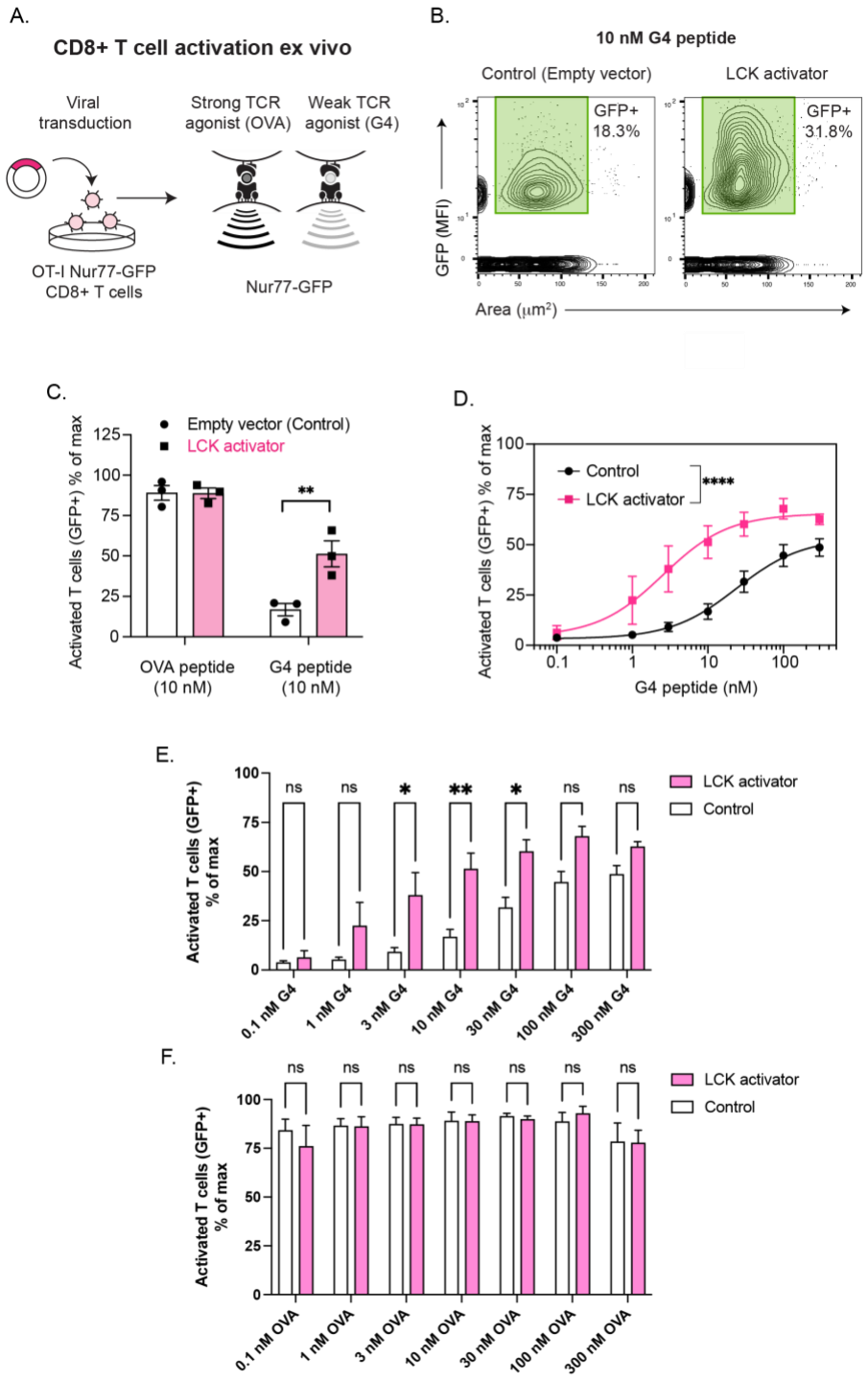

Figure 2-6

LCK activator lowers the threshold for T cell activation.

(A) Primary CD8+ T cells were isolated from OT-I TCR Nur77-GFP reporter transgenic mice and transduced to incorporate the LCK activator (TIP Minimal). (B-F) T cells were co-cultured with

splenocytes that were pulsed with Ovalbumin$_{257-264}$ peptide (OVA), a strong TCR agonist, or a variant peptide that is a weak TCR agonist (G4). (B) Representative Celigo Imaging Cytometer image showing comparison of T cell activation caused by G4 peptide at 10 nM by LCK activator or the control (Empty Vector). (C) Comparison of T cell activation caused by OVA and G4 peptides at 10 nM was quantified using the Nur77-GFP reporter (GFP+). Data were normalized to the maximal value. (n=3, means ± SEM) ** $p < 0.01$ (one-tailed *t* test). (D) G4 peptide dose-response (0.1-300 nM). Data were normalized to the maximal value. (n=3, means ± SEM) **** $p < 0.0001$ (two-way ANOVA). (E) Quantification of T cell activation caused by various doses of G4 peptides using the Nur77-GFP reporter (GFP+). (F) Quantification of T cell activation caused by various doses of OVA peptides using the Nur77-GFP reporter (GFP+).

2.4.7 Increased LCK Activity Sensitizes T cells to Weak Agonist to Produce Cytokines

I also evaluated cytokine production in response to the weak G4 TCR agonist. OT-I T cells purified from C57BL/6 mice (CD45.2+) were co-cultured with peptide-pulsed splenocytes isolated from C57BL/6 BoyJ mice (CD45.1+) for 16 hours in the absence of IL-2 and then treated with Brefeldin A (BFA) prior to fixation and analysis by flow cytometry (Fig. 2.7A). Comparable levels of intracellular IFNγ were found in T cells transduced with either empty vector control or the LCK activator when stimulated with a strong agonist (OVA) peptide but not the control peptide (VSV) (Fig. 2.7B, C). Consistent with the Nur77-GFP reporter system, the LCK activator increased intracellular IFNγ in response to G4 (Fig. 2.7D).

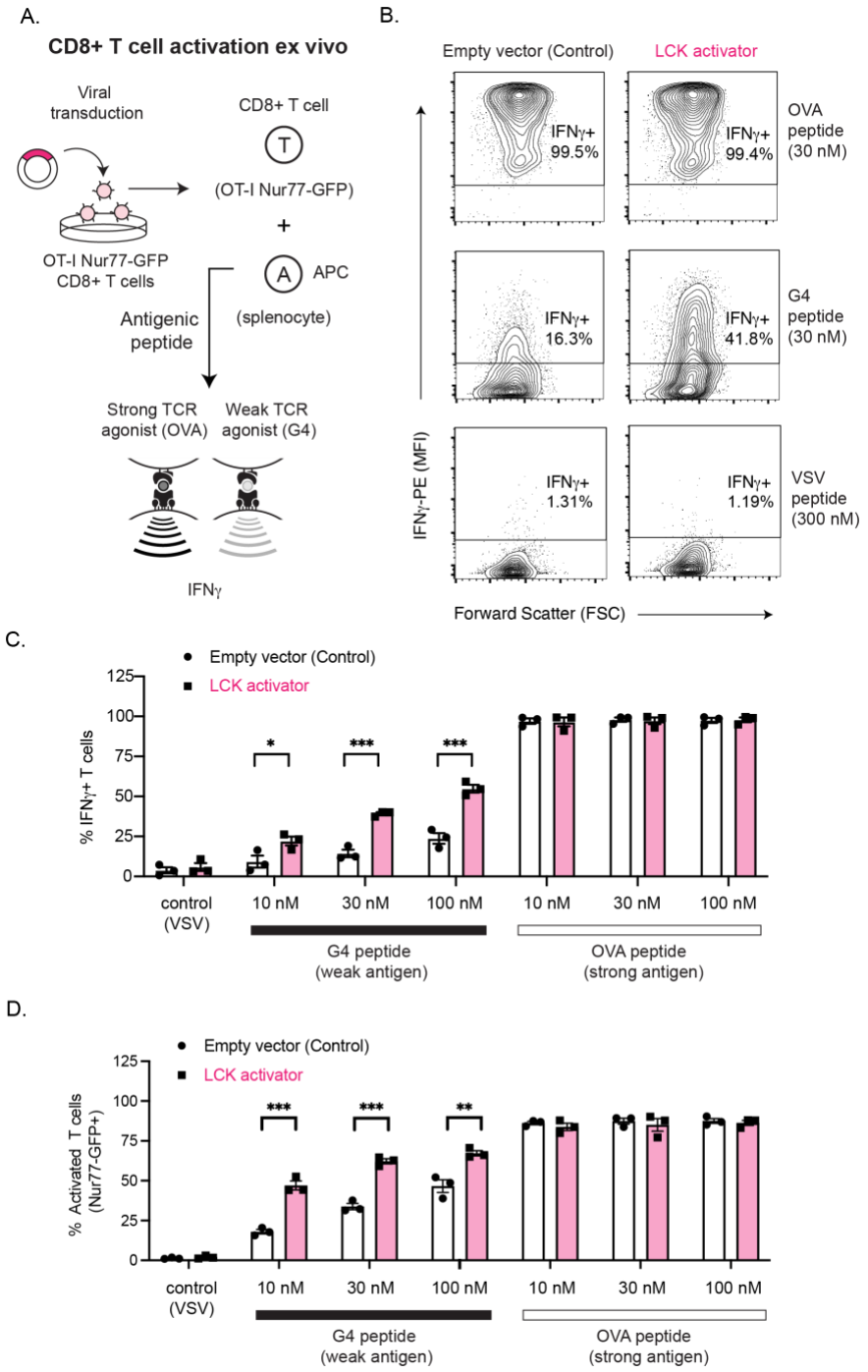

Figure 2-7

Increased LCK activity sensitizes T cells to weak agonist to produce cytokines

(A) Transduced OT-I TCR Nur77-GFP T cells (CD45.2+) were re-stimulated with antigen pulsed splenocytes (CD45.1+) to assess activation and IFNγ levels for 16 hour in the absence

of IL-2. (B) Representative flow cytometer data depicting intracellular IFNγ levels following re-stimulation by OVA (30 nM), G4 (30 nM) or VSV (300 nM) peptides. (C) Quantification of IFNγ T cells by flowcytometry. VSV was included as a negative control (300 nM). Data are representative of three independent experiments (n=3, means ± SEM), * $p < 0.05$, *** $p < 0.001$ (one-tailed *t* test). (D) Quantification of T cell activation caused by various doses of G4 and OVA peptide and VSV as a control using Nur77-GFP reporter (GFP+) by flow cytometry. (n=3, means ± SEM), ** $p < 0.01$, *** $p < 0.001$ (one-tailed *t* test).

2.4.8 LCK Activator May Not Be Efficient to Enhance Anti-Tumor Immunity

Next, we want to evaluate if enhanced antigen recognition by LCK activator could improve T cell mediated anti-tumor immunity. We started from a hot tumor, MC38 colon adenocarcinoma (Fig. 2.8A) to first assess the ex vivo cell-mediated cytotoxicity. I transduced primary OT-I T cells with LCK activator and co-cultured with MC38 cancer cells that are pulsed with peptide antigens for 16 hours in the presence of IL-2. Cell-mediated cytotoxicity was assessed by staining the dead cells using propidium iodide and assessed under Celigo cell cytometer. LCK activator transduced CD8+ T cells could barely enhance the cytotoxic killing when stimulated by weak peptide antigen (G4) pulsed MC38 (Fig. 2.8B, C). We suspect the nature of MC38 cancer cells as an adherent cell line might not provide the context for thorough cell to cell interactions in the ex vivo cell culture setting. We then used EL4 lymphoma cells which are circular by morphology to provide a more suitable context to study antigen recognition. Compared with VSV control, LCK activator marginally increase T cell mediated cytotoxic killing when stimulated by G4 peptide antigen pulsed EL4 cancer cells (Fig. 2.8 B). We wonder if an in vivo tumor setting would be more physiologically relevant to study

enhanced tumor killing in the context of antigen recognition. We transferred the LCK activator transduced OT-I T cells (expanded in IL-2) to EL4-OVA tumor bearing mice and monitored the tumor outgrowth overtime (Fig. 2.8D). LCK activator transduced tumor specific CD8+ T cells didn't demonstrate improvement in controlling tumor outgrowth compared with empty vector control transduced tumor specific CD8+ T cells (Fig. 2.8E, F).

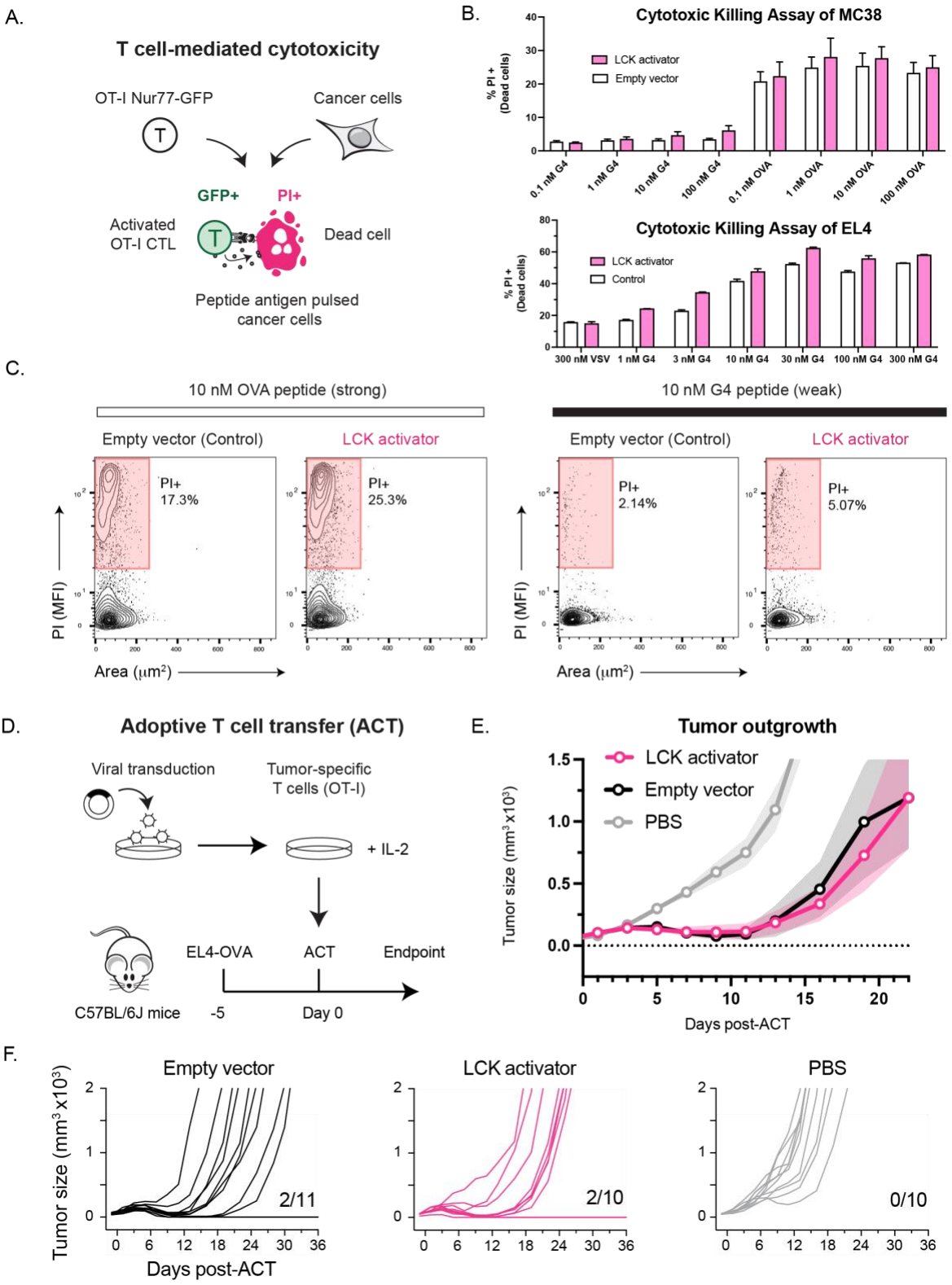

Figure 2-8

LCK activator may not be efficient to enhance anti-tumor immunity.

(A) The ex vivo T cell-mediated cytotoxicity of an LCK activator was assessed by co-culture of OT-I T cells with peptide antigen pulsed MC38 adenocarcinoma or EL4 lymphoma cancer cells for 16 hours in the presence of IL-2. (B) Quantification of T cell-mediated cytotoxicity at Effector : Target (E:T) ratio of 1:1. Cytotoxic T cell lymphocyte assay with MC38 cancer cells (n=3). Cytotoxic T cell lymphocyte assay with EL4 cancer cells (3 technical replicates). (C) A representative Celigo Imaging Cytometer data depicting dead cells (propidium iodide positive, PI+) cells when LCK activator transduced OT-I T cells were co-cultured with OVA peptide (10 nM) or G4 peptide (10 nM) pulsed MC38 cancer cells. (D) OT-I T cells were transduced and adoptively transferred into EL4-OVA tumor bearing mice. (E) Tumor outgrowth was monitored by measurement of tumor size until a humane endpoint was reached. Shaded areas depict means ± SEM (n=10 to 11). (F) Tumor outgrowth of individual mice grouped by treatment. The number of regressed tumors is denoted.

2.5 Discussion

Recent studies have indicated LCK is a promiscuous basally activated kinase in resting Jurkat T cells [49-51]. Increasing the abundance of active LCK can alter affinity discrimination and potentiate T cell activation in response to low affinity antigens. The previous work done by has shown that using CSK inhibitor that increases basal LCK kinase activity lowers the threshold for T cell activation [154]. However, CSK is a master regulator of many SRC family kinases which poses that by directly activating LCK kinase could be a more favorable approach to sensitize T cells in response to weak antigen stimulation. By harnessing the features of wild type viral TIP proteins, we isolated a minimal region to recruit LCK kinase activity to its canonical substrates in early TCR signaling and generated a LCK activator that

has the potential activate a broad range of substrate. We characterized this minimal TIP peptide by removing all the unwanted regions and confirmed its ability to bind to and activate LCK kinase by mutating the sequence that is reported to determine the binding and activation of LCK kinase by wild type TIP protein. To test our hypothesis that whether we could utilize this minimal peptide to activate LCK and sensitizes primary T cells, I delivered this TIP minimal peptide into primary T cells through retroviral transduction and demonstrated its ability to increase basal LCK kinase activity as well as agonist induced TCR signaling. This TIP minimal peptide that directly activates LCK sensitizes T cells against weak antigen stimulation by lowering the activation threshold and increased intracellular cytokine production. However, in EL4 or MC38 tumor models, LCK activator didn't demonstrate a significantly elevated cell-mediated cytotoxicity of CD8+ T cells. It would be more informative to test out the ex vivo cytotoxic killing ability with a less immunogenic tumor model that is attributed to poor antigen recognition but not resulted from low MHC expression. The morphology of the tumor model might play a role in the ex vivo co-culture setting. Therefore, generating weak peptide antigen-expressing tumor model with circular morphology (not adherent cell lines) that is poorly immunogenic would be valuable to test the hypothesis that whether increasing LCK kinase activity would enhance the cytotoxic killing of T cells ex vivo. In terms of in vivo tumor killing, we plan to use a weaker antigen expressing tumor like B16-G4 to see whether the LCK activator can demonstrate a better in vivo anti-tumor effect than the empty vector control group due to their enhanced TCR response.

Chapter 3 Recruitment of LCK Kinase to Activate Targeted STAT Proteins

3.1 Abstract

The efficacy of T cell therapies can be limited if cytokine-induced JAK-STAT signaling is dysregulated or insufficient to sustain functionality. Here, we demonstrate that LCK kinase activity can be recruited to non-canonical protein substrates to directly activate targeted STAT proteins in T cells. STAT activation was accomplished by engineering the Herpesvirus saimiri (HVS) tyrosine kinase interacting protein (TIP) to provide a platform for the enforced recruitment of LCK to STAT proteins. We determined that a minimal region of TIP that binds to LCK could be combined with STAT binding sites derived from endogenous cytokine receptors. These constructs activated targeted STAT proteins in a cytokine-independent manner. A STAT5 activator enabled CD8+ T cells to retain their functionality under suppressive culture conditions. These findings translated to reduced tumor outgrowth in vivo due to enhanced T cell persistence and functionality.

3.2 Introduction

The unique membrane proximal region of LCK associates with the CD4 and CD8 co-receptors [133, 134, 155], which facilitate its recruitment to the antigen-bound TCR to promote phosphorylation of the TCR-associated ζ-chain and the recruitment of ZAP-70 kinase [135,

136]. Activated ZAP-70 phosphorylates LAT, which recruits additional signaling effectors, such as PLCγ1 and GRB2/GADS, to activate the calcium, PKC, and MAPK pathways necessary for T cell activation [137]. In comparison to the restricted substrate profile of ZAP-70, the substrate specificity of LCK is promiscuous, consistent with its capacity to phosphorylate a wider array of protein substrates [138]. These properties appear to have been exploited by HVS, which infects T cells and expresses the tyrosine kinase interacting protein (TIP). TIP is known to bind LCK and disrupt its autoinhibited conformation to cause increased basal LCK kinase activity [139, 141, 156]. The viral TIP protein then recruits LCK to phosphorylate STAT proteins that mediate cytokine-induced JAK-STAT signaling [118, 144, 157]. These observations suggest that HVS has evolved to exploit the promiscuous basal kinase activity of LCK by recruiting it to specific protein substrates to cause their activation.

The activation of signaling pathways in T cells as a therapeutic strategy for cancer treatment has been evaluated using receptor agonists that target costimulatory receptors, such as CD28, 4-1BB, OX40, and CD27, as well as cytokine receptors, such as IL-2R, IL-15R, and IL-12R [158-161]. Despite promising preclinical studies, agonistic antibodies that target costimulatory receptors have thus far lacked sufficient efficacy in clinical trials [162]. Although the cytokine IL-2 has been approved for the treatment of metastatic melanoma and renal cancer [163], its use has been limited by its poor pharmacological properties, toxicity, and low response rate [164]. In contrast to receptor agonists, the targeted activation of intracellular signaling mediators remains a largely unexplored approach to interrogate potential immunomodulatory strategies for therapeutic applications. A notable exception includes cyclic dinucleotides (CDNs) and derivatives that activate STING, an intracellular mediator of the cGAS (cyclic GMP-AMP synthase)-STING

pathway [165]. STING agonists, such as DMXAA, have been evaluated in clinical trials [166]. Yet, despite the therapeutic potential of STING agonists, few activators of intracellular signaling pathways have been developed.

The targeted inhibition of intracellular enzymes is often achieved through small molecules that bind an active site, such as the ATP-binding site of kinases [167]. In contrast, a paucity of intracellular activators could be attributable to fundamental challenges in exploiting generalizable regulatory features known to induce the activation of intracellular proteins. We reasoned that the HVS TIP protein exploited such a general feature – induced regulatory site phosphorylation. However, whether this mechanism could be repurposed to facilitate the targeted phosphorylation of proteins in T cells to activate them required exploration. Given the potential utility of intracellular activators, we determined whether a minimal region of the TIP protein that bound to LCK kinase could be isolated independently from the full-length viral protein. Whether this minimal peptide could recruit LCK to activate cellular targets was evaluated by incorporating STAT binding sites derived from endogenous cytokine receptors to target specific STAT proteins. An IL-2 receptor β subunit (IL-2Rβ) STAT binding site was found to activate STAT5 in ex vivo cultured primary T cells, which translated to reduced tumor outgrowth and enhanced T cell persistence in vivo. Our findings indicate that LCK recruitment to a protein activated by phosphorylation could be exploited as a general mechanism for the development of molecules that activate or otherwise rewire T cell signaling pathways.

3.3 Materials

3.3.1 Animal

Mice were housed in a specific-pathogen-free facility at University of Michigan (U-M) NS were treated according to protocols that were approved by U-M animal care ethics and veterinary committees and are in accordance with NIH guidelines. All mice were bred and maintained on the C57BL/6 genetic background (6 to 12 weeks). The following mice strains were used for this study: C57BL/6 mice (The Jackson Laboratory (JAX)); BoyJ (CD45.1) mice (JAX); OT-I mice (JAX) (49). OT-I Nur77-GFP mice were generated by crossing OT-I and Nur77-GFP transgenic mice. Phoenix cells and EL4-OVA (E.G7-OVA) cells were obtained from ATCC. B16-OVA cells were obtained from the Zou lab (U-M) [168].

3.3.2 Cell Lines

The culture of Jurkat T cells, Primary CD8+ T cells, MC38-OVA/MC38 colon adenocarcinoma cancer cells, E.G7-OVA cells are the same as described. In “Cell lines” in Materials and Methods section in the Chapter 2. B16-OVA cells were maintained in 1% HEPES supplemented DMEM culture medium (10% FBS, 2 mM glutamine).

3.3.3 Plasmids

Site directed mutagenesis (Quikchange) was performed to generate STAT binding sites variants. TIP variants were transferred into the pDONR221 plasmid for Gateway cloning (ThermoFisher). MSCV_IRES_mCherry (#52114) and MSCV_IRES_Thy1.1 (#17442) were obtained from Addgene and modified to generate a destination vector by insertion of a

Gateway cassette. TIP variants were transferred into MSCV destination vectors using LR clonase. The pCL_Eco plasmid was obtained from Addgene (#12371). pBABE_Stat5a1*6 was purchased from Addgene (#130668) to generate MSCV_Stat5a1*6_IRES_Thy1.1 as the construct for CASTAT5.

3.3.4 Antibodies

Antibodies used in this study are listed in Table 1.

Table 1 Antibody list

	Vendor	**Catalog#**
Anti-Mouse/Anti-Rat & Dilution Factor		
CD28 (37.51) (1:200)	BioLegend	102116
CD3ε (145-2C11) (1:200)	BioLegend	100340
CD45.2 PerCP-Cy5.5 (104) (1:200)	BioLegend	109828
CD45.1 FITC (A20) (1:200)	BioLegend	110706
CD90.1 (Thy-1.1) Alexa 647 (OX-7) (1:200)	BioLegend	202508
IFNγ PE (XMG1.2) (1:200)	BioLegend	505808
CD8α PE (53-6.7) (1:200)	BioLegend	100708
CD8α FITC (53-6.7) (1:200)	BioLegend	100706
CD8α BV785 (53-6.7) (1:200)	BioLegend	100750
CD45 Pacific blue (30-F11) (1:200)	BioLegend	103126
PD-1 BV605 (29F.1A12) (1:200)	BioLegend	135220
Granzyme B Alexa Fluor 647 (GB11) (1:200)	BioLegend	515406
AffiniPure Goat Anti-Armenian Hamster IgG (H+L)	Jackson ImmunoResearch	127-005-160
Recombinant murine IL-2	BioLegend	714604
TruStain FcX PLUS (Fc block, anti-mouse CD16/32) (S17011E) (1:1000)	BioLegend	156604
BD CompBeads Anti-Mouse Ig, k	BD Biosciences	51-90-9001229
BD CompBeads Anti-Rat and Anti-Hamster Ig, k	BD Biosciences	51-90-9000949
BD CompBeads Negative Control	BD Biosciences	51-90-9001291

	Vendor	Catalog#
Brilliant Violet 605 Rat IgG2, k isotype Ctrl (RTK2758) (1:200)	BioLegend	400540
Alexa Fluor647 Mouse IgG1, k isotype Ctrl (MOPC-21) (1:200)	BioLegend	400155
Immunoblot		
LCK (D88)	Cell Signaling Technology	2984
SFK pY416 (LCK pY394)	Cell Signaling Technology	2101
LCK pY505	BD Biosciences	612391
Zap70 (D1C10E)	Cell Signaling Technology	3165
Zap70 pY319	Cell Signaling Technology	2701
CD247 pY142 (Zeta-chain pY142)	BD Biosciences	558402
GAPDH (D16H11)	Cell Signaling Technology	5174
Myc-Tag (9B11)	Cell Signaling Technology	2276
STAT1 pY701	Cell Signaling Technology	7649
STAT1 (D1K9Y)	Cell Signaling Technology	14994
STAT2 pY690	Cell Signaling Technology	4441
STAT2 (D9J7L)	Cell Signaling Technology	72604
STAT3 pY705	Cell Signaling Technology	9145
STAT3 (D1B2J)	Cell Signaling Technology	30835
STAT4 pY693 (D2E4)	Cell Signaling Technology	4134
STAT4 (C46B10)	Cell Signaling Technology	2653
STAT5 pY694 (D47E7)	Cell Signaling Technology	4322
STAT5 (D206Y)	Cell Signaling Technology	94205
STAT6 pY641	Cell Signaling Technology	9361
STAT6 (D3H4)	Cell Signaling Technology	5397
Cell Separation		
CD11b Biotin (M1/70)	BioLegend	101204
CD11c Biotin (N418)	BioLegend	117304
CD19 Biotin (6D5)	BioLegend	115504
CD24 Biotin (M1/69)	BioLegend	101804
CD45R/B220 Biotin (RA3-6B2)	BioLegend	103204
CD49b Biotin (DX5)	BioLegend	108904
TER119/Erythroid cells Biotin (TER-119)	BioLegend	116204
CD4 Biotin (GK1.5)	BioLegend	100404
CD8α Biotin (53-6.7)	BioLegend	100704
CD90.1 Biotin (Thy-1.1, clone: OX-7)	BioLegend	202510
MojoSort Streptavadin Nanobeads	BioLegend	480016

3.4 Methods

3.4.1 Isolation and Purification of Primary CD8+ T Cells

Mouse primary CD8+ T cells were isolated and enriched using beads-based negative selection the same ways described in “Isolation and purification of primary CD8+ T cells” in Methods section of the Chapter 2.

3.4.2 Preparation of T Cell Depleted Splenocytes as Antigen Presenting Cells

Splenocytes isolated from BoyJ mice (CD45.1+) without T cell depletion were prepared as antigen presenting cells for the co-culture assay to assess intracellular IFNγ production. Red blood cells were lysed using ammonium-chloride-potassium (ACK) lysis.

3.4.3 Retroviral Transduction of Primary CD8+ T Cells

TIP derived STAT5 activators were delivered into CD8+ T cells using retroviral transduction system. Retrovirus preparation and transduction of primary CD8+ T cells are described in “Retroviral transduction of primary CD8+ T cells” in Methods section of the Chapter 2.

3.4.4 Immunoblot Analysis

Antibodies used in the western blot are listed in Table 1. Phospho-immunoblot of both Jurkat and primary T cells was conducted the same way described in “Immunoblot analysis and Immunoprecipitation” in Methods section of the Chapter 2.

3.4.5 Cytotoxic T Lymphocyte (CTL) Assay by Imaging Cytometry

Cytotoxic T lymphocyte assay was assessed using the same approach as described in "Cytotoxic T lymphocyte (CTL) assay by imaging cytometry" in Methods section of the Chapter 2. The only difference is during the 16 hours of co-culture, the co-culture system were supplemented with or without IL-2 treatment for comparison.

3.4.6 Intracellular Cytokine Release Assay and Flow Cytometric Analysis

Intracellular cytokine production assay was assessed using the same approach as described in "Intracellular cytokine release assay and flow cytometric analysis" in Methods section of the Chapter 2. The only difference is during the 16 hours of co-culture, the co-culture system were supplemented with or without IL-2 treatment for comparison.

3.4.7 Mouse Tumor Model

EL4-OVA (E.G7-OVA) cells (10^6) and B16-OVA cells ($2x10^5$) were subcutaneously implanted into age-matched female C57BL/6J mice (6-8 weeks). On day 5 post E.G7-OVA tumor inoculation, retrovirally transduced OT-I T cells ($3x10^6$) were adoptively transferred into tumor bearing mice. For B16-OVA tumors, transduced OT-I T cells ($4x10^6$) were adoptively transferred on Day 7 post-tumor inoculation. For cohort studies, mice were grouped to ensure that the averaged tumor size was similar for each treatment group prior to ACT. For E.G7-OVA tumors, the averaged tumor size for each group on Day -1 was ~ 49 mm^3. Mice with tumors that were smaller than 20 mm^3 and larger than 75 mm^3 were removed. For B16-OVA tumors, the averaged tumor size for

each treatment group on Day -1 was ~ 17 mm3. Mice with no tumors grew out on Day -1 were excluded from the analysis.

3.4.8 Analysis of Tumor Infiltrating T Cells and Draining Lymph Nodes

Transduced T cells isolated from OT-I mice (CD45.2+) were cultured in complete RPMI culture medium supplemented with IL-2 (10 ng/mL) and expanded for 5 days. The T cells (4x106) were then adoptively transferred into B16-OVA tumor bearing recipient mice (CD45.1+) by intravenous tail vein injection. Day 4 or 11 post ACT, peripheral blood was collected from tumor bearing mice and ACK lysis performed prior to staining. Day 5 or 12 post ACT, mice were euthanized to collect tumors and tumor-draining lymph nodes (TDLN). Tumors were dissociated on ice by mechanical disaggregation and passed through a cell strainer (40 μm) to a prepare a cell suspension. Samples were stained with L/D Zombie Violet dye followed by antibodies against cell surface markers CD45.1, CD45.2, CD8α, PD-1 and Fc block in FACS buffer for 40 min on ice. Cells were then fixed with 2% PFA for 20 min and permeabilized using perm/wash buffer for 20 min at room temperature. Cells were stained with anti-Granzyme B AF647 and washed prior to flow cytometry analysis.

3.4.9 Statistical Analysis

All statistical analyses were performed using GraphPad Prism software (V9.2.0).

3.5 Results

3.5.1 Specific STAT5 Activation is Achieved by Incorporating STAT Binding Site Derived from the IL-2Rβ

Our findings indicated that the capacity of TIP to bind LCK could be isolated from its other functions. We next sought to determine whether the minimal LCK activator could recruit LCK activity to STAT proteins, and thereby activate them in T cells. We therefore restored the STAT binding sites within the minimal TIP variant. Because the STAT binding sites within TIP have been shown to broadly activate multiple STAT proteins [118, 144], we predicted that more specific STAT activation profiles could be achieved by incorporating STAT binding sites derived from endogenous cytokine receptors. Chimeric constructs were generated that replaced the TIP STAT binding sites with STAT binding regions derived from the IFNγ and IL-2Rβ receptors (Fig. 3.1A). Jurkat T cells were transiently transfected, and STAT phosphorylation was assessed by immunoblot (Fig. 3.1B). We determined that the minimal peptide could robustly activate STAT proteins and that a STAT binding site comprised of 4 amino acids derived from the IFNγ or IL-2Rβ receptor was sufficient to recapitulate the phosphorylation of STAT1 and STAT5 respectively, which are known hallmarks of IFNγ or IL-2 receptor signaling [169]. These findings indicated that LCK activity could be recruited to targeted STAT proteins to generate selective intracellular cytokine-independent STAT activators (Fig. 3.1A). We therefore profiled the STAT proteins activated by these constructs (Fig. 3.1B). Phosphorylation of STAT proteins results in their activation and a heatmap was generated to visualize the profile of the STATs activated by each construct (Fig. 3.1C). We also tested whether STAT binding sites were modular by combining the IFNγ and IL-2Rβ receptor binding sites within a single construct. Excitingly, we observed that the STAT binding

sites derived from the IFNγR and IL-2Rβ predominately activated STAT1 and STAT5, respectively. When these sites were placed in series, they were found to be additive and could activate both STAT1 and STAT5 simultaneously.

STAT5 was of particular interest because of its critical role in CD8+ T cell homeostasis and expansion [170-173]. We therefore evaluated whether construct 7 derived from IL-2Rβ could activate endogenous STAT5 in primary CD8+ T cells. This construct was used to transduce CD8+ T cells isolated from mice which were expanded ex vivo for 3 days in the absence of IL-2. We observed that the construct derived from the IL-2Rβ receptor caused a comparable degree of STAT5 phosphorylation to cells expanded in the presence of IL-2 (Fig. 3.1D).

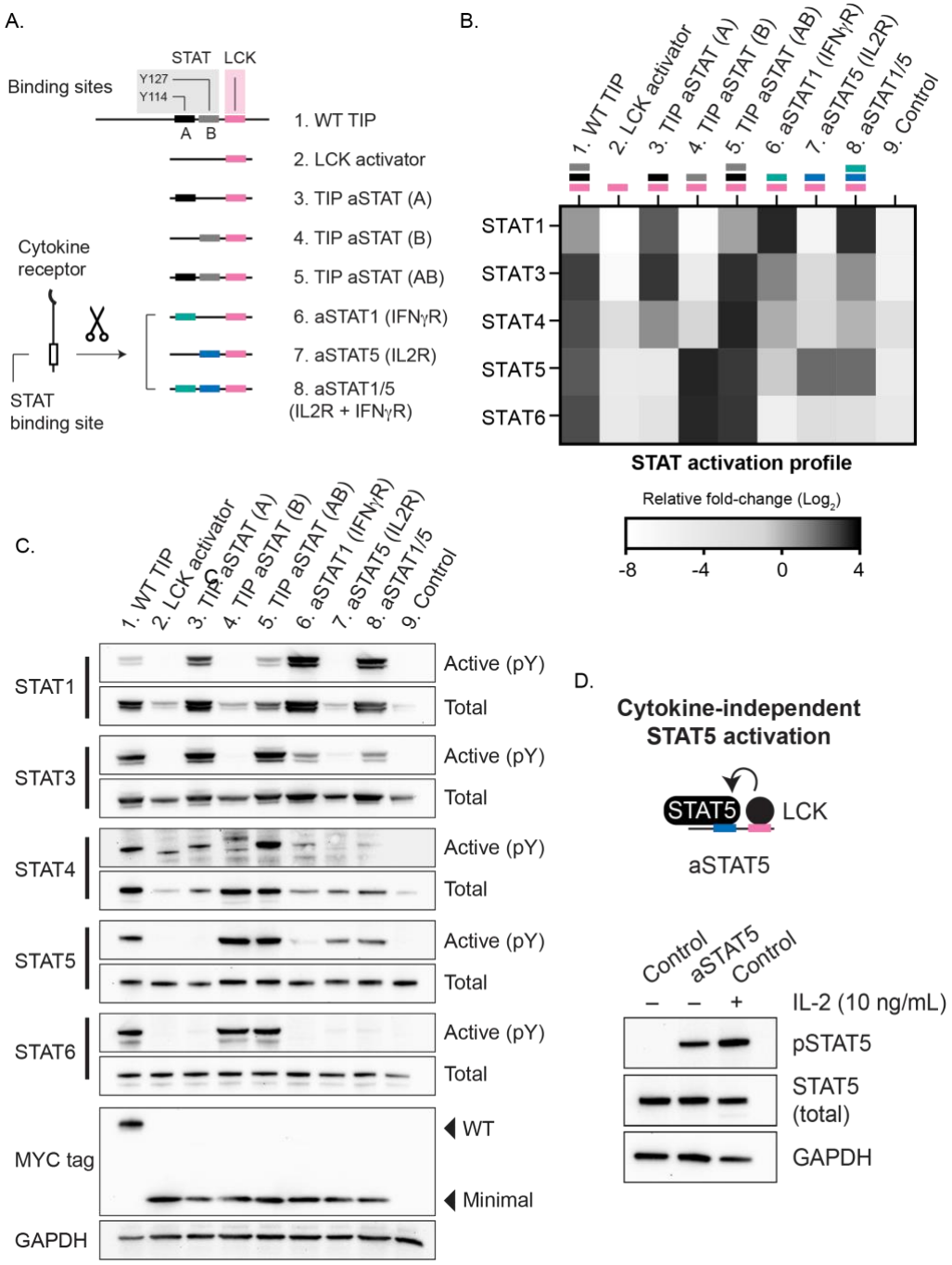

Figure 3-1

Cytokine-independent STAT activation

(A) Restoration of STAT binding sites within the minimal TIP peptide. Chimeric STAT binding sites derived from cytokine receptors were used to evaluate potential cytokine-

independent STAT activators. (B) TIP-derived STAT activators were assessed for their capacity to induce STAT phosphorylation in Jurkat T cells by immunoblot analysis. (C) A heatmap depicting the mean relative extent of STAT phosphorylation (n=3). (D) CD8+ T cells were transduced with empty vector (control) or a STAT5 activator (construct #7, denoted aSTAT5). aSTAT5 cells were cultured without IL-2. Control cells were cultured in the presence of IL-2 (10 ng/mL), and a washout was performed to remove IL-2 16 hours prior to lysis. STAT5 phosphorylation was assessed by immunoblot. Immunoblots are representative of at least three independent experiments (n≥3).

3.5.2 STAT5 Activator Promoted CD8+ T Cell Proliferation but doesn't Cause CD8+ T Cell Immortality

T cells have been shown to undergo leukemic transformation due to aberrant activation of STAT5 [174, 175]. However, another group using a constitutive active mutant form of STAT5 (CASTAT5) showed that CASTAT5-transduced CD4+ T cells did not demonstrate leukemic feature in vivo [114]. Ding's study along with another group using the same CASTAT5 indicated that CASTAT5 transduced CD8+ T cells were not immortal ex vivo [114, 176]. Therefore, we need to assess whether our STAT5 activator modified CD8+ T cells would become immortal or in other words, leukemic. I purified CD8+ T cells and transduced them with STAT5 activator (aSTAT5), TIP Minimal or LCK activator (TIP Min), or Empty vector on day 1 post T cell activation. I cultured the virus transduced CD8+ T cells in the absence of IL-2, monitored the total cell count and live cell count every day or every 2-3 days using Celigo cell cytometer. TIP Minimal or Empty vector transduced CD8+ T cells proliferated aggressively for 2 days post transduction, which is the first 3 days post T cell activation, and started to die off (Fig. 3.2B, C). aSTAT5

promoted CD8+ T cell proliferation in the absence of IL-2 until day 12 post transduction. aSTAT5 modified CD8+ T cells started to die off and then completed lose cell viability at day 30 post transduction (day 31 post T cell activation) (Fig. 3.2A, C)..

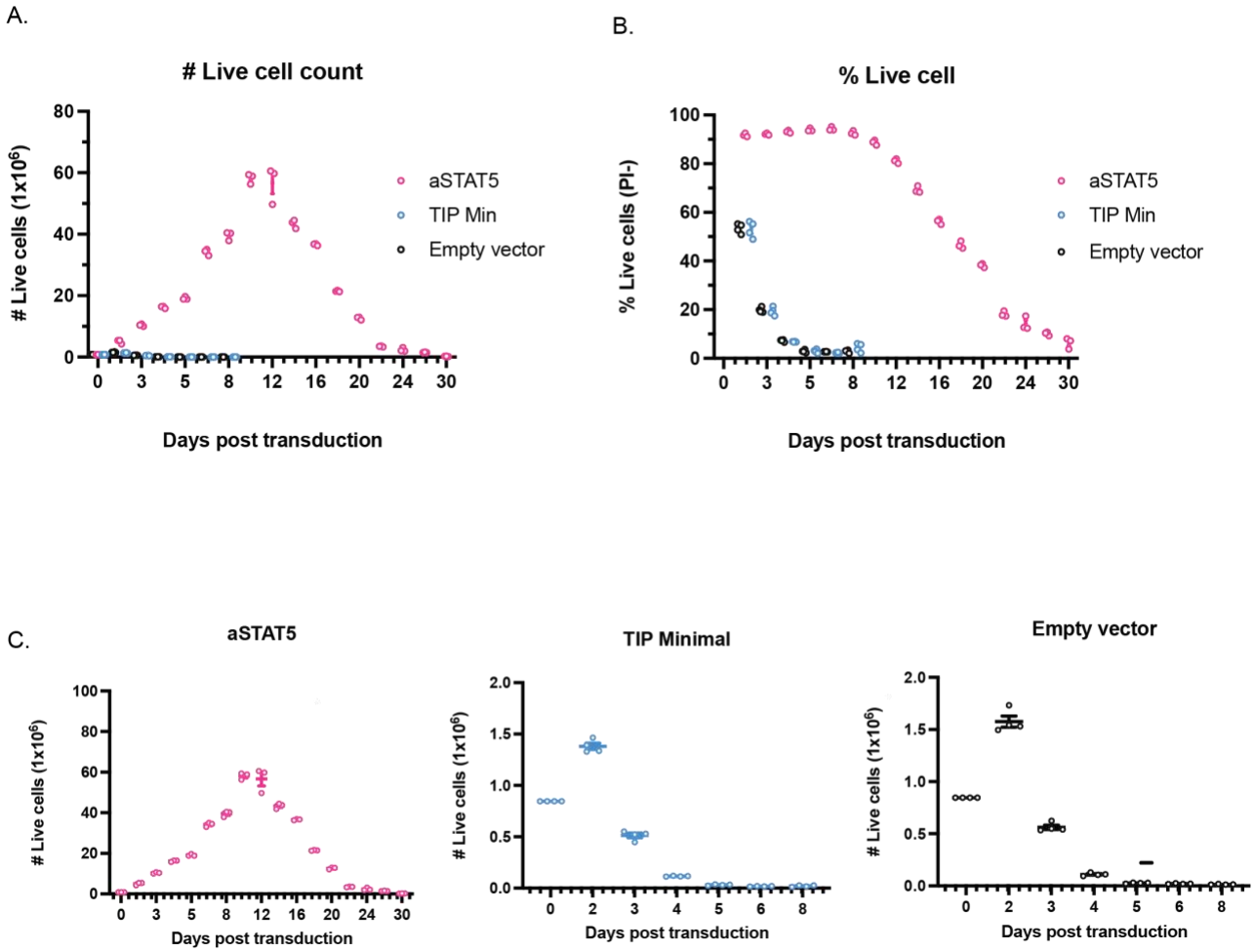

Figure 3-2

STAT5 activator transduced CD8+ T cells doesn't become immortal ex vivo

(A) Total live cell count of aSTAT5, TIP Minimal, Empty Vector transduced CD8+ T cells. (B) Percentage of total live cells of aSTAT5, TIP Minimal, Empty Vector transduced CD8+ T cells. (C) Total live cell count of TIP Minimal, Empty Vector transduced CD8+ T cells, respectively. TIP Minimal and Empty Vector transduced CD8+ T cells day off completely day 8 post transduction therefore we stopped collecting the data for those two groups since then.

3.5.3 Evaluation of Chimeric STAT Bindings Sites within a Minimal TIP Construct

we predicted that more specific STAT activation profiles could be achieved by incorporating STAT binding sites derived from endogenous cytokine receptors. Chimeric constructs were generated that replaced the TIP STAT binding sites with STAT binding regions derived from the IFNγ and IL-2β receptors (Fig. 3.3A). Jurkat T cells were transiently transfected, and STAT phosphorylation was assessed by immunoblot (Fig. 3.3B). We determined that the minimal peptide could robustly activate STAT proteins and that a STAT binding site comprised of 4 amino acids derived from the IFNγ or IL-2Rβ receptor was sufficient to recapitulate the phosphorylation of STAT1 and STAT5 respectively, which are known hallmarks of IFNγ or IL-2 receptor signaling (52). We also profiled the STAT proteins activated by these constructs (Fig.3.1B, 3.3C). We also observed that total STAT protein levels were sensitive to STAT activation (Fig. 3.3C). We evaluated that the minimal TIP construct that binds to LCK and causes the activation of STAT5 through its recruitment to an IL-2Rβ binding site (denoted hereafter as STAT5 activator) (Fig. 3.3A).

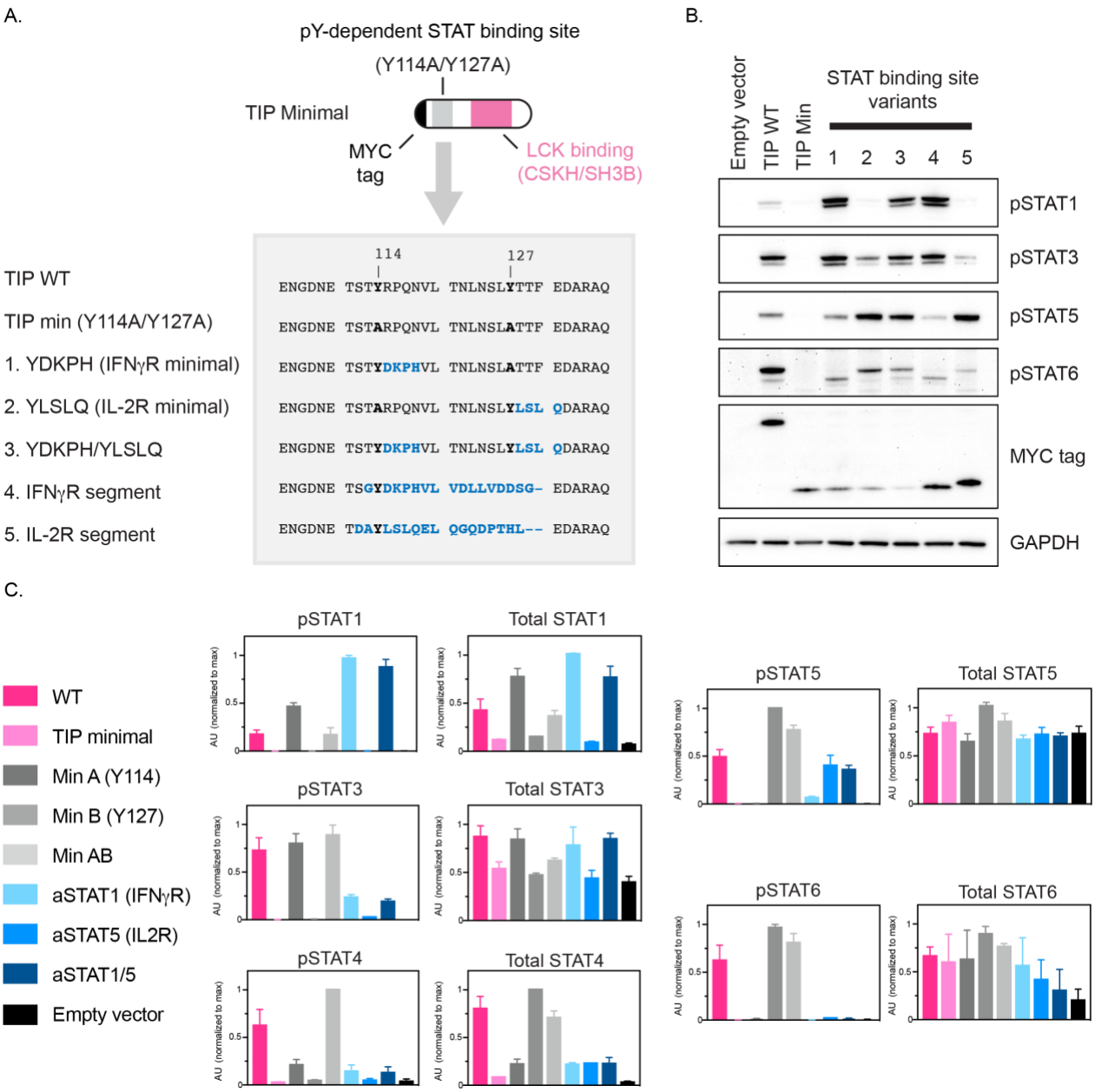

Figure 3-3

Evaluation of chimeric STAT binding sites within a minimal TIP construct

(A) The viral STAT binding sites (Y114 and Y127, denoted site A and B respectively) were restored by site-directed mutagenesis. Chimeric TIP variants were generated by incorporating the STAT1 and STAT5 binding sites from the IFNγ and IL-2 cytokine receptors respectively. Chimeras containing a minimal STAT binding site comprised of 4 amino acids (denoted IFNγR

and IL-2R minimal; constructs 1 and 2, respectively) were compared to segments of the IFNγ and IL-2 receptors that include the STAT binding site (constructs 4 and 5). (B) Constructs were transiently transfected into Jurkat T cells and STAT activation profiles were determined by immunoblot. (C) Quantification of STAT protein phosphorylation and total STAT proteins levels from immunoblot analysis performed in Figure 3.1C (n=3, means ± SEM).

3.5.4 STAT5 Activation Maintains T Cell Functionality in the Absence of Pro-Survival Cytokine

CD8+ T cells require IL-2 to drive their expansion and to differentiate into cytotoxic T lymphocytes (CTL) [108, 177, 178]. We reasoned that because IL-2 activates STAT5, the direct activation of STAT5 could sustain CD8+ T cell survival under suppressive conditions where pro-survival cytokines are depleted. To investigate whether the STAT5 activator can functionally bypass the need for IL-2-induced signaling, we transduced CD8+ T cells with the STAT5 activator and cultured them ex vivo in the absence of IL-2 for 3 days before assessing cell viability by flow cytometry. We observed that the STAT5 activator enabled CD8+ T cells to persist in the absence of IL-2 to a similar degree as control cells cultured in IL-2-containing medium. By contrast, viability was markedly reduced when the control cells were cultured in the absence of IL-2 (Data not shown).

IFNγ is a critical mediator of cellular immunity that is secreted by activated CD8+ T cells. To assess whether the STAT5 activator maintained the functional capacity of CD8+ T cells to produce IFNγ, OT-I Nur77-GFP CD8+ T cells were transduced and co-cultured with peptide-pulsed splenocytes for 16 hours prior to treatment with BFA and fixation (Fig. 3.3A). The

extent of intracellular IFNγ was then determined by flow cytometry. We observed that the STAT5 activator enabled CD8+ T cells to become activated (Nur77-GFP+) and produce IFNγ. However, the proportion of cells with high levels of IFNγ was lower than cells cultured in IL-2 (Fig. 3.3A, B, C, D). Interestingly, the addition of IL-2 to culture medium of cells that expressed the STAT5 activator resulted in levels of IFNγ comparable to the IL-2 treated control (Fig. 3.3B, C, D).

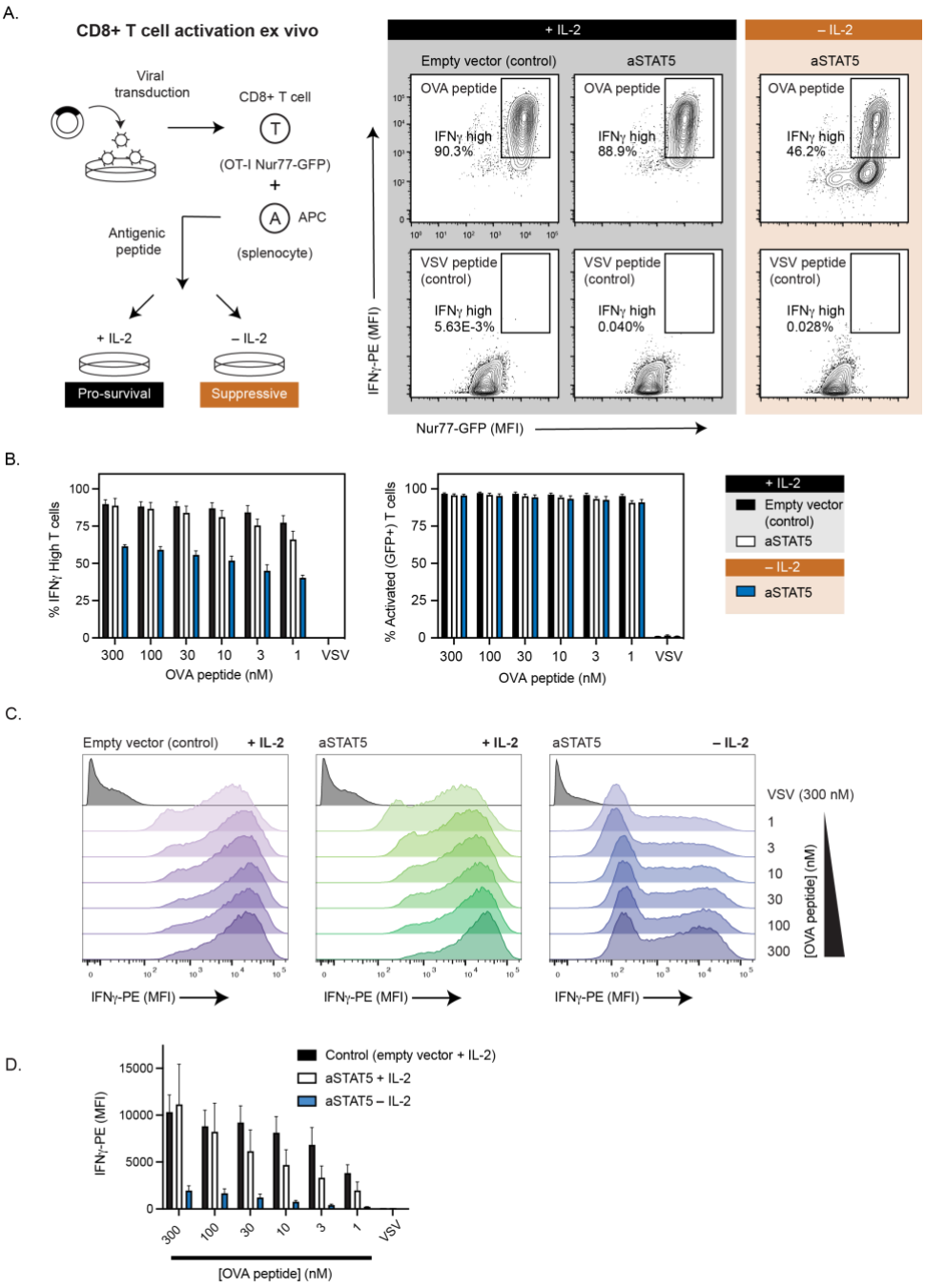

Figure 3-4

Direct activation of endogenous STAT5 maintains CD8+ T cell functionality under suppressive culture conditions

(A) OT-I TCR Nur77-GFP CD8+ T cells were transduced to incorporate a STAT5 activator (aSTAT5) and cultured in the presence or absence of the pro-survival cytokine IL-2 (10 ng/mL)

and re-stimulated to assess activation and IFNγ levels under suppressive culture conditions (– IL-2). Representative data depicting GFP and intracellular IFNγ levels following re-stimulation by OVA (10 nM) or VSV (300 nM) peptides. (B) Quantification of GFP+ and IFNγ+ cells by flow cytometry. Data are representative of three independent experiments (n=3, means ± SEM). (C) Intracellular IFNγ levels were assessed by flow cytometry following restimulation with OVA peptide-pulsed splenocytes (1, 3, 10, 30, 100, 300 nM) or VSV (300 nM). (D) Quantification of the mean fluorescence intensity (MFI) of anti-IFNγ staining (n=3, means ± SEM).

3.5.5 T Cell Mediated-Cytotoxicity in the Absence of IL-2 is Sustained by the STAT5 Activator

A hallmark of CD8+ T cells is their ability to kill infected or malignant cells. We therefore assessed whether T cell-mediated cytotoxicity in the absence of IL-2 could be maintained by the STAT5 activator. OT-I Nur77-GFP CD8+ T cells were transduced and expanded in the presence or absence of IL-2. As previously observed, CD8+ T cells transduced with an empty vector control failed to persist in the absence of IL-2 after 3 days of culture (Data not shown). The expanded T cells were co-cultured with OVA expressing MC38 colon adenocarcinoma cells (MC38-OVA) for 16 hours (Fig. 3.4A). Activated (GFP+) T cells and dead cells, identified by propidium iodide (PI) staining (PI+), were quantified by imaging cytometry (60). We observed that the STAT5 activator was able to maintain the functional capacity of CD8+ T cells to kill MC38-OVA cancer cells to a similar degree as the cells cultured with IL-2. (Fig. 3.4B, C). Interestingly, the STAT5 activator, when combined with IL-2, appeared to enhance killing (Fig. 3.4C). To assess potential differences in antigen recognition, the extent of T cell activation was monitored using the Nur77-GFP reporter (Fig. 3.4B, C).

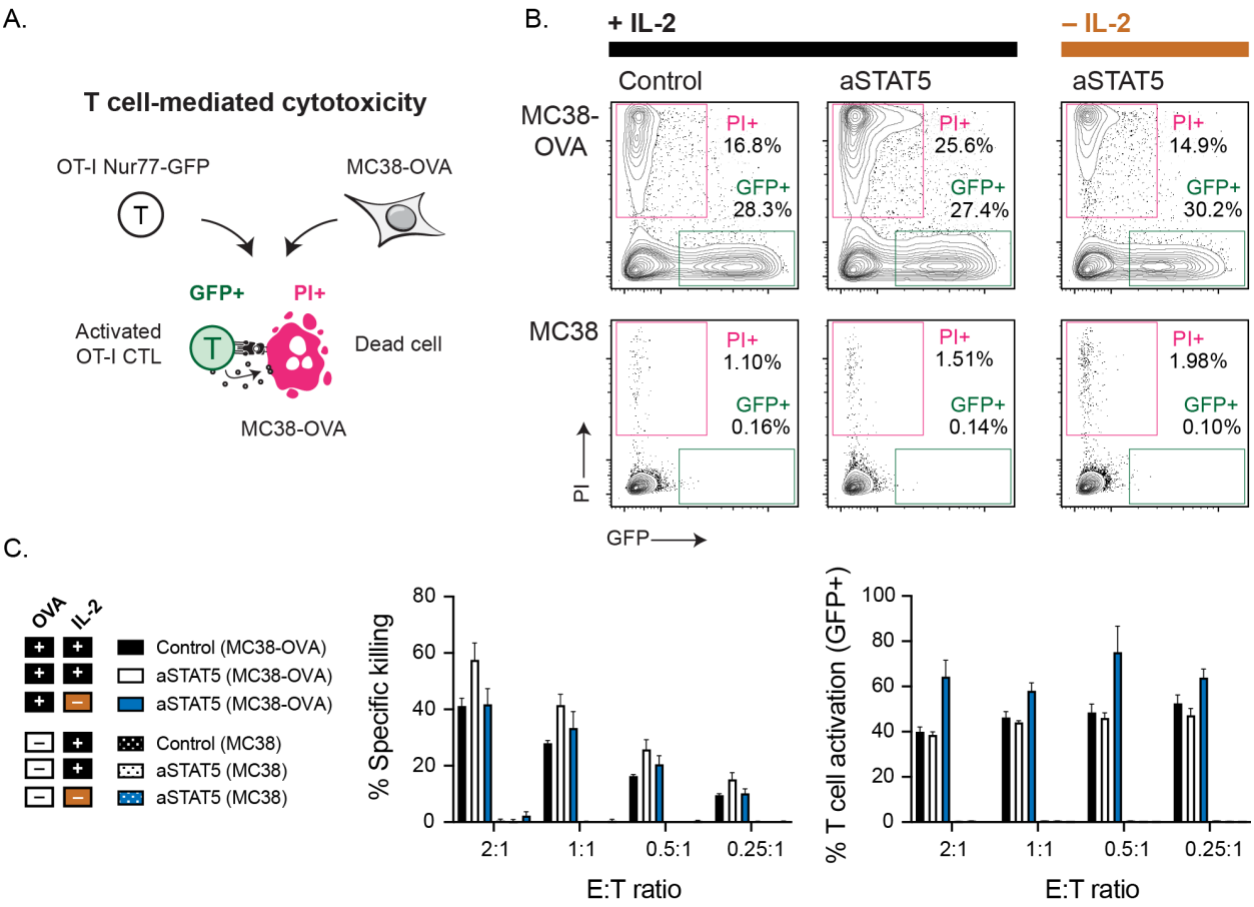

Figure 3-5

A STAT5 activator maintains the cytotoxic capacity of CD8+ T cells

(A) The capacity of a STAT5 activator to sustain T cell-mediated cytotoxicity in the absence of IL-2 was assessed by co-culture of OT-I Nur77-GFP T cells with MC38-OVA cancer cells for 16 hours. (B) Representative data depicting the extent of T cell activation (Nur77-GFP) and cell death (PI) determined by imaging cytometry. (C) Quantification of T cell activation and T cell-mediated cytotoxicity at different E:T ratios. Data are representative of four independent experiments (n=4, means ± SEM).

3.5.6 Tumor-Specific T cells Combined with aSTAT5 Reduces Tumor Outgrowth Following Adoptive Cell Transfer

Our findings indicated that a STAT5 activator enabled CD8+ T cells to persist in the absence of IL-2 and retain their functionality ex vivo. Because pro-survival cytokines can be depleted in tumors, we determined whether the STAT5 activator could enable T cells to better control tumor outgrowth in vivo. We initially evaluated the EL4-OVA syngeneic lymphoma model which was implanted subcutaneously into immunocompetent C57BL/6 mice. The STAT5 activator constructs were incorporated into tumor-specific OT-I T cells by viral transduction and expanded ex vivo for 5 days in the presence of IL-2 (Fig. 3.5A). The T cells were then administered intravenously once tumors were palpable and tumor outgrowth was monitored (Fig. 3.5B, C). We observed that tumor-bearing mice that received OT-I T cells underwent an initial tumor regression that was followed by renewed outgrowth. The STAT5 activator resulted in a more robust initial response to adoptive T cell transfer (ACT), and subsequent tumor outgrowth was delayed to a greater extent (Fig. 3.5B, C). Whereas a minority of control (Empty vector transduced OT-I T cells) treated mice rejected their tumors (2/11), approximately half of the mice that received the STAT5 activator modified OT-I T cell treatment underwent tumor rejection (5/11) (Fig. 3.5C).

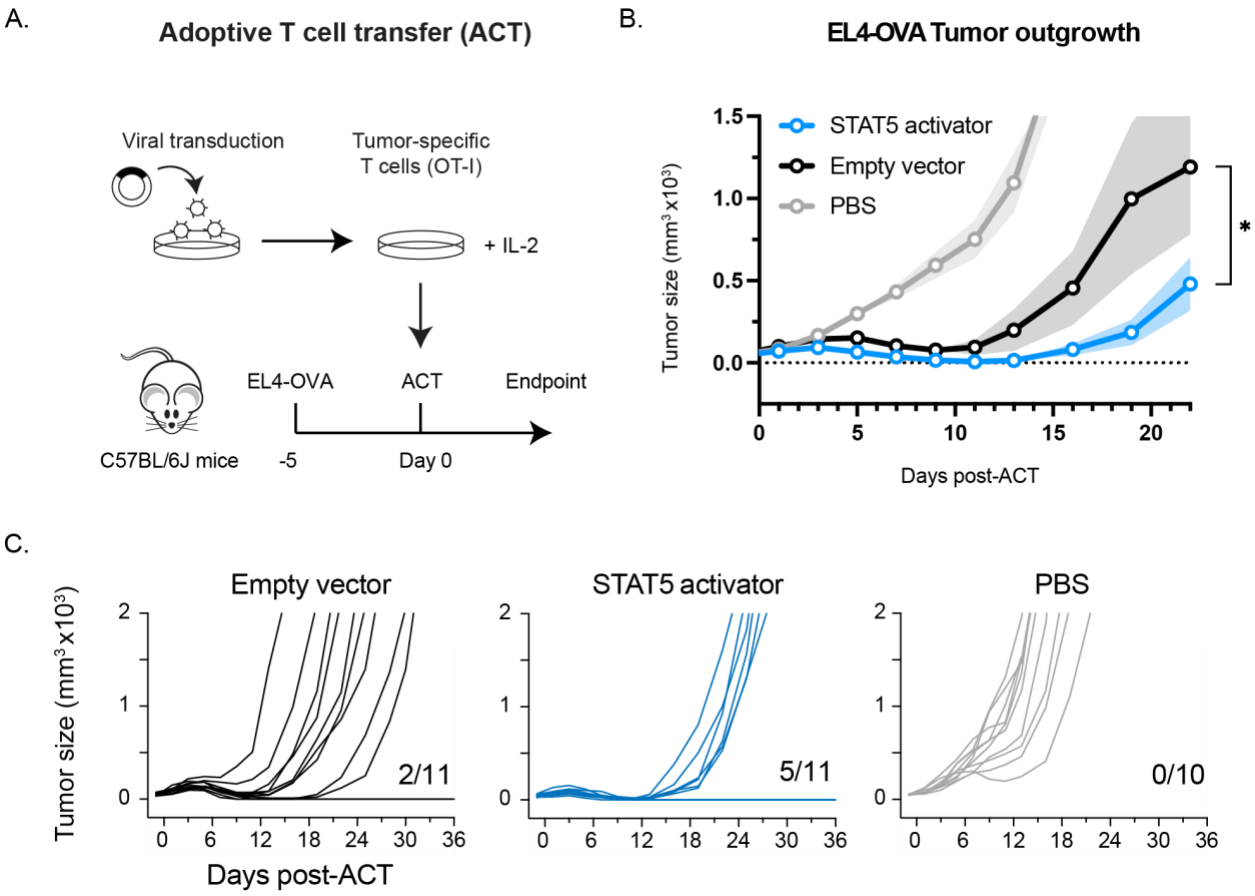

Figure 3-6

Tumor-specific T cells combined with aSTAT5 reduces tumor outgrowth following adoptive cell transfer

(A) OT-I T cells were transduced and adoptively transferred into EL4-OVA tumor bearing mice. (B) Tumor outgrowth was monitored by measurement of tumor size until a humane endpoint was reached. Shaded areas depict means ± SEM (n=10 to 11). * $p < 0.05$ (two-way ANOVA). (C) Tumor outgrowth of individual mice grouped by treatment. The number of regressed tumors is denoted.

3.5.7 aSTAT5 Markedly Slowed Tumor Outgrowth in a Suppressive Tumor Model

We next evaluated the STAT5 activator using the more suppressive B16-OVA melanoma tumor model. B16-OVA was implanted subcutaneously into C57BL/6 mice and tumors were established for 7 days prior to ACT (Fig. 3.6A). OT-I CD8+ T cells that had been transduced with the STAT5 activator or empty vector control were administered intravenously. We observed that the STAT5 activator markedly slowed tumor outgrowth (Fig. 3.6B, C). We also isolated the intact the tumors and weighed them. STAT5 activator group demonstrated a controlled tumor weight compared with the empty vector control group (Fig. 3.6D, E).

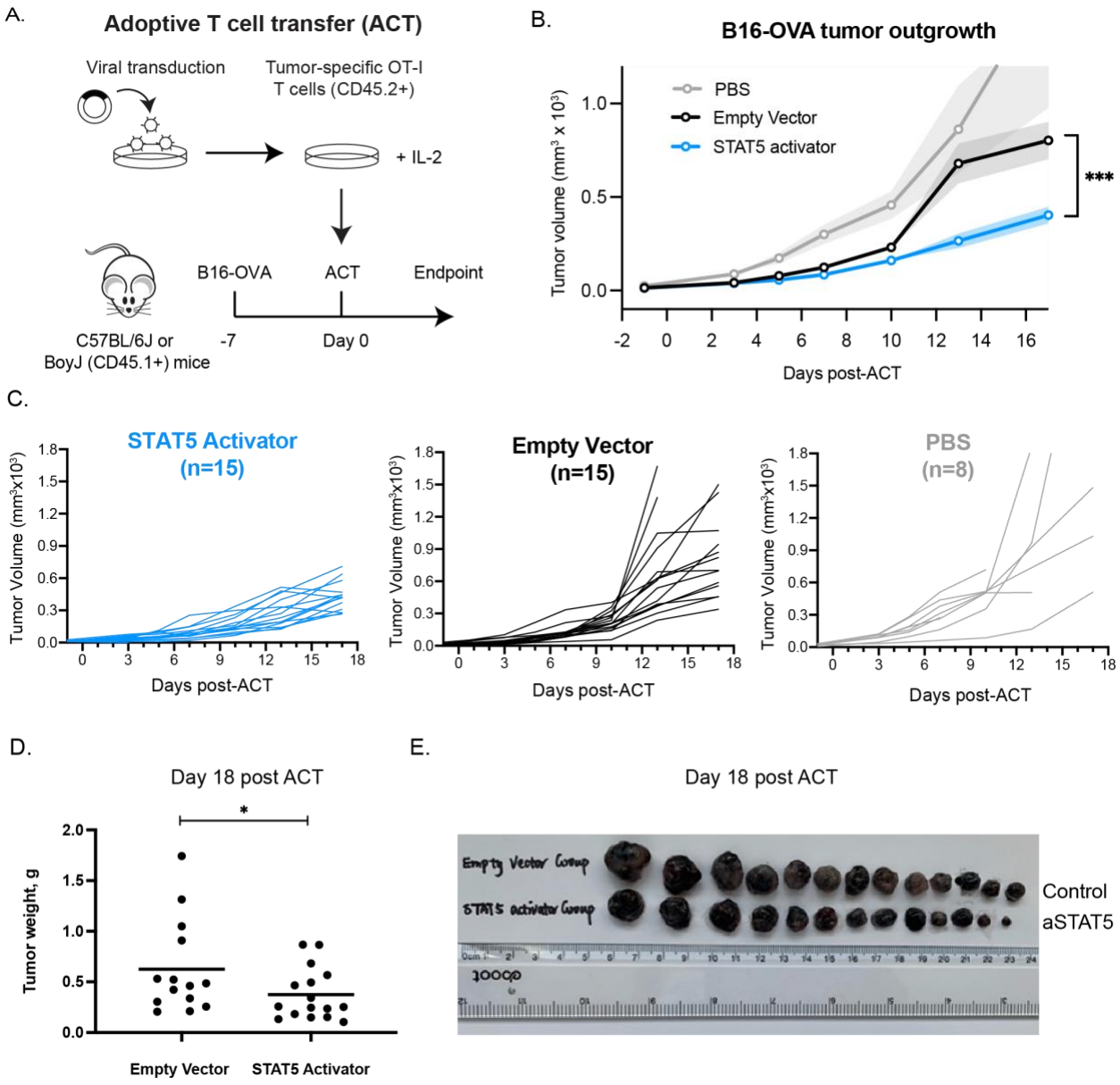

Figure 3-7

STAT5 activator markedly slowed tumor outgrowth in a suppressive tumor model

(A) C57BL/6 mice were subcutaneously inoculated with B16-OVA cells followed by ACT. (B) Tumor outgrowth was monitored across treatment groups, PBS (n=8), Control (empty vector) (n=15), aSTAT5 (n=15). Shaded area represents means ± SEM. *** $p < 0.001$ (two-way ANOVA). (C) Tumor outgrowth of individual mice grouped by treatment. The number of regressed tumors is denoted. (D) All mice were sacrificed on Day 18 post ACT. Tumors

were isolated and weighed. * $p < 0.05$ (One-tailed t test). (E) Tumors photos were taken in alignment on Day 18 post ACT after being sacrificed.

3.5.8 STAT5 Activator Enhances CD8+ T Cell Persistence in Tumors

To address whether the reduced tumor outgrowth caused by the STAT5 activator could be attributed to enhanced T cell persistence and infiltration into B16-OVA tumors in vivo, we isolated blood, tumors, and tumor-draining lymph nodes (TDLN) from BoyJ (CD45.1+) tumor-bearing mice 11-12 days post-ACT (Fig. 3.7A). Few control (empty vector) OT-I T cells could be identified when blood and tumors/tumor draining lymph nodes were collected day 11 or day 12 post ACT (Fig. 3,7B, C). By contrast, we observed a robust population of CD45.2+ adoptively transferred OT-I T cells harboring a STAT5 activator from all the tissues collected on day 11 or day 12 post ACT (Fig. 3,7B, C). The proportion of CD45.2+ OT-I T cells was greatest within the tumor but still readily detected in the blood and TDLN (Fig. 3.7C). The proportion of CD8+ T cells amongst CD45+ cells remained comparable between tumor-bearing mice (Fig. 3.7D). To better understand phenotypic changes caused by the STAT5 activator in vivo, we collected tumors and TDLN 5 days post-ACT. We observed at this earlier timepoint that the increased proportion of STAT5 activator OT-I T cells in the TDLN and tumor was less pronounced (Fig. 3.7E, F).

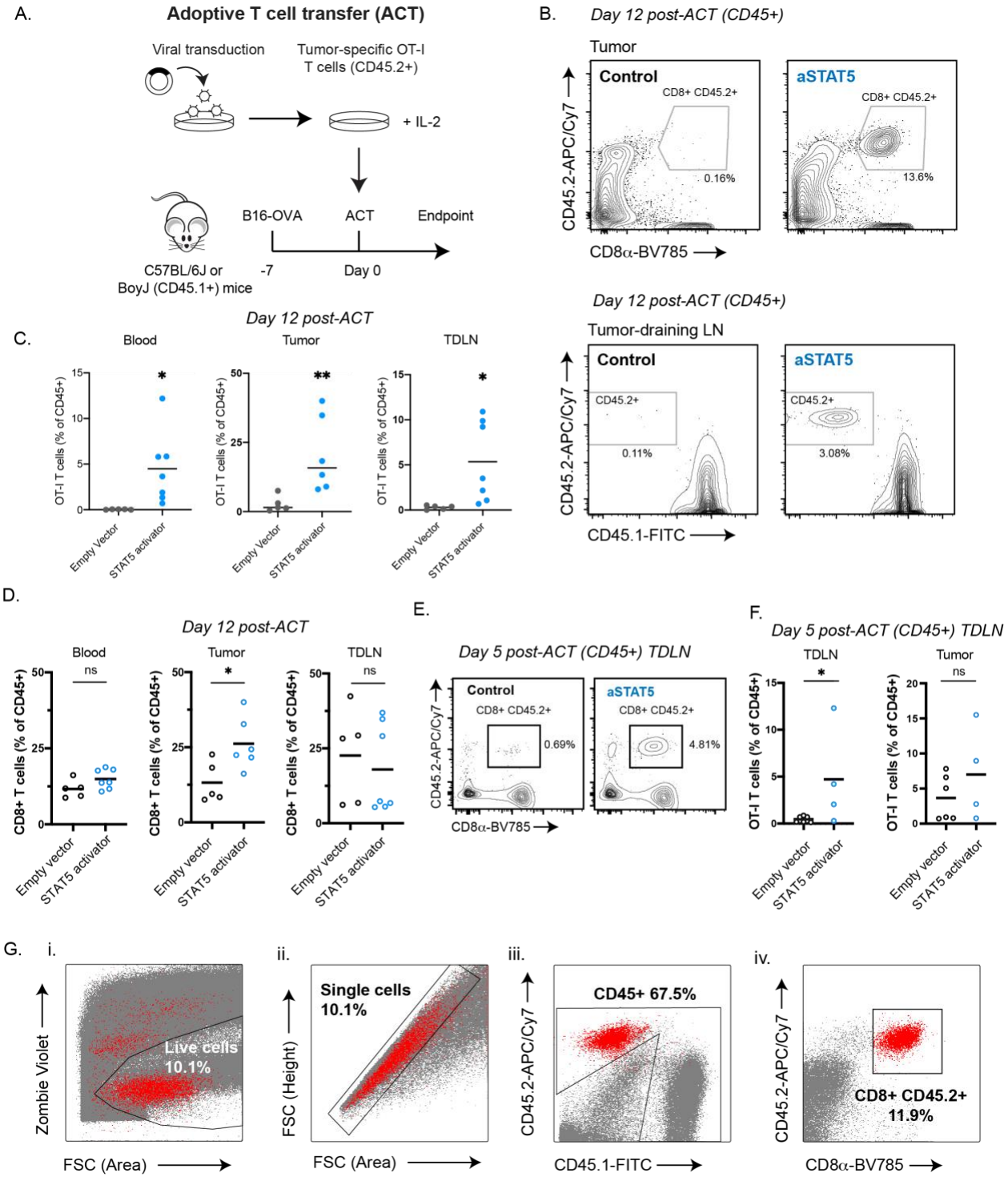

Figure 3-8

Reduced tumor outgrowth due to enhanced T cell persistence following ACT

(A) C57BL/6 mice were subcutaneously inoculated with B16-OVA cells followed by ACT.

(B-D) Tissues collected from BoyJ (CD45.1) mice 11 or 12 days post ACT (Blood: Day 11, Tumors and TDLN: Day 12). (B) Representative flow cytometry data depicting abundance of CD45.2+ OT-I T cells isolated from tumor and tumor-draining lymph node (TDLN) on Day 12 post ACT. (C) Quantification of CD45.2+ OT-I T cells on Day 12 post ACT. One-tailed *t* test (n=5 to 7). (D) Total CD8+ T cells present in blood (Day 11 post ACT), Tumors and TDLN (Day 12 post ACT). Mice were sacrificed to collect tumors and TDLN to analyze OT-I T cells present on day 12 post ACT. Empty vector (n=5), STAT5 activator (n=6 or 7). (EF) Quantification of OT-I T cells present in the TDLN and tumors on day 5 post ACT. (CDF) ns $p > 0.05$, * $p < 0.05$, ** $p < 0.01$(one-tailed *t* test). (G) Gating strategy to identify the adoptively transferred OT-I T cells (CD45.2+ CD8+). (i) Gate 1: Zombie Violet negative (Live cells), (ii) Gate 2: Singlets, (iii) Gate 3: CD45 positive (CD45.2 or CD45.1 positive, Leukocytes), (iv) Gate 4: CD8 and CD45.2 double positive (Adoptively transferred OT-I T cells). Representative image from a aSTAT5 tumor sample depicting the gating strategy described above.

3.5.9 aSTAT5 Enhances CD8+ T Cell Functionality in Tumors

To evaluate readouts of T cell function, we assessed intracellular Granzyme B levels. Because control OT-I T cells were absent by day 12, to provide a benchmark we compared endogenous CD8+ T cells (CD45.1+) to OT-I T cells expressing a STAT5 activator (CD45.2+). The STAT5 activator resulted in uniformly high levels of Granzyme B, a readout of effector function, which was markedly increased in comparison to endogenous CD8+ T cells in both the tumor and TDLN (Fig. 3.8A, B, C, D). To better understand phenotypic changes caused by the STAT5 activator in vivo, we collected tumors and TDLN 5 days post-ACT. We

observed at this earlier timepoint that again the STAT5 activator once again promoted uniformly high Granzyme B levels and numbers of Granzyme B-expressing cells (Fig. 3.8E, G, F, H). Granzyme B levels were lower in control OT-I T cells, similar to endogenous CD8+ T cells, which indicated that high Granzyme B levels were attributable to the STAT5 activator (Fig. 3.8E, G, F, H).

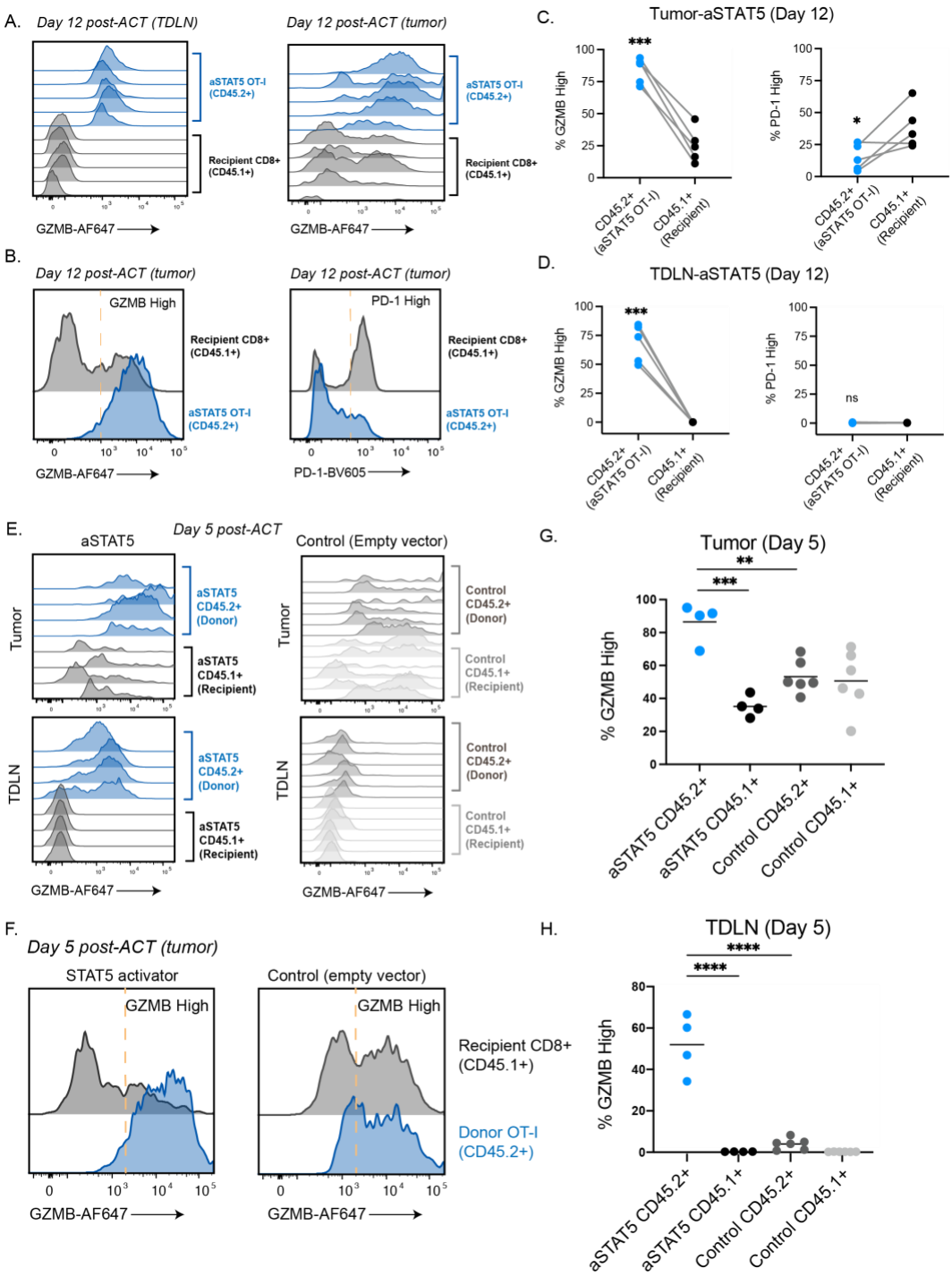

Figure 3-9

Reduced tumor outgrowth due to enhanced T cell functionality following ACT

(A-D) Mice were sacrificed to collect tumors and TDLN to analyze OT-I T cells present on Day 12 post ACT. (A) Flow cytometry data showing Granzyme B (GZMB) level of OT-I T

cells (CD45.2+) and endogenous CD8+ T cells (CD45.1+CD8+) isolated from tumors and TDLN on Day 12 post ACT. (B) Representative histograms depicting the threshold of defining GZMB high of OT-I T cells (CD45.2+) and endogenous CD8+ T cells (CD45.1+CD8+) isolated from tumors on Day 12 post ACT. Quantification of Granzyme B high cells isolated from the tumor (C) and TDLN (D) Paired one-tailed *t test* (n=5). (E-H) Mice were sacrificed to collect tumors and TDLN to analyze OT-I T cells present on Day 5 post ACT. (E） Flow cytometry data showing GZMB level of OT-I T cells (CD45.2+) and endogenous CD8+ T cells (CD45.1+CD8+) isolated from tumors and TDLN on Day 5 post ACT. (F) Representative histograms depicting the threshold of defining GZMB high of OT-I T cells (CD45.2+) and endogenous CD8+ T cells (CD45.1+CD8+) isolated from tumors on Day 5 post ACT. Quantification of Granzyme B high cells isolated from the tumor (G) and TDLN (H) Paired one-tailed *t test* (aSTAT5 n=4, Control n=6).

3.5.10 Assessing Other Functionality of aSTAT5 Modified T Cells within the Tumor

To gain a better understanding of the phenotypical changes of tumor infiltrating T cells modified with our STAT5 activator, we assessed the expression of inhibitory receptors such as PD-1 and LAG-3, as well as an antigen inducible co-stimulatory receptor 4-1BB that is known to activate NFκB. We collected tumors and tumor draining lymph nodes 5 days post adoptive cell transfer. We observed at this earlier timepoint that the STAT5 activator resulted in uniformly lower PD-1 levels on CD8+ T cells both for both adoptively transferred donor T cells (CD45.2+) and recipient T cells (CD45.1+) from tumors (Fig. 3.9A, B, D) but not from tumor draining lymph nodes (Fig. 3.9C, D). We also observed that there is a decrease in LAG-3 level between adoptively transferred T cells and endogenous T cells. But such difference

appears to occur both STAT5 activator group versus empty vector control, only marginally lower in STAT5 activator group (Fig. 3.9E, I). In terms of 4-1BB level, adoptively transferred tumor specific T cells (CD45.2+) demonstrated higher 4-1BB level compared with endogenous T cells (CD45.1+) from the tumors but not from the tumor draining lymph nodes both in STAT5 activator and empty vector group (Fig. 3.9G, H, J).

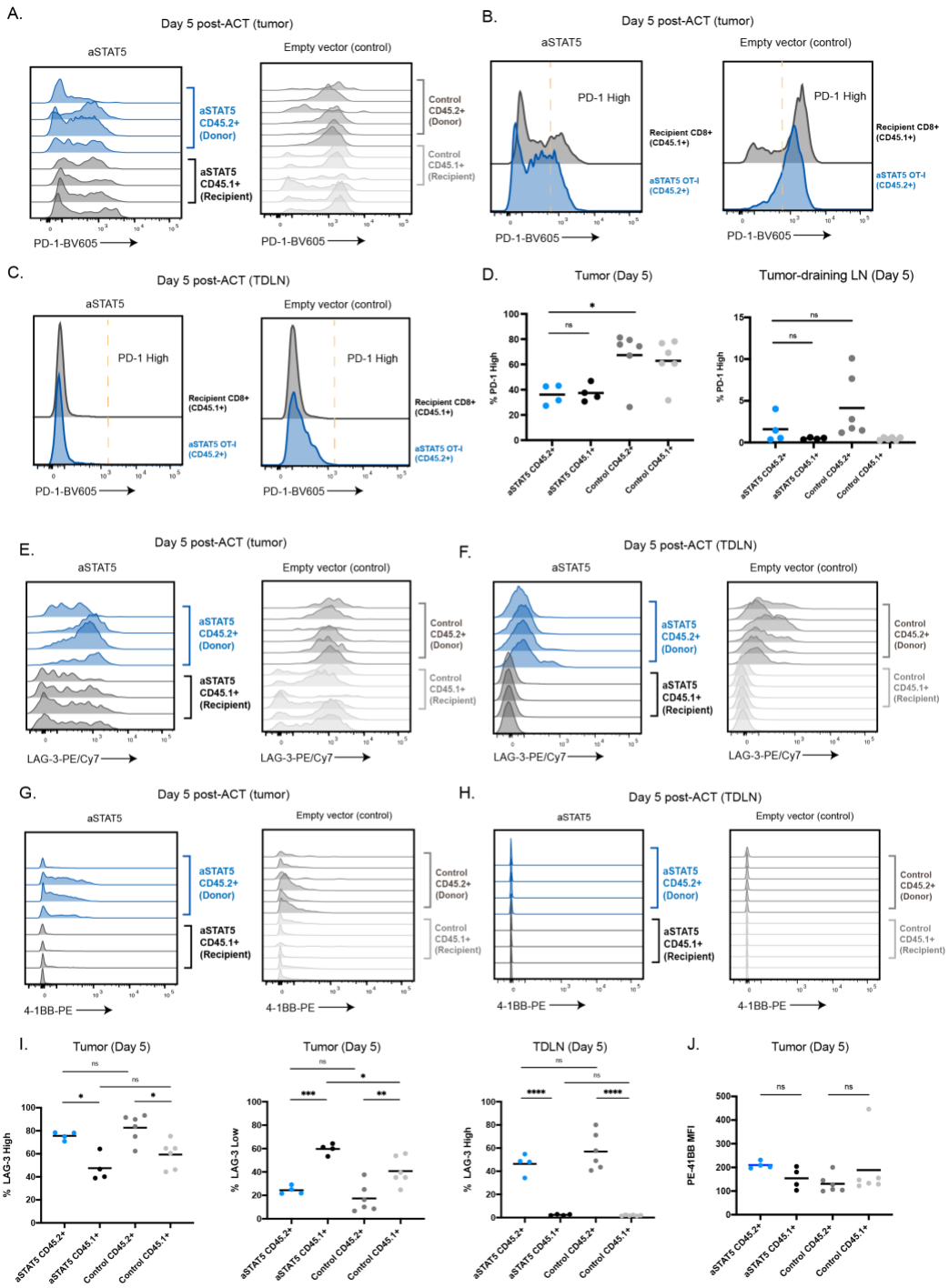

Figure 3-10

Assessment of PD-1, LAG-3, 4-1BB level

(A-J) Mice were sacrificed to collect tumors and TDLN to analyze OT-I T cells present on Day 5 post ACT. (A) Flow cytometry data showing PD-1 levels of OT-I T cells (CD45.2+)

and endogenous CD8+ T cells (CD45.1+CD8+) isolated from tumors. (BC) Representative histograms depicting the threshold of defining PD-1 high of OT-I T cells (CD45.2+) and endogenous CD8+ T cells (CD45.1+CD8+) isolated from tumors (B) and TDLN (C). (D) Quantification of PD-1 high cells isolated from the tumors and TDLN. (E-H） Flow cytometry data showing LAG-3 and 4-1BB level from tumors and TDLN. (I) Quantification of LAG-3 high and low cells isolated from the tumors and TDLN. (J) Quantification of 4-1BB mean florescence intensity (MFI) isolated from the tumors. (DIJ) ns $p > 0.05$, * $p < 0.05$, ** $p < 0.01$, *** $p < 0.001$, **** $p < 0.0001$ (one-way ANOVA).

3.6 Discussion

We have evaluated whether a minimal bifunctional peptide derived from the viral TIP protein could recruit the kinase activity of LCK to targeted STAT proteins in T cells. We determined that when the viral LCK binding site was placed adjacent to STAT binding sites derived from the IL-2 and IFNγ cytokine receptors – STAT proteins became activated. The profile of activated STATs we observed was similar to those reported to result when the cytokines IL-2 and IFNγ bind to their cognate receptors [108, 169, 177]. Interestingly, endogenous STAT binding sites, such as those derived from IFNγR and IL2Rβ, could be placed in series within the peptide to activate combinations of STAT proteins – in this case, STAT1 and STAT5. These findings indicate a generalizable strategy to achieve STAT activation by the enforced recruitment of LCK to targeted STAT proteins. Because LCK is known to possess promiscuous substrate specificity [179], these findings suggest that additional proteins may also be targetable in this manner to cause their phosphorylation at regulatory tyrosine residues

by LCK. The full extent to which proteins can be targeted and regulated by enforced recruitment of LCK remains to be determined.

3.6.1 STAT5 activation is sufficient for maintaining T cell functions

The STAT5-activating cytokine IL-2 is known to be critical to the maintenance of CD8+ T cells, and its depletion by regulatory T cells can suppress CD8+ T cell function [178]. We determined that a cytokine-independent activator of STAT5 allowed T cells to persist and retain their capacity to become activated, produce cytokine, and kill cancer cells under suppressive culture conditions where IL-2 was removed. Our data demonstrate that activation of endogenous STAT5 is sufficient to maintain T cell survival and functionality ex vivo in an IL-2-independent manner. We observed that activation of STAT5 in the absence of IL-2 resulted in T cells that could produce IFNγ following re-stimulation but not to the same extent as T cells cultured in IL-2. The addition of IL-2 restored the ability of T cells that expressed a STAT5 activator to produce IFNγ, indicating that high levels of IFNγ production was caused by IL-2 rather than a less functional T cell state resulting from the STAT5 activator. We also observed cytotoxic potential was modestly increased by the combination of IL-2 and the STAT5 activator.

3.6.2 Targeted STAT5 Activation is Achieved by Our STAT5 Activator to Overcome Suppression

IL-2 has been directly administered to cancer patients as an immunotherapy to counteract the tumor microenvironment of solid tumors that deprives CD8+ T cells of cytokines needed for their survival [149]. It has also been used to promote engraftment of T cell therapies following lymphodepletion and adoptive T cell transfer [169]. However, IL-2 usage has been limited by low response rates as a primary therapy, perhaps in part due to expansion of suppressive regulatory T cells [170], and severe systemic toxicities combined with its poor pharmacological properties [153]. Alternative IL-2 agonists are in development that attempt to address these limitations, but none yet have been clinically approved [150, 171]. The overexpression of a constitutively active STAT5 mutant was found to improve adoptively transferred T cell therapies in preclinical mouse tumor models [103, 104, 172]. Our data demonstrate that endogenous STAT5 can be activated in tumor-specific T cells, which results in reduced tumor outgrowth due to enhanced T cell persistence and functionality within the tumor. We observed that approximately half of EL4-OVA tumors fully regressed following ACT. We did not observe enhanced tumor control by LCK activation alone, perhaps due to the high affinity nature of the OT-I receptor for the WT OVA antigen. Tumors progressed in the more suppressive B16-OVA model, but at a reduced rate. Despite tumor progression, the STAT5 activator markedly extended T cell persistence and T cell functions within the tumor and TDLN.

Chapter 4 Discussion

4.1 Defining CD8+ TIL States by Single Cell RNA Sequencing

Out flow cytometry staining result by looking at T cell effector phenotypes such as Granzyme B and T cell inhibitory receptors such as PD-1 suggest that our STAT5 activator transduced tumor specific T cells become effectors that potentially resist a dysfunctional exhausted T cell fate (Chapter 3 Result 3.5.9, 3.5.10). A recent study investigated T cells expressing constitutively active STAT5 (CASTAT5) in the LCMV chronic infection model and revealed that constitutive STAT5 activation antagonized transcription factor Tox which is associated with T cell exhaustion [109]. The development and application of CASTAT5 has been discussed in Chapter 1.2.3.2. The mechanism of action of CASTA5 is different from our STAT5 activator: CASTAT5 is overexpressed against a background of potentially inactive endogenous STAT5, whereas, the STAT5 activator acts on endogenous STAT5. Therefore, it would be informative to study our STAT5 activator in CD8+ T cells with the current available STAT5 activation strategies such as CASTAT5 in an in vivo tumor model to uncover if STAT5 activator has any edges. By comparing CASTAT5 and STAT5 activator side by side, the different mechanisms of STAT5 activation can be compared, which could guide efforts to translate these findings to clinical applications.

Recent preclinical studies show that the treatment of tumor of tumor-bearing mice or mice infected with a chronic infection induces a unique phenotype of antigen-specific T cells, which was called “better effectors” or KILR cells [168-172]. The hallmark of these cell is the expression of cytotoxic

molecules (including Granzyme B), but also other markers such as NK receptors (including cytotoxic NKG2D/KLRK1) or type I interferon-induced genes. Moreover, it has been shown that IL-2 induces the expression of CD25, the subunit of IL-2 receptor [108]. Single-cell RNA sequencing (sgcRNAseq) can distinguish cell types, lineages, and states in the context of heterogenous tissues. Therefore, we are interested in providing a comprehensive transcriptome landscape of the aSTAT5-expressing OT-I T cells in the tumor by using single cell RNA sequencing. Two batches of B16-OVA infiltrating CD8+ T cells across different treatment groups including empty vector control, TIP Minimal (LCK activator), STAT5 activator, and CASTAT5 have been enriched both on Day 5 and Day 12 post adoptive cell transfer to conduct a whole transcriptome analysis on a single cell level (Fig. 4.1, 4.2). We will be conducting comparisons between adoptively transferred tumor specific CD8+ T cells (donor, CD45.2+) versus the intra-tumoral recipient CD8+ T cells (CD45.1+) using sgcRNAseq. As we expected, we observed substantially more CD8+ T cells with the aSTAT5 and CASTAT groups – about 50% of leukocytes (CD45+) cells within the B16-OVA tumors are CD8+ T cells (Fig. 4.2). The sorted samples will be processed at the U-M Advanced Genomics Core (AGC) with 5' Gene Expression Libraries using 10X Genomics. The single cell samples have passed the quality control at the Advanced Genomics Core and reach 20K per sample for AGC to prepare the 5' Gene Expression Libraries. This data should provide a comprehensive analysis of STAT5 activator modified tumor specific T cells isolating from B16-OVA tumors and conduct the comparison between our donor CD8+ T cells and recipient CD8+ T cells at a single cell level.

Research previously conducted using the CASTAT5 only compared the CD8+ T cells from the control group versus CD8+ T cells from the treatment group as a whole. Our research would dig

further into the differences of transferred versus endogenous CD8+ T cells to provide a comprehensive comparison of two kinds of tumor infiltrating CD8+ T cells following adoptive cell transfer. A recent study using B16 murine melanoma model with paired single cell RNA sequencing of CD8 T cells infiltrating B16 murine melanoma tumors identified four distinct tumor infiltrating CD8+ T cell states: Naive, Effector Memory Like, Memory Like, and Exhausted [180]. Among the four populations, it was validated by another two groups that tumor specific PMEL TILS were enriched in exhausted and memory like states [181, 182]. Exhausted tumor infiltrating T cells are characterized by high expression of the inhibitory receptors PD-1 and TIM-3 and lack of transcription factor 1 (Tcf1) [183]. Memory-Like tumor infiltrating T cells has self-renewal capacity and co-express Tcf1 and PD-1 [183]. Stemness was assessed by Tcf7, Lef1, Sell, Il7r [183]. Cytotoxicity was assessed by looking at Prf1, Fasl, Gzmb [183]. Inhibition/exhaustion was assessed by Pdcd1, Havcr2, Tigit, Lag3, Ctla4 [183].

Specifically, this group studied B16/pMEL model and they identified four groups of tumor infiltrating CD8+ T cells. Cluster 1 (Naive cluster – highest level of stemness, lowest inhibition and cytotoxicity), was defined by high expression of markers of naive/memory (Tcf7, Sell, Ccr7, Lef1, Il7r) and no expression of cytotoxicity genes or inhibitory receptors, compatible with a naive or central memory state. Cluster 2 (Effector memory like cluster - intermediate levels of cytotoxicity and stemness, with low levels of inhibition) expressed high levels of memory-related genes (Tcf7, Lef1, Il7r) with cytotoxicity genes (Gzmb, Gzmk). Expression of granzymes and lack of Sell and Ccr7 expression suggested an effector memory rather than a central memory phenotype. Cluster 3 (Memory cluster – higher levels of stemness compared to exhausted, lower levels of inhibition and very low levels of cytotoxicity), was defined by the co-expression of inhibitory

receptors (Pdcd1, Tigit, and Lag3 but not Havcr2 or Entpd1) and memory-related genes (Tcf7, Lef1, Sell), and low levels of cytotoxic genes, compatible with the recently described memory-like subset [181, 182]. Cluster 4 (Exhausted cluster – lowest level of stemness, highest level of inhibition and cytotoxicity) was defined by high expression of inhibitory receptors pdcd1, Havcr2, Ctla4, Tigit, and Lag3, and exhaustion-related transcription factors as such Batf and Tox, which is essential to establish and maintain the epigenetic T cell exhaustion program enabling T cells to persist in the context of chronic antigenic stimulation, and high expression of cytotoxic molecules (Gzmb, Prf1, Fasl), compatible with an exhausted state.

We have taken a similar approach to identity these four populations of our B16-OVA infiltrating T cells and assess their transcriptome landscape both qualitatively and quantitatively. My data showed that not only the adoptively transferred aSTAT5 OT-I T cells had relatively low surface levels of the inhibitory receptor PD-1, but also the endogenous T cells had decreased PD-1 levels (Chapter 3 Result 3.5.10). Using the single cell RNA sequencing data, we could answer how do aSTAT5 OT-I T cells (CD45.2+) reduce the PD-1 levels of the endogenous wild type CD8+ T cells (recipient, CD45.1+) and is it attributed to a production of specific cytokines, such as IL-2, secreted by aSTAT5 OT-I T cells. Moreover, including CASTAT5 in this analysis would be able to tell us whether our viral TIP peptide derived STAT5 activator has any edges. The specific protocol for sample preparation, workflow and results for the samples that were collected Day 5 post ACT were described in detail as below (Fig. 4.1, 4.2) [114].

4.1.1 B16-OVA Infiltrating CD8+ T Cell Preparation for Single Cell RNA Sequencing

B16-OVA cells ($4x10^5$ or $5x10^5$) cells were subcutaneously injected into age-matched female BoyJ mice (6-8 weeks). On day 8 post tumor inoculation, transduced CD8+ OT-I T cells ($4x10^6$) were adoptively transferred into tumor bearing mice. Tumors were collected post 5 or 12 days of tumor implantation, manually dissociated and digested enzymatically with Collagenase/Hyaluronidase (STEMCELL Technologies, #07912) and DNase I solution (STEMCELL Technologies, #07900). Digested tumors were mashed through 70 μm filters (Fisher Scientific, #22363548). Red blood cells were lysed with Ammonium Chloride Solution (STEMCELL Technologies, #07800). CD45+ tumor infiltrating leukocytes were purified by immunomagnetic positive selection using EasySep Mouse TIL (CD45) Positive Selection Kit (STEMCELL Technologies, #100-0350). For higher recovery, cells were resuspended to 10-25 million cells/mL in r.t. FACS buffer. For each 1 mL of sample, 100 μL of Selection Antibody Cocktail and 50 μL of RapidSpheres were added. Samples were stained with L/D Zombie Violet dye followed by Fc block on ice for 10 min. To label specific cell populations of interest for 10x Genomics, TotalSeq-C antibodies were used. Each master mix of staining will have one of the TotalSeq-C HashTag antibodies (either 1 or 2 or 3) to ensure that each mouse will receive one of the TotalSeq-C HashTag antibodies only to identify that sample in the single cell RNA sequencing dataset. Three master mixes of TotalSeq-C antibodies, fluorescent antibodies, and TotalSeq-C Hashtag antibodies were prepared, respectively. Each master mix has one of the TotalSeq-C HashTag antibodies (either 1 or 2 or 3). Cells were stained with the master mix with corresponding TotalSeq-C HashTag antibodies (1, 2, or 3) on ice for 30 min. CD8+ T cells were sorted by flow cytometry (ThermoFisher Bigfoot Spectral Cell Sorter) using L/D staining and fluorescent antibodies against cell surface markers CD45, CD8α and CD8β (Gating: Lymphocytes > Single cells > Live cells > CD45+ > CD8α + CD8β +). Cells from the same treatment group but collected from different mice that were stained with unique TotalSeq-C

HashTag antibodies (1, 2 or 3) were pooled in ice-cold plain RPMI medium with 0.5% BSA after sorting to target 20K cells per sample. Flow sorted tumor infiltrating CD8+ T cells were then used for single-cell RNA sequence purpose (4 samples, 20K per sample). 10x genomics single-cell gene expression sample processing and sequencing were conducted by U-M Advanced Genomics Core (AGC) using Single Cell 5' Library. After receiving the data from AGC, we will work with our collaborator for a comprehensive transcriptome analysis at a single cell level. TotalSeq-C antibodies we used are as below: TotalSeq™-C0002 anti-mouse CD8α Antibody (53-6.7) (1:50) (BioLegend, 100785), TotalSeq™-C0178 anti-mouse CD45.1 Antibody (A20) (1:50) (BioLegend, 110757), TotalSeq™-C0157 anti-mouse CD45.2 Antibody (104) (1:50) (BioLegend, 109855), TotalSeq™-C0981 anti-mouse TCR Vα2 Antibody (B20.1) (1:50) (BioLegend, 127829), TotalSeq™-C0380 anti-mouse CD90.1 (Thy1.1) Antibody (OX-7) (1:50) (BioLegend, 202551), TotalSeq™-C0301 anti-mouse Hashtag 1 Antibody (M1/42; 30-F11) (1:50) (BioLegend, 155861), TotalSeq™-C0302 anti-mouse Hashtag 2 Antibody (M1/42; 30-F11) (1:50) (BioLegend, 155863), TotalSeq™-C0303 anti-mouse Hashtag 3 Antibody (M1/42; 30-F11) (1:50) (BioLegend, 155865).

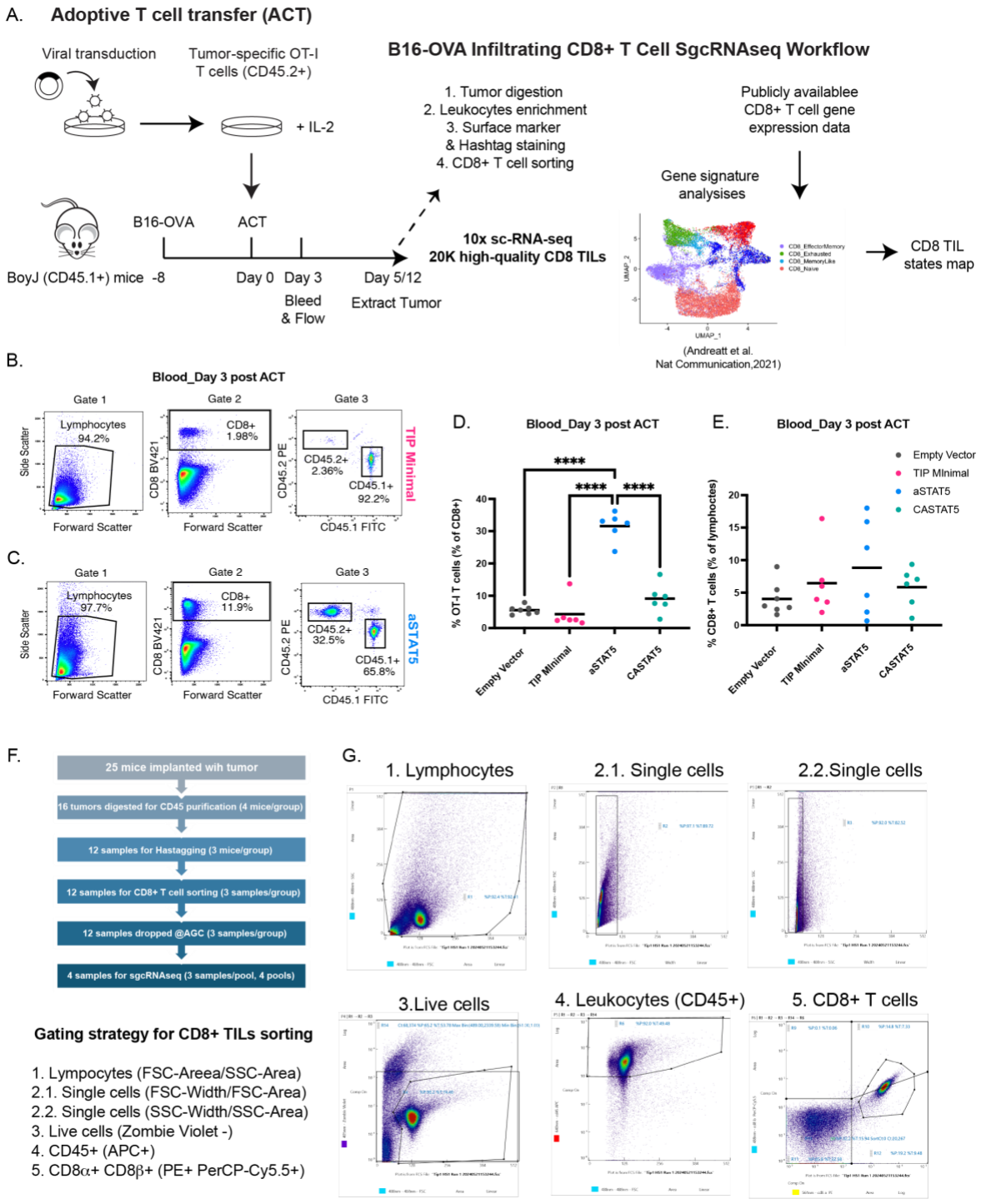

Figure 4-1

B16-OVA infiltrating CD8+ T cell preparation for single cell RNA sequencing

(A) B16-OVA infiltrating CD8+ T cell single cell RNA sequencing preparation workflow. (BC) Representative flow cytometry blot with gating strategy (Lymphocyets > CD8+ > CD45.2+ (donor

OT-I T cells) or CD45.1+ (recipient) from blood collected on Day 3 post adoptive cell transfer to identify the portion of adoptively transferred OT-I T cells (CD45.2+) (B) TIP Minimal, (C) aSTAT5. (D) Quantification of OT-I CD45.2+ T cells % among all the CD8+ T cells. C57BL/6 BoyJ (CD45.1) mice were subcutaneously inoculated with B16-OVA cells followed by ACT. Blood collected 3 days post ACT. Quantification of CD45.2+ OT-I T cells. One-way ANOVA, Sidak's multiple comparisons. Empty Vector (n=7), TIP Minimal (n=6), aSTAT5 (n=6), CASTAT5 n=6. **** $p < 0.0001$. (E) CD8+ T cells % among all the lymphocytes. C57BL/6 BoyJ (CD45.1) mice were subcutaneously inoculated with B16-OVA cells followed by ACT. Blood collected 3 days post ACT. Quantification of CD45.2+ OT-I T cells. One-way ANOVA, Sidak's multiple comparisons. Empty Vector (n=7), TIP Minimal (n=6), aSTAT5 (n=6), CASTAT5 n=6. ns $p > 0.05$. (F) The reverse triangle demonstrates the sample size and workflow from tumor implantation, to tumor digestion and leukocytes enrichment (CD45+), hashtag staining, CD8+ single cell sorting and sample pooling for RNA sample preparation at advanced genomics core. Lower panel shows the gating strategy for CD8+ TILs single cell sorting after leukocyte enrichment. (G) Representative flow cytometry result showing the purity of CD8+ T cells after the single cell sorting.

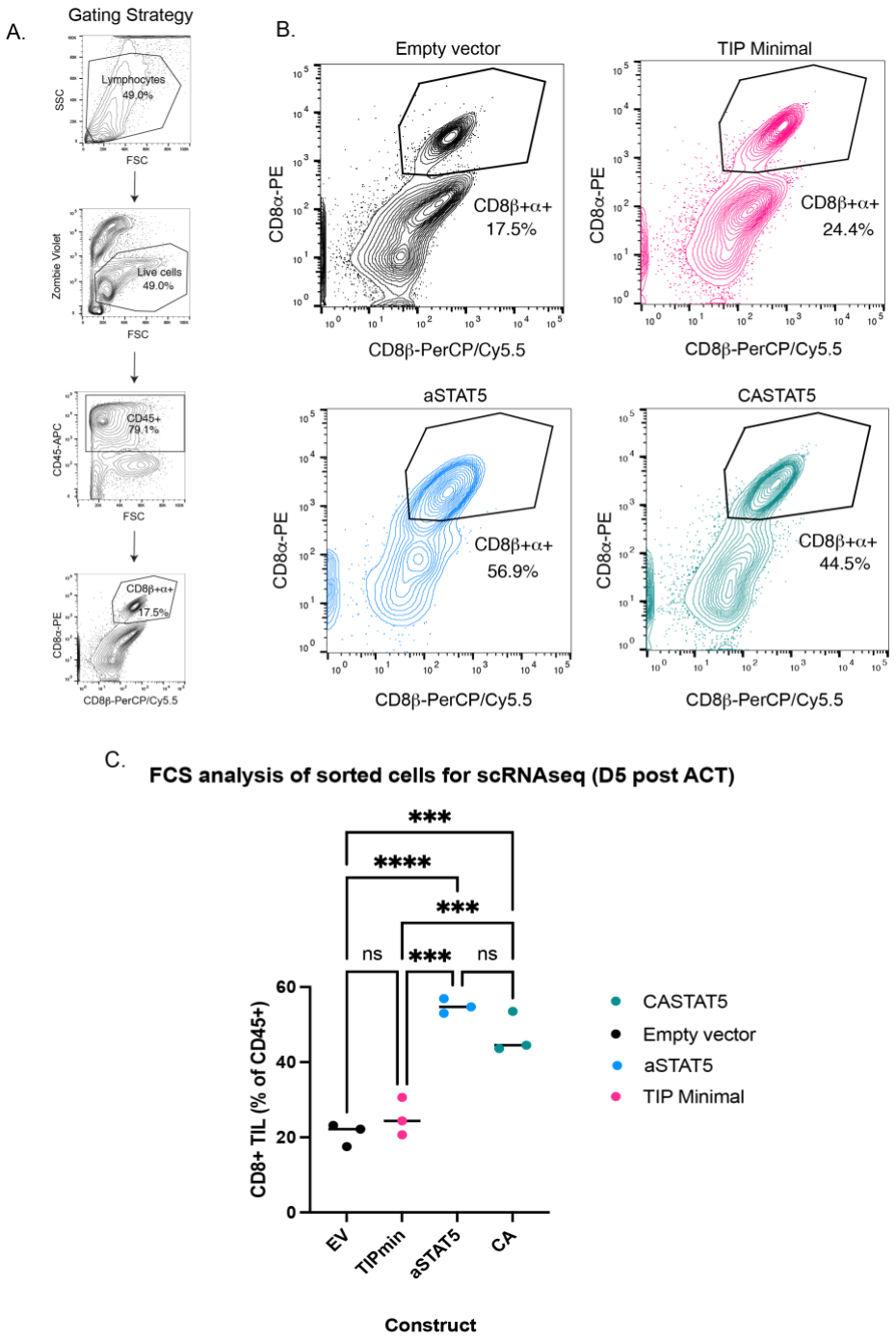

Figure 4-2 Substantial increases in CD8+ T cell modified with aSTAT5 from B16-OVA infiltrating leukocytes

Tumors were isolated on day 5 post ACT. CD45+ T cells were enriched for CD8+ T cell single cell sorting to prepare for the single cell RNA sequencing. Sorted samples were re-analyzed using

gating strategy from a representative flow cytometry blot of an empty vector control sample. Gating strategy: Lymphocytes > Live cells > CD45+ > CD8β+ CD8α+. (B) Representative flow cytometry blot demonstrating percentage of CD8+ T cells (CD8β+ CD8α+) among leukocytes (CD45+) from all four treatment groups. Black: Empty vector. Red: TIP Minimal. Blue: aSTAT5 (STAT5 activator). Green: CASTAT5 (Constitutively active mutant of STAT5). (C) Quantification of CD8 TIL (% of CD45+). Each dot represents an individual mouse. ns $p > 0.05$, * $p < 0.05$, ** $p < 0.01$, *** $p < 0.001$, **** $p < 0.0001$ (one-way ANOVA with Sidak's multiple comparisons).

4.2 If Optimal Model Systems are Needed to Re-Assess if LCK Activator Could Promote Killing of Tumors with Weak Antigens?

Tyrosine-protein kinase-interacting protein (TIP), expressed by Herpesvirus saimiri, co-opts LCK kinase by recruiting it to either canonical or non-canonical substrates to hijack signaling pathways in T cells. We evaluated whether a minimal region of TIP could be isolated from the full-length viral protein (Chapter 2 Result 2.4.1). We have demonstrated that this minimal viral TIP protein enhances TCR signaling, lowers T cell activation threshold, as well as boosted antigen recognition ex vivo by functioning as a direct LCK activator (Chapter 2 Result 2.4.4, 2.4.6, 2.4.7). However, the TIP Minimal peptide (LCK activator) didn't demonstrate a significant enhancement in ex vivo cytotoxic killing or control in tumor suppression in vivo (Chapter 2 Result 2.4.8). Multifaceted factors including antigen affinity, proper interaction between TCR and pMHC, MHC expression and etc., can affect antigen recognition. We suspect such suboptimal result could be limited to current tumor models we are using with regard to tumor antigen affinity, MHC expression, and T cell-cancer cell interaction. A

comprehensive interaction between T cells and cancer cells is suggested to not only provides immunological synapse that gathers a complex classes of receptors but also exert mechanical force that helps to initiate TCR signaling, and therefore subsequence T cell mediated cytotoxicity [184-187]. Even though MC38 expresses high levels of MHC-I for antigen presentation, it is an adherent colon adenocarcinoma [188]. Such adherent nature might be suboptimal for T cell and cancer cell interaction in an ex vivo cell culture to study whether enhanced antigen recognition benefits cancer killing. Therefore, suspension cancer cell lines such as EL4 lymphoma cells especially EL4-G4 cancer cells or other ex vivo 3D culture might provide better condition to study antigen recognition of cancer cells in an ex vivo setting. In terms of the in vivo anti-tumor immunity using EL4-OVA/OT-I T cell system (Chapter 2 Result 2.4.8), we suspect the failure of tumor outgrowth control of our LCK activator transduced OT-I T cells could be attributed to the fact that those tumor specific T cells already have high affinity to the EL4-OVA tumors. Therefore, the question of whether enhanced antigen recognition by the LCK activator could enhance anti-tumor immunity in vivo remains to be explored by potentially using B16-G4 tumors or other tumor models with high MHC expression with a low affinity antigen.

A recent studies using a one of the BMS-684 series that inhibit DAGKα/ζ which also resides in early TCR signaling [74]. They have shown that inhibiting DAGKα/ζ enhances the priming of tumor specific T cells as well as T cell proliferation and cytokine production. Particularly, they use $TRP1^{high}$ and $TRP1^{low}$ trans-nuclear mice bearing CD8 T cells that recognize an epitope from the melanoma self-antigen tyrosinase-related protein 1 (Tyrp1) with different affinities. $TRP1^{high}$ mice carry donor nuclei from melanoma antigen TYRP1-specific CD8+ T

cells. Activated and naive CD8+ T cells from these mice show a high affinity for TYRP1 antigen and function to slow the progression of a subcutaneous B16 melanoma in vivo [189]. TRP1^{low} mice carry donor nuclei from melanoma antigen TYRP1-specific CD8+ T cells [189]. Activated CD8+ T cells from these mice exhibit a low affinity for TYRP1 antigen. Instead of manipulating antigen affinity on tumor cells, this model provides an alternative approach to study antigen affinity and CD8+ T cell killing by using tumor specific CD8+ T cells with difference TCR affinity to the same tumor antigen. This model may be useful for studying the functional attributes of T cells conferred by TCR affinity and for screening immunomodulatory cancer therapies. Therefore, we could potentially use CD8+ T cells from TRP1^{high} and TRP1^{low} mice with subcutaneously implanted C2VTrp1 tumor model, a mouse pancreatic cancer cell line engineered to express a TRP1 transgene, or B16F10 model to assess our LCK activator in an in vivo tumor model.

4.3 Regulatable System to Tune LCK Activity and potentially STAT5 Activation

A potential complication of STAT5 activation is the risk of lymphoproliferative disease [190]. Recent strategies have been developed to incorporate control mechanisms, such as kill switches and regulatable gene circuits, to mitigate the potential toxicities associated with T cell therapies [191-193]. Therefore, one of the future directions is to further develop our TIP derived viral peptide into a gene regulatable system for a controllable gene expression (Fig. 4.2A). We have incorporated out TIP Minimal into an “all-in-one” dox-inducible expression system. To demonstrate that we can affect changes in basal LCK activation, the minimal LCK agonist was incorporated into an inducible expression system and delivered with lentivirus (Fig. 4.2B, C). Because doxycycline can be administered to mice, the effects of rewiring

antigen recognition can now be assessed in vivo using adoptively transferred T cells. Beyond that, if LCK kinase activity can be regulated in primary T cells and potentially in vivo, regulatable STAT5 or other protein activation that are recruited to the TIP Minimal and be activated by LCK as non-canonical substrate can potentially be achieved in a translational setting.

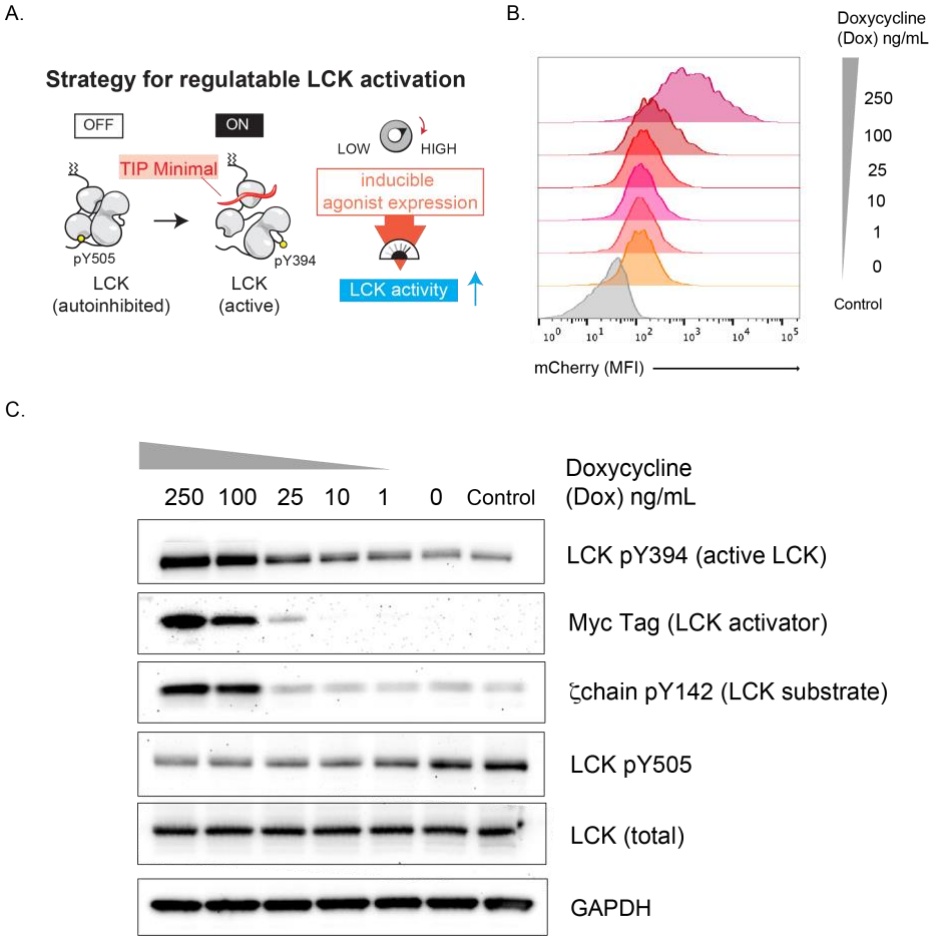

Figure 4-3

Regulatable LCK activation with doxycycline inducible system

Illustration of Doxycycline (Dox) inducible expression of LCK. (B) pINDUCER21_mCherry plasmid were transfected into LX293T cells to produce lentiviruses. Jurkat T cells were

transduced with lentiviruses carrying the dox-inducible plasmid. mCherry expression was induced by adding various doses of doxycycline and mCherruy level were analyzed using flow cytometry. Histogram is representative of one biological experiment. Un-transduced Jurkat T cells were included as control. (B) Jurkat T cells were transduced with an "all-in-one" dox-inducible expression vector. Addition of doxycycline causes the regulatable expression of TIP Minimal (LCK activator) which causes robust activation of LCK as assessed by immunoblot (t=16 hours).

4.4 Future Directions

4.4.1 A Generalized Platform to Recruit LCK Kinase to Intracellular Protein of Interest?

Our study demonstrated that endogenous STAT binding sites, such as those derived from IFNγR and IL2Rβ, could be placed in series within the peptide to activate combinations of STAT proteins. These findings indicate a generalizable strategy to achieve STAT activation by the enforced recruitment of LCK to targeted STAT proteins. Because LCK is known to possess promiscuous substrate specificity [179], these findings suggest that additional proteins may also be targetable in this manner to cause their phosphorylation at regulatory tyrosine residues by LCK. The full extent to which proteins can be targeted and regulated by enforced recruitment of LCK remains to be determined. We hypothesize that if an intracellular protein is regulated by phosphorylation and intramolecular interaction with an SH2 domain, it could potentially be activated by LCK in this "TIP" dependent manner. Its SH2 domain could be recruited to the tyrosine phosphorylated site that is integrated on the TIP Minimal peptide. Due to the proximity, the protein itself could be phosphorylated by LCK kinase to promote its further activation or inhibition. If the minimal

tyrosine binding sequence for a protein's SH2 domain has been identified and such protein's activity is regulated through intramolecular interaction by phosphorylation, we can integrate that minimal SH2 binding sequence into the TIP Minimal to recruit our protein of interest to be phosphorylated and regulated by LCK kinase. Therefore, the TIP derived peptide provides a novel platform for the design of T cell or B cell intracellular activator or maybe even inhibitor by re-engineering this viral protein to recruit LCK kinase activity to its non-canonical substrate.

4.4.2 Potential in Hardwiring STAT5 Activator into Other Translational Models to Overcome T Cell Exhaustion

We determined that when the viral LCK binding site was placed adjacent to STAT binding sites derived from the IL-2 and IFNγ cytokine receptors that STAT proteins could be recruited to LCK to become phosphorylated and activated (Chapter 3 Result 3.5.1, 3.5.3). The profile of activated STAT proteins we observed was similar to those reported to result when the cytokines IL-2 and IFNγ binding to their cognate receptors [108, 169, 177]. We determined that a STAT5 activator (aSTAT5) allowed CD8+ T cells to retain their capacity to produce IFNγ and kill cancer cells ex vivo (Chapter 3 Result 3.5.4, 3.5.5). We therefore incorporated aSTAT5 into tumor-specific T cells (TST) and transferred them into tumor-bearing mice. We determined that aSTAT5 TST caused potent tumor regression in a "hot" tumor and controlled tumor outgrowth due to improved T cell persistence and functionality in a poorly immunogenic tumor model (Chapter 3 Result 3.5.6, 3.5.7, 3.5.8, 3.5.9, 3.5.10). Our findings highlight that T cells can be improved to resist the miscommunication that cancer causes by targeting intracellular signaling pathways.

Efforts are ongoing to develop more efficacious and safe T cell therapies, which could be combined with targeted STAT activation [120, 194]. Tumor infiltrating lymphocytes (TIL) isolated from patients, CAR-T, and TCR-T cells used therapeutically have shown limited efficacy in solid tumors due to suppressive barriers that prevent T cell function [195]. Because the cytokine milieu within tumors results in T cell dysfunction, T cells have been engineered to secrete soluble cytokines such as IL-2 and IL-12 [196, 197], or installed with orthogonal cytokine receptors [198]. Our findings indicate that these cytokine signals could be "hardwired" into T cell therapies by direct activation of STAT proteins. Moreover, despite side effects, T cell therapies typically require a preconditioning regimen where the patient undergoes lymphodepletion prior to ACT to improve the engraftment of the transferred T cells, a major determinant of therapeutic outcome [199]. We observed that preconditioning was not required for the robust engraftment of T cells that expressed a STAT5 activator. Moreover, we observed persistent Granzyme B levels in vivo and reduced expression of the inhibitory PD-1 receptor, which indicate improved functionality in vivo. These observations are consistent with recent findings that STAT5 opposes the activity of TOX, a transcriptional driver of T cell exhaustion [109], which suggests a STAT5 activator could be used to stave off or reverse an exhausted T cell state by applying STAT5 activation in potentially CAR-T or TCR-T models. Because TIP essentially is a viral protein, the LCK binding motif may be different in different species. Human T cells might be favorable to assess the translational value of this TIP derived STAT5 activator. Therefore, one of the future directions would be to assess the feasibility of TIP-derived T cell activators as potential human therapeutics. We envision that tumor infiltrating lymphocytes could be expanded from patient-derived tumors as combined with

xenograft mouse models to assess whether reactivity against the tumor can be improved using our TIP-derived T cell activators.

Rosenberg's group for the first time utilized human tumor infiltrating lymphocytes (TILs) for adoptive cell transfer in the treatment of advanced melanoma because TILs would be enriched for tumor specific T cells [200]. In their study, patient-derived tumors were excised and enzymatically digested to obtain single cell suspensions and grown in high does IL-2 (6000 IU/mL). The cytotoxicity of those ex vivo expanded tumor derived lymphocytes was assessed by ex vivo cytotoxic T cell lymphocytes assay where lymphocytes were co-cultured with tumor cells ex vivo to select individual lymphocyte cultures with high cytotoxic killing functions. Using this approach, Rosenberg's group harvested approximately 10^{11} lymphocytes in approximately 5-6 weeks for infusion into patients. They found that adoptive transfer of those TILs could achieve advanced tumor regression. Human TILs grown from resected melanomas in the presence of recombinant IL-2 demonstrated effective tumor control against autologous melanomas [201]. Therefore, incorporating our STAT5 activator into tumor patient derived tumor infiltrating lymphocytes to assess if our STAT5 activator could bypass the need of ex vivo expansion with IL-2 and further prolong the persistence of those TILs in vivo would be a valuable route to pursue in the future.

4.4.3 Investigating the Negative Feedback Mechanism

Since the LCK activator can be incorporated into T cells by viral transduction to cause a sustained kinase activation over days. We hypothesized that sustained increase in LCK activity will cause negative feedback that acts to desensitize the TCR signaling pathway. In the same experiment

conducted in Chapter 2 Result 2.4.4 “TIP Minimal Enhances LCK Activation and TCR Signaling in Primary T Cells” where we observed that increased LCK activity caused an expected increase in phosphorylation of its substrates, such as ZAP-70 kinase. At the same time, I also probed for LAT and PLCγ1 phosphorylation. LAT is an adaptor protein that acts as a hub for the recruitment of signaling proteins and is required for T cell function. When LAT is phosphorylated by ZAP-70, it recruits proteins such as PLCγ1, and recruits SOS, SLP-76 and ITK. LAT is required for calcium mobilization and RAS-ERK signaling pathways. We observed that sustained LCK activation caused reduced LAT phosphorylation, a ZAP-70 substrate, as well as PLCγ1 (Fig. 4.3A). Similar results were obtained by 5 hours of CSK inhibition (data not shown) (Fig. 4.3B). These data suggest a negative feedback mechanism that restrain agonist-induced T cell activation . By incorporating LCK activator into primary T cells, we have evaluated whether tonic TCR signaling could be recapitulated ex vivo by sustained activation of LCK over several days. I expanded primary CD8+ T cells and incorporated LCK activator by viral transduction. Our LCK activator sustained increased LCK activity over 4 days of culture (Fig. 4.3C). We also observed that hallmarks of tonic TCR signaling were recapitulated, demonstrated by phosphorylation of the TCR-associated ζ-chain and ZAP-70 kinase in the absence of a TCR agonist, as well as increased global protein tyrosine phosphorylation (pY total) (Fig. 4.3C). Therefore, we hypothesized that tonic signaling could cause desensitization of the TCR signaling pathway. By collaborating with Monica Chanda, a graduate student in the lab, we conducted initial RNA-sequencing analysis on the un-stimulated LCK activator transduced CD8+ T cells and empty vector transduced CD8+ T cells as control to evaluate whether tonic signals caused adaptive changes in gene expression. Through comparative RNA-sequencing analysis, we identified 1502 differentially expressed genes ($p < 0.05$), including interesting candidates implicated in dampened T cell responses, such as LAG-

3, which encodes an inhibitory receptor, PD-L1, Egr3, and Nr4a3 (Fig. 4.3D). Altogether, we aim to determine the composition of LAT signaling complexes to elucidate how negative composition of LAT signaling complexes to elucidate how negative feedback loops contribute to ligand discrimination (Fig. 4.3B) as well as to determine how adaptive changes that occur over days change the assembly of signaling complexes (Fig. 4.3E), which is now being investigated by Zehui Gu, a graduate student in the Courtney Lab by conducting mass spectrometry analysis.

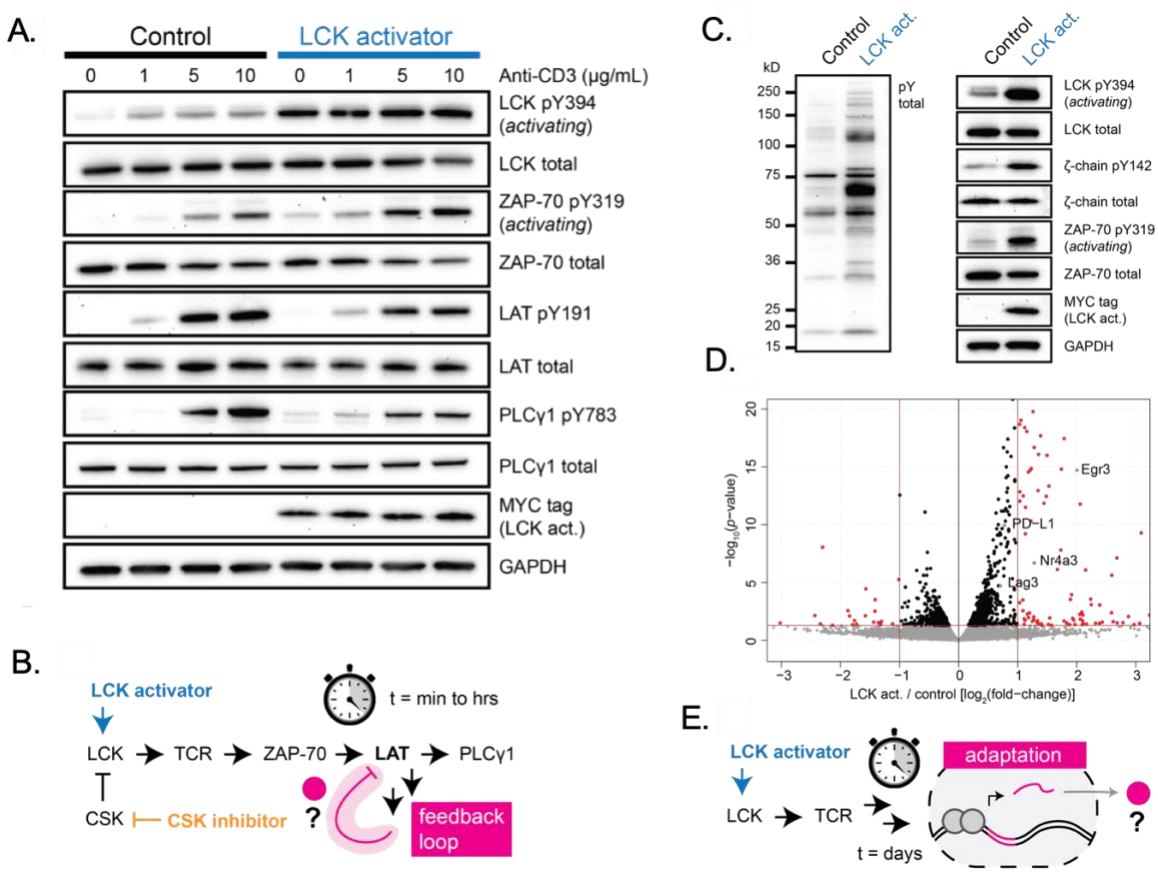

Figure 4-4

A negative feedback mechanism revealed by chronic LCK activation

(A) Sustained LCK activity by a LCK activator. T cells were stimulated for 2 minutes with an anti-CD3 agonist antibody. Protein phosphorylation was assessed by immunoblot. (n=3). (B)

Determining the composition of LAT signaling complexes to elucidate how negative feedback loops contribute to ligand discrimination. (C) Increased basal LCK kinase activity recapitulates tonic TCR signaling in resting ex vivo cultured CD8+ T cells. Protein phosphorylation was assessed by immunoblot (n=3). (D) T cells were cultured ex vivo for 4 days. RNA was isolated and analyzed by RNA-seq. Differential expression was determined from read count data using the DESeq2 package in R studio. DESeq2 uses a negative binomial distribution model for differential expression analysis. The log_2fold change and p-value are plotted with a significance threshold of 0.05. (E) We will temporally resolve adaptive changes caused by tonic TCR signaling by RNA-sequencing.

Bibliography

1. Daniels, M.A. and E. Teixeiro, *TCR Signaling in T Cell Memory.* Front Immunol, 2015. **6**: p. 617.
2. Godfrey, D.I., J. Kennedy, T. Suda, and A. Zlotnik, *A developmental pathway involving four phenotypically and functionally distinct subsets of CD3-CD4-CD8- triple-negative adult mouse thymocytes defined by CD44 and CD25 expression.* J Immunol, 1993. **150**(10): p. 4244-52.
3. Germain, R.N., *T-cell development and the CD4-CD8 lineage decision.* Nat Rev Immunol, 2002. **2**(5): p. 309-22.
4. Borgulya, P., H. Kishi, Y. Uematsu, and H. von Boehmer, *Exclusion and inclusion of alpha and beta T cell receptor alleles.* Cell, 1992. **69**(3): p. 529-37.
5. von Boehmer, H., et al., *Crucial function of the pre-T-cell receptor (TCR) in TCR beta selection, TCR beta allelic exclusion and alpha beta versus gamma delta lineage commitment.* Immunol Rev, 1998. **165**: p. 111-9.
6. Germain, R.N. and I. Stefanova, *The dynamics of T cell receptor signaling: complex orchestration and the key roles of tempo and cooperation.* Annu Rev Immunol, 1999. **17**: p. 467-522.
7. Robey, E. and B.J. Fowlkes, *Selective events in T cell development.* Annu Rev Immunol, 1994. **12**: p. 675-705.

8. von Boehmer, H., H.S. Teh, and P. Kisielow, *The thymus selects the useful, neglects the useless and destroys the harmful.* Immunol Today, 1989. **10**(2): p. 57-61.

9. Matzinger, P. and S. Guerder, *Does T-cell tolerance require a dedicated antigen-presenting cell?* Nature, 1989. **338**(6210): p. 74-6.

10. Kambayashi, T. and T.M. Laufer, *Atypical MHC class II-expressing antigen-presenting cells: can anything replace a dendritic cell?* Nat Rev Immunol, 2014. **14**(11): p. 719-30.

11. Luckheeram, R.V., R. Zhou, A.D. Verma, and B. Xia, *CD4(+)T cells: differentiation and functions.* Clin Dev Immunol, 2012. **2012**: p. 925135.

12. Constant, S.L. and K. Bottomly, *Induction of Th1 and Th2 CD4+ T cell responses: the alternative approaches.* Annu Rev Immunol, 1997. **15**: p. 297-322.

13. Walker, J.A. and A.N.J. McKenzie, *T(H)2 cell development and function.* Nat Rev Immunol, 2018. **18**(2): p. 121-133.

14. Martin-Orozco, N., et al., *T helper 17 cells promote cytotoxic T cell activation in tumor immunity.* Immunity, 2009. **31**(5): p. 787-98.

15. Aydemir, T.B., J.P. Liuzzi, S. McClellan, and R.J. Cousins, *Zinc transporter ZIP8 (SLC39A8) and zinc influence IFN-gamma expression in activated human T cells.* J Leukoc Biol, 2009. **86**(2): p. 337-48.

16. Vinuesa, C.G., M.A. Linterman, D. Yu, and I.C. MacLennan, *Follicular Helper T Cells.* Annu Rev Immunol, 2016. **34**: p. 335-68.

17. Tran, D.Q., *TGF-beta: the sword, the wand, and the shield of FOXP3(+) regulatory T cells.* J Mol Cell Biol, 2012. **4**(1): p. 29-37.

18. Courtney, A.H., W.L. Lo, and A. Weiss, *TCR Signaling: Mechanisms of Initiation and Propagation.* Trends Biochem Sci, 2018. **43**(2): p. 108-123.

19. Balagopalan, L., et al., *The LAT story: a tale of cooperativity, coordination, and choreography.* Cold Spring Harb Perspect Biol, 2010. **2**(8): p. a005512.

20. Wange, R.L., *LAT, the linker for activation of T cells: a bridge between T cell-specific and general signaling pathways.* Sci STKE, 2000. **2000**(63): p. re1.

21. Pardigon, N., et al., *Role of co-stimulation in CD8+ T cell activation.* Int Immunol, 1998. **10**(5): p. 619-30.

22. Raskov, H., A. Orhan, J.P. Christensen, and I. Gogenur, *Cytotoxic CD8(+) T cells in cancer and cancer immunotherapy.* Br J Cancer, 2021. **124**(2): p. 359-367.

23. Chen, L. and D.B. Flies, *Molecular mechanisms of T cell co-stimulation and co-inhibition.* Nat Rev Immunol, 2013. **13**(4): p. 227-42.

24. Yoshinaga, S.K., et al., *T-cell co-stimulation through B7RP-1 and ICOS.* Nature, 1999. **402**(6763): p. 827-32.

25. Suresh, M., A. Singh, and C. Fischer, *Role of tumor necrosis factor receptors in regulating CD8 T-cell responses during acute lymphocytic choriomeningitis virus infection.* J Virol, 2005. **79**(1): p. 202-13.

26. Ye, L.L., et al., *The Significance of Tumor Necrosis Factor Receptor Type II in CD8(+) Regulatory T Cells and CD8(+) Effector T Cells.* Front Immunol, 2018. **9**: p. 583.

27. Sansom, D.M., *CD28, CTLA-4 and their ligands: who does what and to whom?* Immunology, 2000. **101**(2): p. 169-77.

28. Boomer, J.S. and J.M. Green, *An enigmatic tail of CD28 signaling.* Cold Spring Harb Perspect Biol, 2010. **2**(8): p. a002436.

29. Janardhan, S.V., K. Praveen, R. Marks, and T.F. Gajewski, *Evidence implicating the Ras pathway in multiple CD28 costimulatory functions in CD4+ T cells.* PLoS One, 2011. **6**(9): p. e24931.

30. Ikeda, H., L.J. Old, and R.D. Schreiber, *The roles of IFN gamma in protection against tumor development and cancer immunoediting.* Cytokine Growth Factor Rev, 2002. **13**(2): p. 95-109.

31. O'Shea, J.J., M. Gadina, and R.D. Schreiber, *Cytokine signaling in 2002: new surprises in the Jak/Stat pathway.* Cell, 2002. **109 Suppl**: p. S121-31.

32. Hanahan, D. and R.A. Weinberg, *Hallmarks of cancer: the next generation.* Cell, 2011. **144**(5): p. 646-74.

33. Gonzalez, H., C. Hagerling, and Z. Werb, *Roles of the immune system in cancer: from tumor initiation to metastatic progression.* Genes Dev, 2018. **32**(19-20): p. 1267-1284.

34. Robbins, P.F., et al., *Mining exomic sequencing data to identify mutated antigens recognized by adoptively transferred tumor-reactive T cells.* Nat Med, 2013. **19**(6): p. 747-52.

35. Segal, N.H., et al., *Epitope landscape in breast and colorectal cancer.* Cancer Res, 2008. **68**(3): p. 889-92.

36. Dotiwala, F., et al., *Killer lymphocytes use granulysin, perforin and granzymes to kill intracellular parasites.* Nat Med, 2016. **22**(2): p. 210-6.

37. Akira, S., et al., *Molecular cloning of APRF, a novel IFN-stimulated gene factor 3 p91-related transcription factor involved in the gp130-mediated signaling pathway.* Cell, 1994. **77**(1): p. 63-71.

38. Metkar, S.S., et al., *Cytotoxic cell granule-mediated apoptosis: perforin delivers granzyme B-serglycin complexes into target cells without plasma membrane pore formation.* Immunity, 2002. **16**(3): p. 417-28.

39. Chen, D.S. and I. Mellman, *Oncology meets immunology: the cancer-immunity cycle.* Immunity, 2013. **39**(1): p. 1-10.

40. Ferguson, T.A., J. Choi, and D.R. Green, *Armed response: how dying cells influence T-cell functions.* Immunol Rev, 2011. **241**(1): p. 77-88.

41. Gajewski, T.F., H. Schreiber, and Y.X. Fu, *Innate and adaptive immune cells in the tumor microenvironment.* Nat Immunol, 2013. **14**(10): p. 1014-22.

42. Motz, G.T. and G. Coukos, *Deciphering and reversing tumor immune suppression.* Immunity, 2013. **39**(1): p. 61-73.

43. Pardoll, D.M., *The blockade of immune checkpoints in cancer immunotherapy.* Nat Rev Cancer, 2012. **12**(4): p. 252-64.

44. Sharma, P., et al., *Immune checkpoint therapy-current perspectives and future directions.* Cell, 2023. **186**(8): p. 1652-1669.

45. Wang, D.R., X.L. Wu, and Y.L. Sun, *Therapeutic targets and biomarkers of tumor immunotherapy: response versus non-response.* Signal Transduct Target Ther, 2022. **7**(1): p. 331.

46. Ostios-Garcia, L., et al., *Safety and Efficacy of PD-1 Inhibitors Among HIV-Positive Patients With Non-Small Cell Lung Cancer.* J Thorac Oncol, 2018. **13**(7): p. 1037-1042.

47. Xu-Monette, Z.Y., J. Zhou, and K.H. Young, *PD-1 expression and clinical PD-1 blockade in B-cell lymphomas.* Blood, 2018. **131**(1): p. 68-83.

48. Annibali, O., et al., *PD-1 /PD-L1 checkpoint in hematological malignancies.* Leuk Res, 2018. **67**: p. 45-55.

49. Manz, B.N., et al., *Small molecule inhibition of Csk alters affinity recognition by T cells.* Elife, 2015. **4**.

50. Nika, K., et al., *Constitutively active Lck kinase in T cells drives antigen receptor signal transduction.* Immunity, 2010. **32**(6): p. 766-77.

51. Courtney, A.H., et al., *CD45 functions as a signaling gatekeeper in T cells.* Sci Signal, 2019. **12**(604).

52. Chow, L.M., M. Fournel, D. Davidson, and A. Veillette, *Negative regulation of T-cell receptor signalling by tyrosine protein kinase p50csk.* Nature, 1993. **365**(6442): p. 156-60.

53. Inderberg, E.M., et al., *Human c-SRC kinase (CSK) overexpression makes T cells dummy.* Cancer Immunol Immunother, 2018. **67**(4): p. 525-536.

54. Imamoto, A. and P. Soriano, *Disruption of the csk gene, encoding a negative regulator of Src family tyrosine kinases, leads to neural tube defects and embryonic lethality in mice.* Cell, 1993. **73**(6): p. 1117-24.

55. Schmedt, C., et al., *Csk controls antigen receptor-mediated development and selection of T-lineage cells.* Nature, 1998. **394**(6696): p. 901-4.

56. Tan, Y.X., et al., *Inhibition of the kinase Csk in thymocytes reveals a requirement for actin remodeling in the initiation of full TCR signaling.* Nat Immunol, 2014. **15**(2): p. 186-94.

57. D, P.O.M., *Recent advances in inhibitors of C-terminal SRC kinase.* Future Med Chem, 2020. **12**(16): p. 1447-1449.

58. Kiefer, F., et al., *HPK1, a hematopoietic protein kinase activating the SAPK/JNK pathway.* EMBO J, 1996. **15**(24): p. 7013-25.

59. Ling, P., et al., *Involvement of hematopoietic progenitor kinase 1 in T cell receptor signaling.* J Biol Chem, 2001. **276**(22): p. 18908-14.

60. Patzak, I.M., et al., *HPK1 competes with ADAP for SLP-76 binding and via Rap1 negatively affects T-cell adhesion.* Eur J Immunol, 2010. **40**(11): p. 3220-5.

61. Hernandez, S., et al., *The Kinase Activity of Hematopoietic Progenitor Kinase 1 Is Essential for the Regulation of T Cell Function.* Cell Rep, 2018. **25**(1): p. 80-94.

62. Shui, J.W., et al., *Hematopoietic progenitor kinase 1 negatively regulates T cell receptor signaling and T cell-mediated immune responses.* Nat Immunol, 2007. **8**(1): p. 84-91.

63. Wang, X., et al., *Attenuation of T cell receptor signaling by serine phosphorylation-mediated lysine 30 ubiquitination of SLP-76 protein.* J Biol Chem, 2012. **287**(41): p. 34091-100.

64. Di Bartolo, V., et al., *A novel pathway down-modulating T cell activation involves HPK-1-dependent recruitment of 14-3-3 proteins on SLP-76.* J Exp Med, 2007. **204**(3): p. 681-91.

65. Sauer, K., et al., *Hematopoietic progenitor kinase 1 associates physically and functionally with the adaptor proteins B cell linker protein and SLP-76 in lymphocytes.* J Biol Chem, 2001. **276**(48): p. 45207-16.

66. Le Bras, S., et al., *Recruitment of the actin-binding protein HIP-55 to the immunological synapse regulates T cell receptor signaling and endocytosis.* J Biol Chem, 2004. **279**(15): p. 15550-60.

67. Liou, J., et al., *HPK1 is activated by lymphocyte antigen receptors and negatively regulates AP-1.* Immunity, 2000. **12**(4): p. 399-408.

68. You, D., et al., *Enhanced antitumor immunity by a novel small molecule HPK1 inhibitor.* J Immunother Cancer, 2021. **9**(1).

69. Lim, P.S., C.R. Sutton, and S. Rao, *Protein kinase C in the immune system: from signalling to chromatin regulation.* Immunology, 2015. **146**(4): p. 508-22.

70. Joshi, R.P., et al., *The zeta isoform of diacylglycerol kinase plays a predominant role in regulatory T cell development and TCR-mediated ras signaling.* Sci Signal, 2013. **6**(303): p. ra102.

71. Sanjuan, M.A., D.R. Jones, M. Izquierdo, and I. Merida, *Role of diacylglycerol kinase alpha in the attenuation of receptor signaling.* J Cell Biol, 2001. **153**(1): p. 207-20.

72. Zhong, X.P., et al., *Regulation of T cell receptor-induced activation of the Ras-ERK pathway by diacylglycerol kinase zeta.* J Biol Chem, 2002. **277**(34): p. 31089-98.

73. Wichroski, M., et al., *DGKalpha/zeta inhibitors combine with PD-1 checkpoint therapy to promote T cell-mediated antitumor immunity.* Sci Transl Med, 2023. **15**(719): p. eadh1892.

74. Kureshi, R., et al., *DGKalpha/zeta inhibition lowers the TCR affinity threshold and potentiates antitumor immunity.* Sci Adv, 2023. **9**(47): p. eadk1853.

75. Schmidt, M.H.H. and I. Dikic, *The Cbl interactome and its functions.* Nat Rev Mol Cell Biol, 2005. **6**(12): p. 907-18.

76. Thien, C.B. and W.Y. Langdon, *Cbl: many adaptations to regulate protein tyrosine kinases.* Nat Rev Mol Cell Biol, 2001. **2**(4): p. 294-307.

77. Wang, H.Y., et al., *Cbl promotes ubiquitination of the T cell receptor zeta through an adaptor function of Zap-70.* J Biol Chem, 2001. **276**(28): p. 26004-11.

78. Murphy, M.A., et al., *Tissue hyperplasia and enhanced T-cell signalling via ZAP-70 in c-Cbl-deficient mice.* Mol Cell Biol, 1998. **18**(8): p. 4872-82.

79. Naramura, M., H.K. Kole, R.J. Hu, and H. Gu, *Altered thymic positive selection and intracellular signals in Cbl-deficient mice.* Proc Natl Acad Sci U S A, 1998. **95**(26): p. 15547-52.

80. Bachmaier, K., et al., *Negative regulation of lymphocyte activation and autoimmunity by the molecular adaptor Cbl-b.* Nature, 2000. **403**(6766): p. 211-6.

81. Chiang, Y.J., et al., *Cbl-b regulates the CD28 dependence of T-cell activation.* Nature, 2000. **403**(6766): p. 216-20.

82. Fang, D. and Y.C. Liu, *Proteolysis-independent regulation of PI3K by Cbl-b-mediated ubiquitination in T cells.* Nat Immunol, 2001. **2**(9): p. 870-5.

83. Nguyen, T.T.T., et al., *Cbl-b deficiency prevents functional but not phenotypic T cell anergy.* J Exp Med, 2021. **218**(7).

84. Qiao, G., et al., *E3 ubiquitin ligase Cbl-b suppresses proallergic T cell development and allergic airway inflammation.* Cell Rep, 2014. **6**(4): p. 709-23.

85. Loeser, S., et al., *Spontaneous tumor rejection by cbl-b-deficient CD8+ T cells.* J Exp Med, 2007. **204**(4): p. 879-91.

86. Kumar, J., et al., *Deletion of Cbl-b inhibits CD8(+) T-cell exhaustion and promotes CAR T-cell function.* J Immunother Cancer, 2021. **9**(1).

87. Xie, P., et al., *TNF receptor-associated factor 3 is required for T cell-mediated immunity and TCR/CD28 signaling.* J Immunol, 2011. **186**(1): p. 143-55.

88. Arkee, T., B.S. Hostager, J.C.D. Houtman, and G.A. Bishop, *TRAF3 in T Cells Restrains Negative Regulators of LAT to Promote TCR/CD28 Signaling.* J Immunol, 2021. **207**(1): p. 322-332.

89. Prell, R.A., et al., *OX40-mediated memory T cell generation is TNF receptor-associated factor 2 dependent.* J Immunol, 2003. **171**(11): p. 5997-6005.

90. Saoulli, K., et al., *CD28-independent, TRAF2-dependent costimulation of resting T cells by 4-1BB ligand.* J Exp Med, 1998. **187**(11): p. 1849-62.

91. Cannons, J.L., E.M. Bertram, and T.H. Watts, *Cutting edge: profound defect in T cell responses in TNF receptor-associated factor 2 dominant negative mice.* J Immunol, 2002. **169**(6): p. 2828-31.

92. Lah, S., et al., *Engineering second-generation TCR-T cells by site-specific integration of TRAF-binding motifs into the CD247 locus.* J Immunother Cancer, 2023. **11**(4).

93. Rota, G., et al., *Shp-2 Is Dispensable for Establishing T Cell Exhaustion and for PD-1 Signaling In Vivo.* Cell Rep, 2018. **23**(1): p. 39-49.

94. Yuan, X., et al., *Recent Advances of SHP2 Inhibitors in Cancer Therapy: Current Development and Clinical Application.* J Med Chem, 2020. **63**(20): p. 11368-11396.

95. Naing, A., et al., *Phase I Dose Escalation Study of Sodium Stibogluconate (SSG), a Protein Tyrosine Phosphatase Inhibitor, Combined with Interferon Alpha for Patients with Solid Tumors.* J Cancer, 2011. **2**: p. 81-9.

96. Stromnes, I.M., et al., *Abrogation of SRC homology region 2 domain-containing phosphatase 1 in tumor-specific T cells improves efficacy of adoptive immunotherapy by enhancing the effector function and accumulation of short-lived effector T cells in vivo.* J Immunol, 2012. **189**(4): p. 1812-25.

97. Trengove, M.C. and A.C. Ward, *SOCS proteins in development and disease.* Am J Clin Exp Immunol, 2013. **2**(1): p. 1-29.

98. Zhang, J.G., et al., *The conserved SOCS box motif in suppressors of cytokine signaling binds to elongins B and C and may couple bound proteins to proteasomal degradation.* Proc Natl Acad Sci U S A, 1999. **96**(5): p. 2071-6.

99. Kamizono, S., et al., *The SOCS box of SOCS-1 accelerates ubiquitin-dependent proteolysis of TEL-JAK2.* J Biol Chem, 2001. **276**(16): p. 12530-8.

100. Yasukawa, H., et al., *The JAK-binding protein JAB inhibits Janus tyrosine kinase activity through binding in the activation loop.* EMBO J, 1999. **18**(5): p. 1309-20.

101. Naka, T., et al., *Structure and function of a new STAT-induced STAT inhibitor.* Nature, 1997. **387**(6636): p. 924-9.

102. Endo, T.A., et al., *A new protein containing an SH2 domain that inhibits JAK kinases.* Nature, 1997. **387**(6636): p. 921-4.

103. Palmer, D.C. and N.P. Restifo, *Suppressors of cytokine signaling (SOCS) in T cell differentiation, maturation, and function.* Trends Immunol, 2009. **30**(12): p. 592-602.

104. Palmer, D.C., et al., *Cish actively silences TCR signaling in CD8+ T cells to maintain tumor tolerance.* J Exp Med, 2015. **212**(12): p. 2095-113.

105. Guittard, G., et al., *The Cish SH2 domain is essential for PLC-gamma1 regulation in TCR stimulated CD8(+) T cells.* Sci Rep, 2018. **8**(1): p. 5336.

106. Lv, J., et al., *Disruption of CISH promotes the antitumor activity of human T cells and decreases PD-1 expression levels.* Mol Ther Oncolytics, 2023. **28**: p. 46-58.

107. Jin, J., et al., *CISH impairs lysosomal function in activated T cells resulting in mitochondrial DNA release and inflammaging.* Nat Aging, 2023. **3**(5): p. 600-616.

108. Tripathi, P., et al., *STAT5 is critical to maintain effector CD8+ T cell responses.* J Immunol, 2010. **185**(4): p. 2116-24.

109. Beltra, J.C., et al., *Stat5 opposes the transcription factor Tox and rewires exhausted CD8(+) T cells toward durable effector-like states during chronic antigen exposure.* Immunity, 2023. **56**(12): p. 2699-2718 e11.

110. Scott, A.C., et al., *TOX is a critical regulator of tumour-specific T cell differentiation.* Nature, 2019. **571**(7764): p. 270-274.

111. Heltemes-Harris, L.M. and M.A. Farrar, *Constitutively active STAT5 constructs.* Methods Mol Biol, 2013. **967**: p. 225-32.

112. Onishi, M., et al., *Identification and characterization of a constitutively active STAT5 mutant that promotes cell proliferation.* Mol Cell Biol, 1998. **18**(7): p. 3871-9.

113. Grange, M., et al., *Activated STAT5 promotes long-lived cytotoxic CD8+ T cells that induce regression of autochthonous melanoma.* Cancer Res, 2012. **72**(1): p. 76-87.

114. Ding, Z.C., et al., *Persistent STAT5 activation reprograms the epigenetic landscape in CD4(+) T cells to drive polyfunctionality and antitumor immunity.* Sci Immunol, 2020. **5**(52).

115. Schreiber, R.D., L.J. Old, and M.J. Smyth, *Cancer immunoediting: integrating immunity's roles in cancer suppression and promotion.* Science, 2011. **331**(6024): p. 1565-70.

116. Laletin, V., et al., *Negative intracellular regulators of T-cell receptor (TCR) signaling as potential antitumor immunotherapy targets.* J Immunother Cancer, 2023. **11**(5).

117. Kraft, M.S., et al., *Herpesvirus saimiri transforms human T-cell clones to stable growth without inducing resistance to apoptosis.* J Virol, 1998. **72**(4): p. 3138-45.

118. Lund, T.C., et al., *Activation of STAT transcription factors by herpesvirus Saimiri Tip-484 requires p56lck.* J Virol, 1997. **71**(9): p. 6677-82.

119. Gross, G., T. Waks, and Z. Eshhar, *Expression of immunoglobulin-T-cell receptor chimeric molecules as functional receptors with antibody-type specificity.* Proc Natl Acad Sci U S A, 1989. **86**(24): p. 10024-8.

120. June, C.H., et al., *CAR T cell immunotherapy for human cancer.* Science, 2018. **359**(6382): p. 1361-1365.

121. Porter, D.L., et al., *Chimeric antigen receptor-modified T cells in chronic lymphoid leukemia.* N Engl J Med, 2011. **365**(8): p. 725-33.

122. Kochenderfer, J.N., et al., *Eradication of B-lineage cells and regression of lymphoma in a patient treated with autologous T cells genetically engineered to recognize CD19.* Blood, 2010. **116**(20): p. 4099-102.

123. Straus, D.B. and A. Weiss, *Genetic evidence for the involvement of the lck tyrosine kinase in signal transduction through the T cell antigen receptor.* Cell, 1992. **70**(4): p. 585-93.

124. Raab, M., et al., *p56Lck and p59Fyn regulate CD28 binding to phosphatidylinositol 3-kinase, growth factor receptor-bound protein GRB-2, and T cell-specific protein-tyrosine kinase ITK: implications for T-cell costimulation.* Proc Natl Acad Sci U S A, 1995. **92**(19): p. 8891-5.

125. Hui, E., et al., *T cell costimulatory receptor CD28 is a primary target for PD-1-mediated inhibition.* Science, 2017. **355**(6332): p. 1428-1433.

126. Heyeck, S.D., H.M. Wilcox, S.C. Bunnell, and L.J. Berg, *Lck phosphorylates the activation loop tyrosine of the Itk kinase domain and activates Itk kinase activity.* J Biol Chem, 1997. **272**(40): p. 25401-8.

127. van Oers, N.S., N. Killeen, and A. Weiss, *Lck regulates the tyrosine phosphorylation of the T cell receptor subunits and ZAP-70 in murine thymocytes.* J Exp Med, 1996. **183**(3): p. 1053-62.

128. Bergman, M., et al., *The human p50csk tyrosine kinase phosphorylates p56lck at Tyr-505 and down regulates its catalytic activity.* EMBO J, 1992. **11**(8): p. 2919-24.

129. Levinson, N.M., M.A. Seeliger, P.A. Cole, and J. Kuriyan, *Structural basis for the recognition of c-Src by its inactivator Csk.* Cell, 2008. **134**(1): p. 124-34.

130. Mustelin, T., K.M. Coggeshall, and A. Altman, *Rapid activation of the T-cell tyrosine protein kinase pp56lck by the CD45 phosphotyrosine phosphatase.* Proc Natl Acad Sci U S A, 1989. **86**(16): p. 6302-6.

131. Ostergaard, H.L., et al., *Expression of CD45 alters phosphorylation of the lck-encoded tyrosine protein kinase in murine lymphoma T-cell lines.* Proc Natl Acad Sci U S A, 1989. **86**(22): p. 8959-63.

132. Yamaguchi, H. and W.A. Hendrickson, *Structural basis for activation of human lymphocyte kinase Lck upon tyrosine phosphorylation.* Nature, 1996. **384**(6608): p. 484-9.

133. Rudd, C.E., et al., *The CD4 receptor is complexed in detergent lysates to a protein-tyrosine kinase (pp58) from human T lymphocytes.* Proc Natl Acad Sci U S A, 1988. **85**(14): p. 5190-4.

134. Shaw, A.S., et al., *Short related sequences in the cytoplasmic domains of CD4 and CD8 mediate binding to the amino-terminal domain of the p56lck tyrosine protein kinase.* Mol Cell Biol, 1990. **10**(5): p. 1853-62.

135. Barber, E.K., et al., *The CD4 and CD8 antigens are coupled to a protein-tyrosine kinase (p56lck) that phosphorylates the CD3 complex.* Proc Natl Acad Sci U S A, 1989. **86**(9): p. 3277-81.

136. Chan, A.C., M. Iwashima, C.W. Turck, and A. Weiss, *ZAP-70: a 70 kd protein-tyrosine kinase that associates with the TCR zeta chain.* Cell, 1992. **71**(4): p. 649-62.

137. Zhang, W., et al., *LAT: the ZAP-70 tyrosine kinase substrate that links T cell receptor to cellular activation.* Cell, 1998. **92**(1): p. 83-92.

138. Shah, N.H., et al., *An electrostatic selection mechanism controls sequential kinase signaling downstream of the T cell receptor.* Elife, 2016. **5**.

139. Wiese, N., et al., *Selective activation of T cell kinase p56lck by Herpesvirus saimiri protein tip.* J Biol Chem, 1996. **271**(2): p. 847-52.

140. Bauer, F., et al., *Characterization of Lck-binding elements in the herpesviral regulatory Tip protein.* Biochemistry, 2004. **43**(47): p. 14932-9.

141. Jung, J.U., et al., *Identification of Lck-binding elements in tip of herpesvirus saimiri.* J Biol Chem, 1995. **270**(35): p. 20660-7.

142. Au-Yeung, B.B., et al., *IL-2 Modulates the TCR Signaling Threshold for CD8 but Not CD4 T Cell Proliferation on a Single-Cell Level.* J Immunol, 2017. **198**(6): p. 2445-2456.

143. Biesinger, B., et al., *Stable growth transformation of human T lymphocytes by herpesvirus saimiri.* Proc Natl Acad Sci U S A, 1992. **89**(7): p. 3116-9.

144. Kim, Y., et al., *Activation of the STAT6 transcription factor in Jurkat T-cells by the herpesvirus saimiri Tip protein.* J Gen Virol, 2012. **93**(Pt 2): p. 330-340.

145. Park, J., et al., *Herpesviral protein targets a cellular WD repeat endosomal protein to downregulate T lymphocyte receptor expression.* Immunity, 2002. **17**(2): p. 221-33.

146. Min, C.K., et al., *Role of amphipathic helix of a herpesviral protein in membrane deformation and T cell receptor downregulation.* PLoS Pathog, 2008. **4**(11): p. e1000209.

147. Kingston, D., et al., *Inhibition of retromer activity by herpesvirus saimiri tip leads to CD4 downregulation and efficient T cell transformation.* J Virol, 2011. **85**(20): p. 10627-38.

148. Heck, E., et al., *Growth transformation of human T cells by herpesvirus saimiri requires multiple Tip-Lck interaction motifs.* J Virol, 2006. **80**(20): p. 9934-42.

149. Sigalov, A.B., *Novel mechanistic insights into viral modulation of immune receptor signaling.* PLoS Pathog, 2009. **5**(7): p. e1000404.

150. Moran, A.E., et al., *T cell receptor signal strength in Treg and iNKT cell development demonstrated by a novel fluorescent reporter mouse.* J Exp Med, 2011. **208**(6): p. 1279-89.

151. Hogquist, K.A., et al., *T cell receptor antagonist peptides induce positive selection.* Cell, 1994. **76**(1): p. 17-27.

152. Zikherman, J., R. Parameswaran, and A. Weiss, *Endogenous antigen tunes the responsiveness of naive B cells but not T cells.* Nature, 2012. **489**(7414): p. 160-4.

153. Daniels, M.A., et al., *Thymic selection threshold defined by compartmentalization of Ras/MAPK signalling.* Nature, 2006. **444**(7120): p. 724-9.

154. Courtney, A.H., et al., *A Phosphosite within the SH2 Domain of Lck Regulates Its Activation by CD45.* Mol Cell, 2017. **67**(3): p. 498-511 e6.

155. Turner, J.M., et al., *Interaction of the unique N-terminal region of tyrosine kinase p56lck with cytoplasmic domains of CD4 and CD8 is mediated by cysteine motifs.* Cell, 1990. **60**(5): p. 755-65.

156. Chapman, T.L., et al., *Characterization of the interaction between the herpes simplex virus type I Fc receptor and immunoglobulin G.* J Biol Chem, 1999. **274**(11): p. 6911-9.

157. Villarino, A.V., Y. Kanno, J.R. Ferdinand, and J.J. O'Shea, *Mechanisms of Jak/STAT signaling in immunity and disease.* J Immunol, 2015. **194**(1): p. 21-7.

158. Melero, I., et al., *Immunostimulatory monoclonal antibodies for cancer therapy.* Nat Rev Cancer, 2007. **7**(2): p. 95-106.

159. Xin Yu, J., V.M. Hubbard-Lucey, and J. Tang, *Immuno-oncology drug development goes global.* Nat Rev Drug Discov, 2019. **18**(12): p. 899-900.

160. Rosenberg, S.A., *IL-2: the first effective immunotherapy for human cancer.* J Immunol, 2014. **192**(12): p. 5451-8.

161. Jackson, S.R., J. Yuan, and R.M. Teague, *Targeting CD8+ T-cell tolerance for cancer immunotherapy.* Immunotherapy, 2014. **6**(7): p. 833-52.

162. Kraehenbuehl, L., et al., *Enhancing immunotherapy in cancer by targeting emerging immunomodulatory pathways.* Nat Rev Clin Oncol, 2022. **19**(1): p. 37-50.

163. Lotze, M.T., et al., *High-dose recombinant interleukin 2 in the treatment of patients with disseminated cancer. Responses, treatment-related morbidity, and histologic findings.* JAMA, 1986. **256**(22): p. 3117-24.

164. Lotze, M.T., et al., *Clinical effects and toxicity of interleukin-2 in patients with cancer.* Cancer, 1986. **58**(12): p. 2764-72.

165. Amouzegar, A., et al., *STING Agonists as Cancer Therapeutics.* Cancers (Basel), 2021. **13**(11).

166. Le Naour, J., et al., *Trial watch: STING agonists in cancer therapy.* Oncoimmunology, 2020. **9**(1): p. 1777624.

167. Noble, M.E., J.A. Endicott, and L.N. Johnson, *Protein kinase inhibitors: insights into drug design from structure.* Science, 2004. **303**(5665): p. 1800-5.

168. Wang, W., et al., *CD8(+) T cells regulate tumour ferroptosis during cancer immunotherapy.* Nature, 2019. **569**(7755): p. 270-274.

169. Morris, R., N.J. Kershaw, and J.J. Babon, *The molecular details of cytokine signaling via the JAK/STAT pathway.* Protein Sci, 2018. **27**(12): p. 1984-2009.

170. Kelly, J., et al., *A role for Stat5 in CD8+ T cell homeostasis.* J Immunol, 2003. **170**(1): p. 210-7.

171. Moriggl, R., et al., *Stat5 is required for IL-2-induced cell cycle progression of peripheral T cells.* Immunity, 1999. **10**(2): p. 249-59.

172. Nosaka, T., et al., *STAT5 as a molecular regulator of proliferation, differentiation and apoptosis in hematopoietic cells.* EMBO J, 1999. **18**(17): p. 4754-65.

173. Burchill, M.A., et al., *Distinct effects of STAT5 activation on CD4+ and CD8+ T cell homeostasis: development of CD4+CD25+ regulatory T cells versus CD8+ memory T cells.* J Immunol, 2003. **171**(11): p. 5853-64.

174. Ribeiro, D., et al., *STAT5 is essential for IL-7-mediated viability, growth, and proliferation of T-cell acute lymphoblastic leukemia cells.* Blood Adv, 2018. **2**(17): p. 2199-2213.

175. Shuai, K., et al., *Constitutive activation of STAT5 by the BCR-ABL oncogene in chronic myelogenous leukemia.* Oncogene, 1996. **13**(2): p. 247-54.

176. Hand, T.W., et al., *Differential effects of STAT5 and PI3K/AKT signaling on effector and memory CD8 T-cell survival.* Proc Natl Acad Sci U S A, 2010. **107**(38): p. 16601-6.

177. D'Souza, W.N. and L. Lefrancois, *IL-2 is not required for the initiation of CD8 T cell cycling but sustains expansion.* J Immunol, 2003. **171**(11): p. 5727-35.

178. Chinen, T., et al., *An essential role for the IL-2 receptor in T(reg) cell function.* Nat Immunol, 2016. **17**(11): p. 1322-1333.

179. Shah, N.H., M. Lobel, A. Weiss, and J. Kuriyan, *Fine-tuning of substrate preferences of the Src-family kinase Lck revealed through a high-throughput specificity screen.* Elife, 2018. **7**.

180. Andreatta, M., et al., *Interpretation of T cell states from single-cell transcriptomics data using reference atlases.* Nat Commun, 2021. **12**(1): p. 2965.

181. Miller, B.C., et al., *Subsets of exhausted CD8(+) T cells differentially mediate tumor control and respond to checkpoint blockade.* Nat Immunol, 2019. **20**(3): p. 326-336.

182. Siddiqui, I., et al., *Intratumoral Tcf1(+)PD-1(+)CD8(+) T Cells with Stem-like Properties Promote Tumor Control in Response to Vaccination and Checkpoint Blockade Immunotherapy.* Immunity, 2019. **50**(1): p. 195-211 e10.

183. Carmona, S.J., et al., *Deciphering the transcriptomic landscape of tumor-infiltrating CD8 lymphocytes in B16 melanoma tumors with single-cell RNA-Seq.* Oncoimmunology, 2020. **9**(1): p. 1737369.

184. Huppa, J.B. and M.M. Davis, *T-cell-antigen recognition and the immunological synapse.* Nat Rev Immunol, 2003. **3**(12): p. 973-83.

185. Basu, R. and M. Huse, *Mechanical Communication at the Immunological Synapse.* Trends Cell Biol, 2017. **27**(4): p. 241-254.

186. Feng, Y., E.L. Reinherz, and M.J. Lang, *alphabeta T Cell Receptor Mechanosensing Forces out Serial Engagement.* Trends Immunol, 2018. **39**(8): p. 596-609.

187. Dustin, M.L., *The immunological synapse.* Cancer Immunol Res, 2014. **2**(11): p. 1023-33.

188. Nagato, T., Y.R. Lee, Y. Harabuchi, and E. Celis, *Combinatorial immunotherapy of polyinosinic-polycytidylic acid and blockade of programmed death-ligand 1 induce*

effective CD8 T-cell responses against established tumors. Clin Cancer Res, 2014. **20**(5): p. 1223-34.

189. Dougan, S.K., et al., *Transnuclear TRP1-specific CD8 T cells with high or low affinity TCRs show equivalent antitumor activity.* Cancer Immunol Res, 2013. **1**(2): p. 99-111.

190. Maurer, B., et al., *High activation of STAT5A drives peripheral T-cell lymphoma and leukemia.* Haematologica, 2020. **105**(2): p. 435-447.

191. Li, H.S., et al., *Multidimensional control of therapeutic human cell function with synthetic gene circuits.* Science, 2022. **378**(6625): p. 1227-1234.

192. Di Stasi, A., et al., *Inducible apoptosis as a safety switch for adoptive cell therapy.* N Engl J Med, 2011. **365**(18): p. 1673-83.

193. Straathof, K.C., et al., *An inducible caspase 9 safety switch for T-cell therapy.* Blood, 2005. **105**(11): p. 4247-54.

194. Rafiq, S., C.S. Hackett, and R.J. Brentjens, *Engineering strategies to overcome the current roadblocks in CAR T cell therapy.* Nat Rev Clin Oncol, 2020. **17**(3): p. 147-167.

195. Mellman, I., D.S. Chen, T. Powles, and S.J. Turley, *The cancer-immunity cycle: Indication, genotype, and immunotype.* Immunity, 2023. **56**(10): p. 2188-2205.

196. Allen, G.M., et al., *Synthetic cytokine circuits that drive T cells into immune-excluded tumors.* Science, 2022. **378**(6625): p. eaba1624.

197. Liu, E., et al., *Use of CAR-Transduced Natural Killer Cells in CD19-Positive Lymphoid Tumors.* N Engl J Med, 2020. **382**(6): p. 545-553.

198. Sockolosky, J.T., et al., *Selective targeting of engineered T cells using orthogonal IL-2 cytokine-receptor complexes.* Science, 2018. **359**(6379): p. 1037-1042.

199. Rosenberg, S.A. and N.P. Restifo, *Adoptive cell transfer as personalized immunotherapy for human cancer.* Science, 2015. **348**(6230): p. 62-8.

200. Rosenberg, S.A., et al., *Gene transfer into humans--immunotherapy of patients with advanced melanoma, using tumor-infiltrating lymphocytes modified by retroviral gene transduction.* N Engl J Med, 1990. **323**(9): p. 570-8.

201. Muul, L.M., P.J. Spiess, E.P. Director, and S.A. Rosenberg, *Identification of specific cytolytic immune responses against autologous tumor in humans bearing malignant melanoma.* J Immunol, 1987. **138**(3): p. 989-95.